Field Guide Book for the course “Geologic Field Excursion” National Central University, Taiwan

14th January ~ 19th January 2018, Taiwan

Field Guide Book

Tectonics, Sedimentation and Geomorphology of the Active Taiwan Mountain Belt

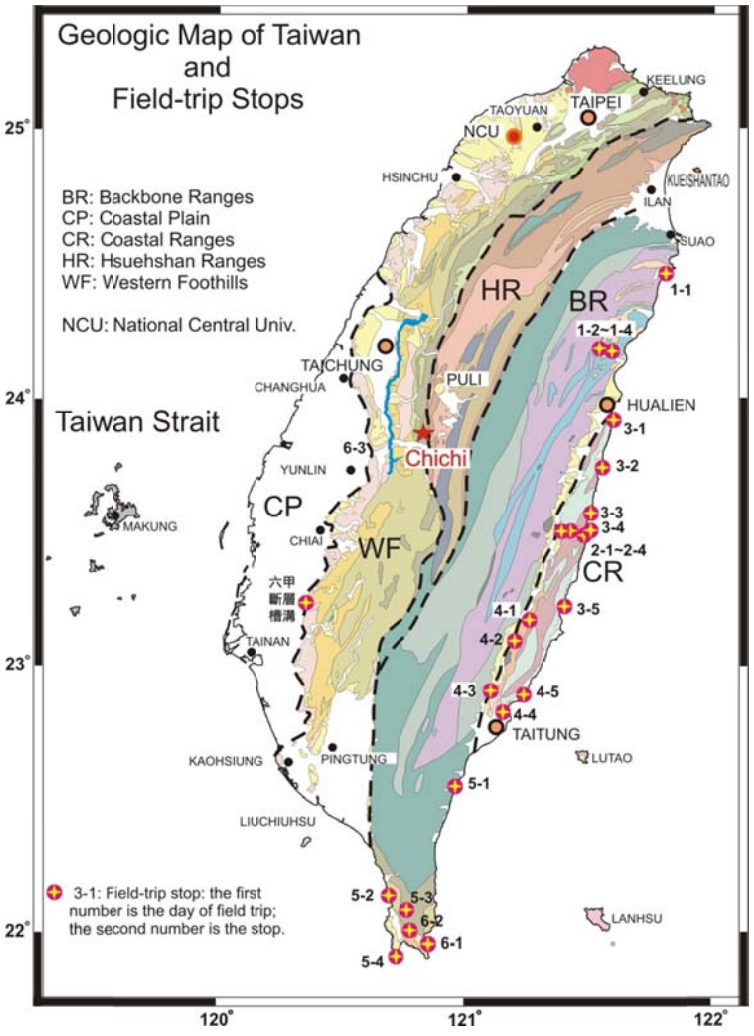

Field Guides:

Andrew Tien-Shun Lin (林殿順),

Wen-Jen Huang (黃文正),

Li-Wei Kuo (郭力維)

National Central University, Taiwan

Tectonics, sedimentation and geomorphology of the active Taiwan mountain belt

Purposes

The island of Taiwan is located on the active convergent boundary between the Philippine Sea plate and the Chinese continental margin. The collision between the Luzon volcanic arc and the Chinese continental margin since late Miocene has resulted in a foreland basin in western Taiwan of Eurasian Plate affinity and a forearc basin and related volcanic arcs in eastern Taiwan, pertaining to the Philippine Sea Plate. The arc-continent collision has caused intense crustal thickening and shortening in the rising mountain range. The mountain building process is very much alive and can be well illustrated by the rugged topography, rapid uplift and denudation, young tectonic landforms, active faulting, and numerous earthquakes.

The 6-day field excursion will make a round trip of the Taiwan island, examining late Paleozoic to Mesozoic metamorphic core in the Central Range for the first day. The second and third days will visit the accreted Coastal Range (a volcanic arc) to see arc volcanics, forearc-basin sediments, and mélange as various active tectonic features. The fourth and fifth days will start by examining the structures of the metamorphosed Miocene slate in the Central Range at the SE coast of Taiwan followed by visiting the Hengchun Peninsula. The Hengchun Peninsula features Miocene continental slope deposits with fan turbidites and canyon-infills accumulated before arc-continent collision, tectonic mélange, and uplifted limestones accumulated in the actively deforming accretionary wedge. The final day starts by visiting the late Miocene deep-sea turbidites at Chialoshui and the Kengting Melange in the morning. We then head back to National Central University in the afternoon and will make a short stop at the Chushan Chelungpu Preservation Museum in central Taiwan.

Selection for the proposed outcrop visits is based on the outcrop experience for the students. We choose outcrops that students haven't visited during their undergraduate study with an emphasis on the Coastal Range and the Hengchun Peninsula. We hope that students will have a holistic understanding on Taiwan tectonics and geology as well as geomorphology after the trip.

1. Introduction

This field excursion provides an opportunity to overview the sedimentation, tectonics, and geomorphology of the Taiwan mountain belt, especially for the Coastal

Range and the Hengchun Peninsula. Figure 1-1 shows the field-trip stops on top of the geological map of Taiwan. Figure 1-2 gives detail geological features in central Taiwan to give impression of the general geology that we may observe during our trip. This figure also illustrates the geology in the Central Range where the highest grade of metamorphic rocks are exposed.

A list of field trip stops and brief explanations of geology for each location, field leaders and assistants and their contacts can be found in Appendix 1. Appendix 2 gives a geologic map of Taiwan.

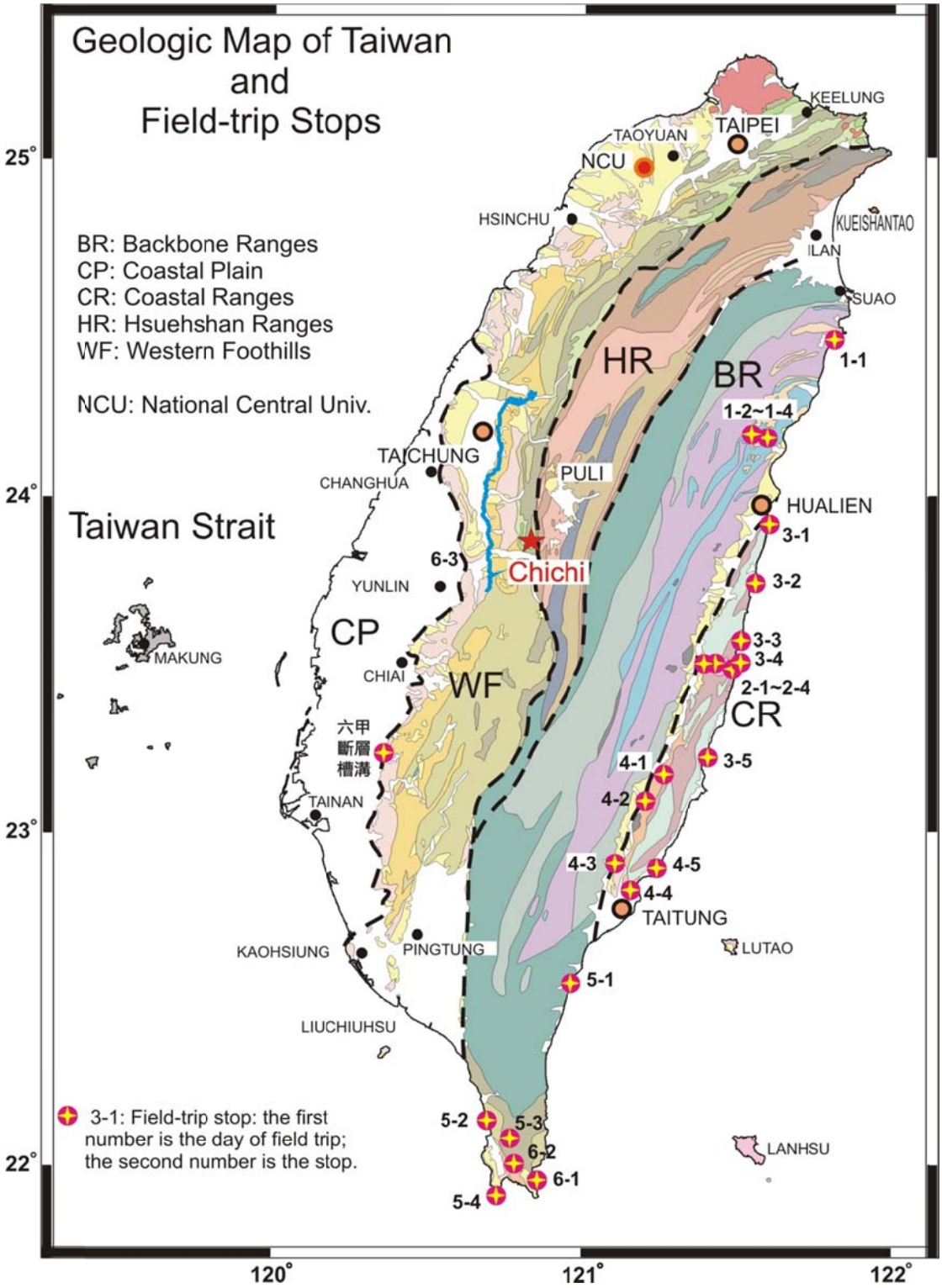

Fig. 1-1. Major stratigraphic units of Taiwan and field trip stops (red circles with stars). Blue line in west-central Taiwan indicates surface ruptures caused by the 1999 Chichi earthquake with its epicenter marked by a red star.

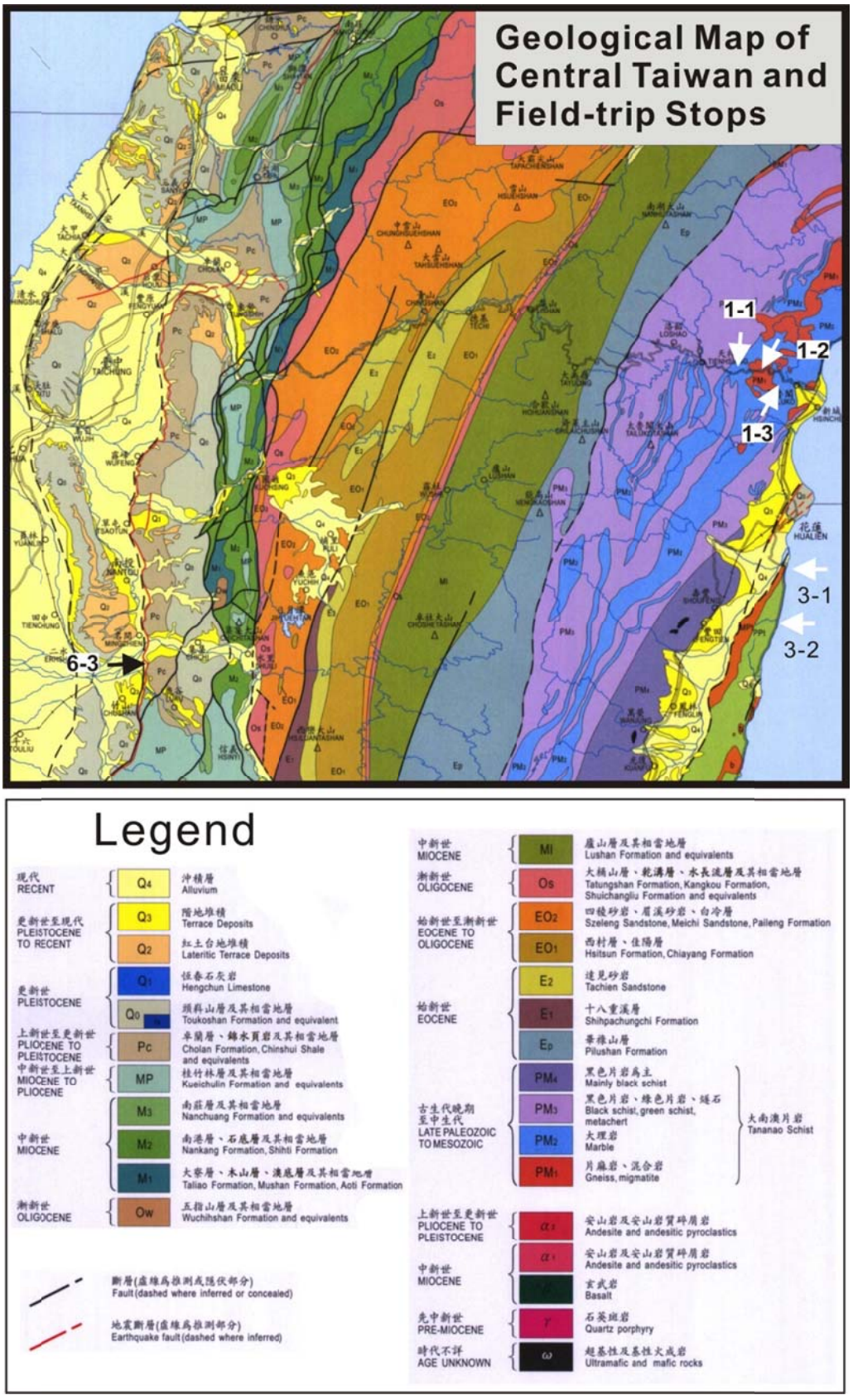

Fig. 1-2. Geologic map of central Taiwan (after Ho, 1988). Boxes show **l**ocations for more detailed geologic maps shown in the following figures. Field stops are **i**ndicated by arrows with numbers.

2. Tectonic Framework and Geologic Provinces

The Taiwan orogen resulted from the oblique collision of the Philippine Sea plate with the Eurasian plate (Figs. 2-1, 2-2), as manifested by the overriding of the Luzon arc onto the Chinese passive margin (e.g., Chai, 1972; Suppe, 1981) since 6.5-5 Ma (e.g., Teng, 1990; Lin and Watts, 2002). Overthrusting of the Luzon arc on the northern South China Sea margin has exhumed material that was previously located in the outer part of the rifted South China Sea margin (Fig. 2-3). Figure 2-3 shows that to the west of the Taiwan orogen, four rifted basins separated by basement highs can be recognized from the Cenozoic sediment isopach map from Lin et al. (2003)'s study. These basins, namely the Nanjihtao (NJB), Penghu (PHB), Taihsi (TB) and Tainan (TNB) basins (Sun, 1982), are Tertiary rifted basins related to the opening of the South China Sea (Lin et al., 2003).

The Taiwan orogenic belt comprises four geologic provinces (Ho, 1988, Fig.2-3). From east to west, they are the Coastal Range (CoR), the Backbone Range (BR), the Hsuehshan Range (HR), and the Western Foothills (WF). The terrains are of Eurasian plate affinity with the exception of the Coastal Range, which incorporates the accreted volcanic arc and belongs to the Philippine Sea plate. The Backbone Range and Hsuehshan Range are collectively referred to as the Central Range, which comprises the main body of the Taiwan orogen. The Central Range consists of pre-Tertiary continental basement unconformably overlain by metamorphosed Eocene to Miocene clastics deposited during the Paleogene rifting and Oligocene-Miocene post-breakup phases related to the opening of the South China Sea (e.g., Lin et al., 2003). The WF province is a west-vergent, fold-and-thrust belt comprising an Oligocene-Pleistocene siliciclastic sequence that accumulated on a passive margin and, subsequently, in a foreland basin setting because of the convergence between the Philippine Sea plate and Eurasian plate.

This field trip is designed to investigate all the geological provinces mentioned above. We therefore briefly describe the geology for the above geo-provinces as follows.

2.1 Backbone Range

The Backbone Range comprises the tectonized pre-Tertiary basement (Tananao Schist) and a metamorphosed Cenozoic sedimentary cover (see Fig. 2-3 for exposed rock formations). It is bordered to the east by the Longitudinal Valley (LV in Fig.2-3, the suture zone between the accreted Luzon arc and the Asian continent (Ho, 1988; Tsai, 1986). To the west, the Lishan Fault and the Chaochou Fault separate it from the Hsuehshan Range and the Western Foothills, respectively.

The pre-Tertiary basement rocks (Tananao Schist) consist of schist and marble, as well as scattered gneiss and amphibolite bodies (Yen, 1954, 1960, 1967). It is bounded to the east by a Mesozoic tectonic melange with high rank greenschist facies mineral assemblages. The geological history of the Tananao Schist can be traced back to the Paleozoic and involves multiple crustal deformation and metamorphism in the Mesozoic and Tertiary (Ernst and Jahn, 1987). Three major metamorphic stages or thermal events since late Mesozoic are recognized:

(1) late Mesozoic: A high-grade metamorphism of upper amphibolite facies coupled with granitoid intrusions occurred during ~110 to 77 Ma (Jahn and Liou, 1977; Jahn et al., 1986; Lan et al., 1990; Lo and Yui, 1996; Lan et al., 1996) or during 95-82 Ma (Lo and Onstott, 1995). This thermal event is generally correlated to the westward subduction of a paleo-Pacific plate beneath the Asian continental margin (Jahn et al., 1981; Liou, 1981; Ernst et al., 1981). Yen (1963) coined this subduction event the Nanao Orogeny;

(2) late Paleogene: Jahn et al. (1986) and Lan et al. (1990) recognized a greenschist facies metamorphism during ~40-35 Ma. Jahn et al. (1986) correlated this event to the opening of the South China Sea. However, Lo and Onstott (1995) argued that the above K-Ar age may be merely due to the effects of mixing and/or the partial resetting of isotopic systems by the metamorphism related to the late Cenozoic arc-continent collision;

(3) late Neogene: An up to greenschist facies metamorphism that occurred later than ~12 Ma has been widely reported in the literature (Yen and Rosenblum., 1964; Jahn and Liou, 1977; Jahn et al., 1981; Liou, 1981; Jahn et al., 1986; Ernst and Jahn, 1987; Yui and Lo, 1989; Lan et al., 1990; Lo and Yui, 1996). This thermal event is correlated to result from the arc-continent collision (Jahn and Liou, 1977; Jahn et al., 1981; Liou, 1981; Jahn et al., 1986; Ernst and Jahn, 1987; Yui and Lo, 1989; Lan et al., 1990; Teng, 1990; Lo and Yui, 1996).

The Cenozoic sedimentary cover is floored by a Paleocene unconformity and consists of Eocene and Miocene clastics which unconformably overlie the pre-Tertiary basement. The entire Eocene sequence is represented by a single rock formation (i.e., the Pilushan Formation), which consists mainly of slate with a minor amount of metamorphosed sandstone, marly limestone, and volcanics. At its top, an Oligocene unconformity separates the Eocene clastics from the overlying Miocene sediments, the Lushan Formation, which in the southern Backbone Range is floored by an upper Oligocene sandstone succession, the Likuan Formation (Chang, 1963, 1970, 1972; Huang, 1980a). The Paleocene and Oligocene unconformities were commonly overprinted by later shear movements resulting in their common associations with mylonite zones (Lee and Yang, 1994). The overprinted features and

a general lack of index fossils have made the recognition of these two unconformities ambiguous, at least in the literature if not in the field.

2.2 Hsuehshan Range

The Hsuehshan Range contains a thick, continuous Eocene to Miocene succession Chen, 1977; Ho, 1988; Teng et al., 1991). It is bordered to its east and west by the Lishan fault and the Chuchih fault, respectively. The northern Hsuehshan Range consists mainly of thick Oligocene sequences with minor upper Eocene and Miocene strata. The southern Hsueshan Range is dominated by thicker, middle to upper Eocene strata and thinner Oligocene sediments (Chen, 1977, 1979; Huang, 1980b). According to Teng et al. (1991), the Miocene sediments appear to have originally formed sheet-like layers of uniform thickness that blanketed the entire region from the Taiwan Strait to the northern Backbone Range. By contrast, the Oligocene sediments appear to have formed a SE-thickening wedge confined between the Taiwan Strait and the Backbone Range (Teng et al., 1991).

Teng et al. (1991) therefore suggested that the Oligocene strata of the northern Hsuehshan Range must have initially been deposited in a half-graben that they coined the “Hsuehshan trough”. The Paleogene Hsuehshan trough is thought to be bordered by an offshore basement high. Teng et al. (1991) assumed that the Paleogene offshore basement high corresponds to the present-day Backbone Range now separated from the Hsuehshan Range to its west by the Lishan Fault, an east-vergent backthrust (Clark et al., 1993; Lee et al., 1997). The Lishan Fault is thus postulated to be the west-dipping major normal fault bounding the Paleogene Hsuehshan trough and the offshore basement high during the Paleogene time (Teng et al., 1991).

2.3 Western Foothills

The Western Foothills is characterized by a series of west-facing fold-and-thrust sheet. It comprises largely the Oligocene to Pleistocene fluvial to shelf clastic sediments with no distinct depositional break (Chou, 1973, 1980; Huang and Cheng, 1983). The Oligocene to late Miocene series was laid down in the northern passive margin of the South China Sea but the latest Miocene to Pleistocene sequence was accumulated in the foreland basin in front of the rising and southwesterly migrating Taiwan orogen since collision between the Luzon arc and Asian continent initiated at about 6.5 Ma (Covey, 1986; Teng, 1990; Yu and Chou, 2001; Lin et al., 2003).

The Taiwan mountain building process is very much alive as evidenced by numerous earthquakes and active fault structures. The latest major earthquake is the devastating 1999 Chichi earthquake (M_w=7.6) with surface rupture of about 100 km

in length that occurs primarily along the pre-existing Chelungpu fault in central Taiwan (the red star shown in Fig. 2-3). In central Taiwan, three thrust sheets are recognized in the Foothills region. From east to west, they are the Shuangtung fault, the Chelungpu fault, and the Changhua fault. The latter is characterized by gentle anticlinal folds on the hangingwall whilst the formers exhibit more or less parallel hanging wall bedding dips and fault dips.

2.4 Coastal Range

The Coastal Range (Fig. 2-5) in eastern Taiwan is the extinct, accreted portion of the Luzon arc-trench system that sutured onto the Asian continent along the Longitudinal Valley between the Central Range and the Coastal Range (Ho, 1988; Tsai, 1986). It comprises an upper Miocene arc basement (the Tuluanshan Formation) with a patchy occurrence of limestone at its top (the Kankou Limestone), overlain by a thick Plio-Pleistocene turbidite sequence (the Takangkou Formation) which is then topped by an upper Pleistocene, non-marine conglomerate unit (the Pinanshan Conglomerate).

As shown in Fig. 2-5, in the southwest of the Coastal Range, a thin slice of tectonic mélange, the Lichi Melange (3.5-2.5Ma), is exposed along the tectonic suture on the overriding plate. Remnants of oceanic facies that formerly lay between the Asian continental margin and the volcanic arc are preserved in exotic blocks of the Lichi Melange. These blocks of ophiolite consist of upper parts of the lower Miocene oceanic crust, including gabbro, peridotite, pillow basalt, and red clay, which are interpreted to be of the South China Sea affinity (Ernst et al., 1985; Chung and Sun, 1992).

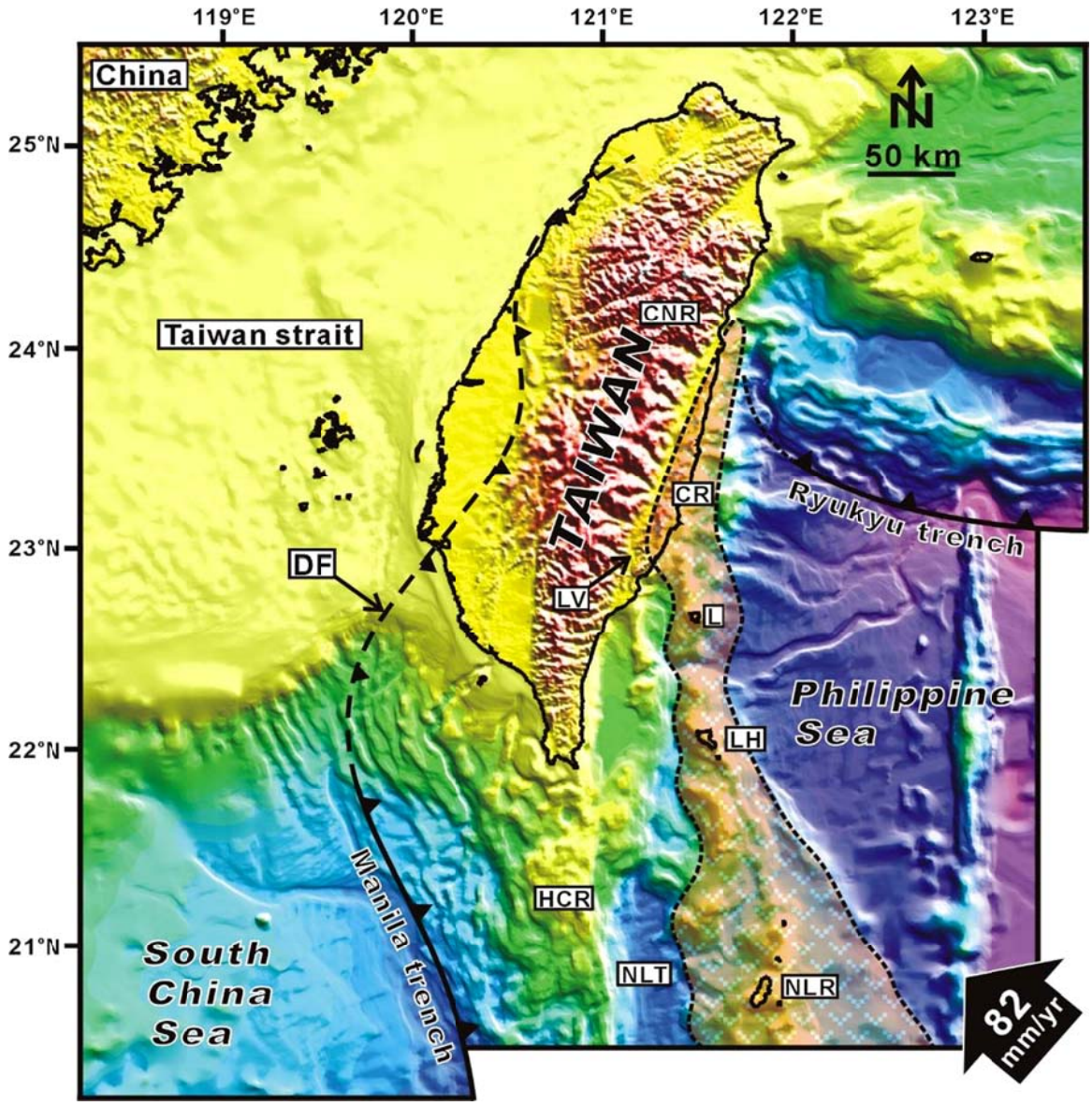

Fig. 2-1. Tectonic framework of the Taiwan collision belt between the Eurasian continent and the Philippine Sea plate (Chang et al., 2003). Large black arrow shows convergence between the volcanic arc and the continent margin (Yu et al., 1997). CeR = Central Range; CoR = Coastal Range; DF = deformation front; HCR= Hengchun Ridge; LV= Longitudinal Valley; NLR = North Luzon Ridge.

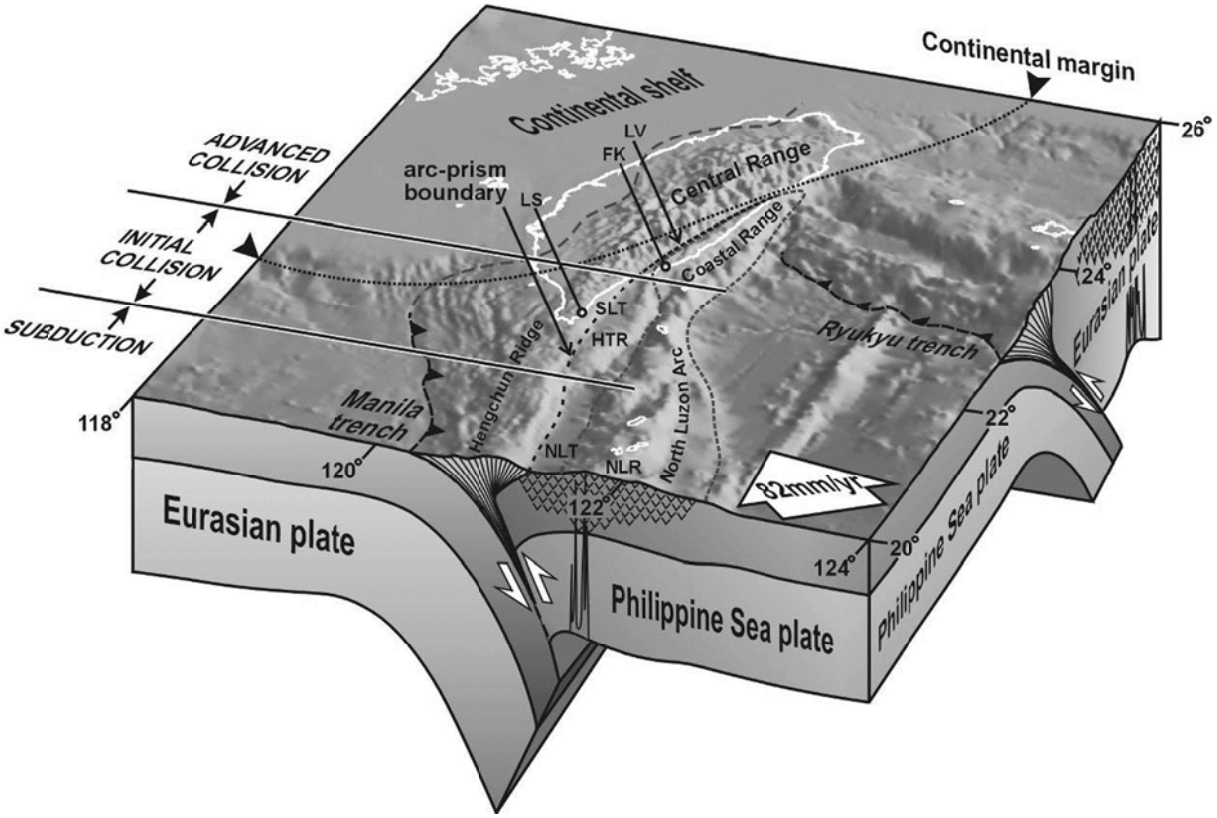

Fig. 2-2. Block diagram showing arc-continent collision and tectonic setting of Taiwan. Taiwan is situated in the active arc-continent collision region between the Eurasian continent and the Philippine Sea plate. South of Taiwan, the oceanic crust of the South China Sea (32-15 Ma) is subducting beneath the Philippine Sea plate along the Manila trench. To the east, the Philippine Sea plate is being consumed beneath the Eurasian continent along the Ryukyu trench. The Philippine Sea plate is moving northwestward at 310° with a rate of 82 mm/yr (Yu, Chen & Kuo, 1997). The Luzon arc (trending at about 355°) on the Philippine Sea plate is colliding with the Asian continent (trending at about 060°) and formed the Coastal Range in the eastern Taiwan. Because the Quaternary collision that forms the Taiwan island is a typical oblique arc-continent collision, the orogenic belt has been propagating southward (Suppe, 1981). Onland in Taiwan, one observes the outcome of this collision; in the area off southeastern Taiwan, the process of subduction is still ongoing. FK: Fukang Sandstone; HTR: Huatung Ridge; LS: Loshui Sandstone; LV: Longitudinal Valley fault zone; NLR: North Luzon Ridge; NLT: North Luzon Trough; SLT: Southern Longitudinal Trough (Chang et al., 2001).

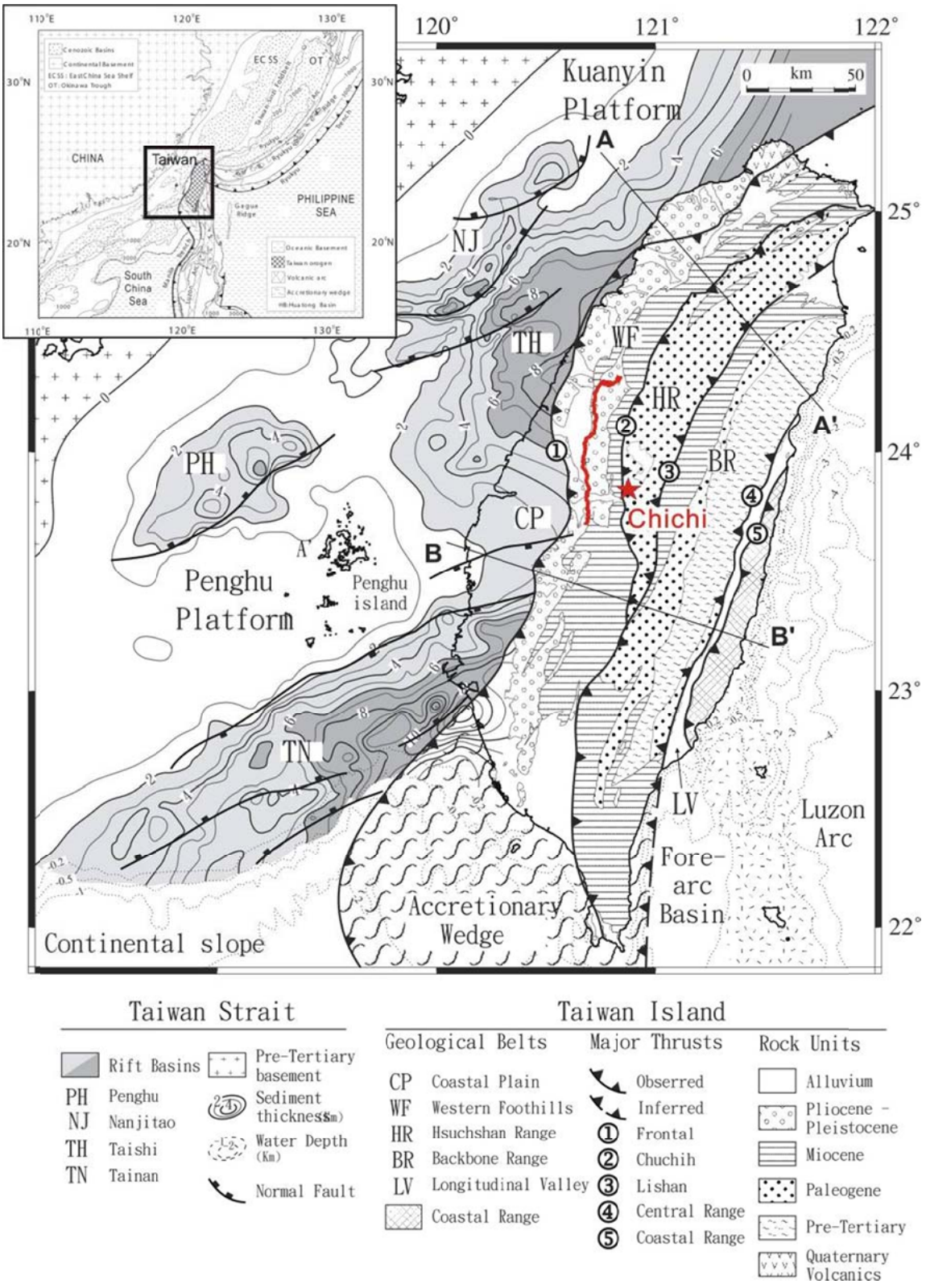

Fig. 2-3. Cenozoic geology of Taiwan and Taiwan Strait (after Teng and Lin, 2004). Summarized from Ho (1988), Teng (1992), Liu et al. (1997), Lin et al. (2003). The red line shows the surface rupture caused by the 1999 Chichi earthquake (denoted by the red star). Sections A-A' and B-B' shown in Fig. 2-4.

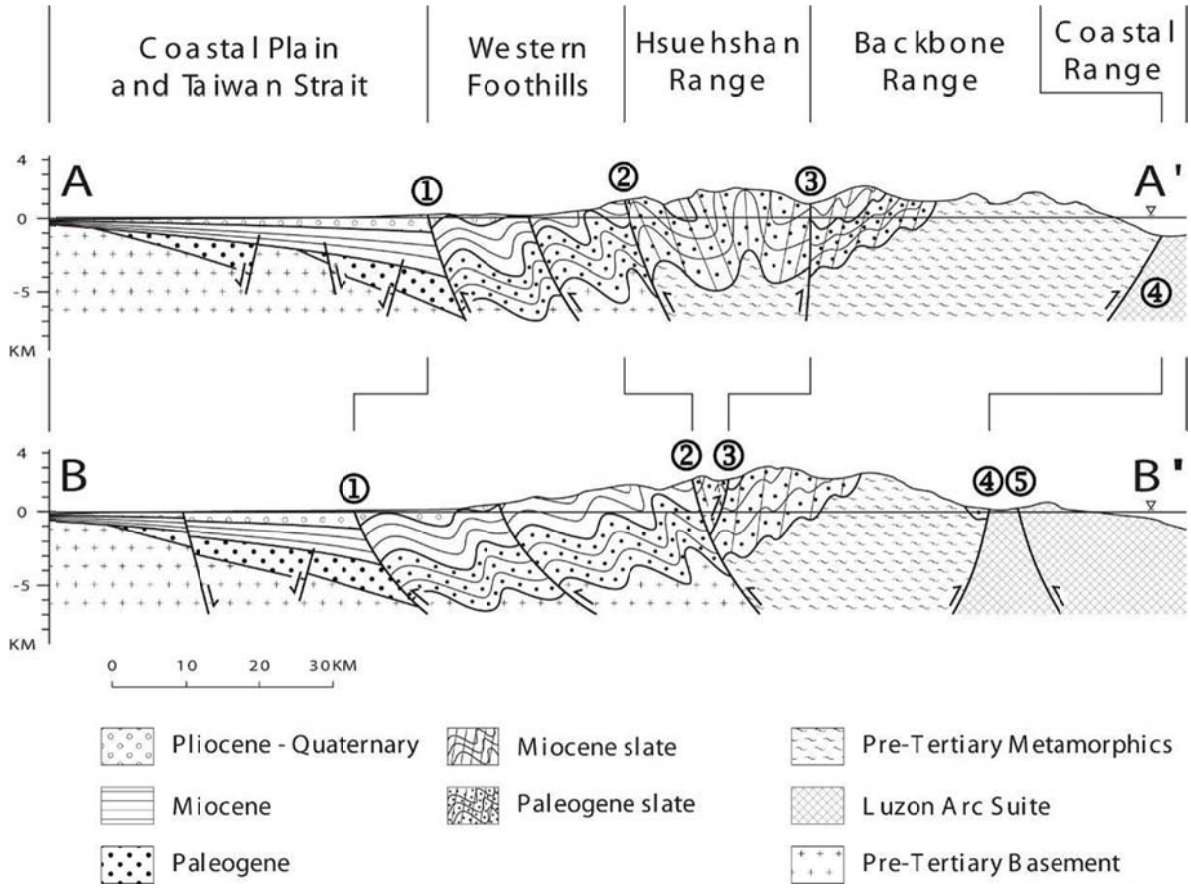

Fig. 2-4. Geological framework and lithotectonic belts of Taiwan (after Teng and Lin, 2004). Locations and major thrust 1-5 shown in Fig. 2-3. Summarized from Ho (1988), Teng et al. (1991) and Lin et al. (2003).

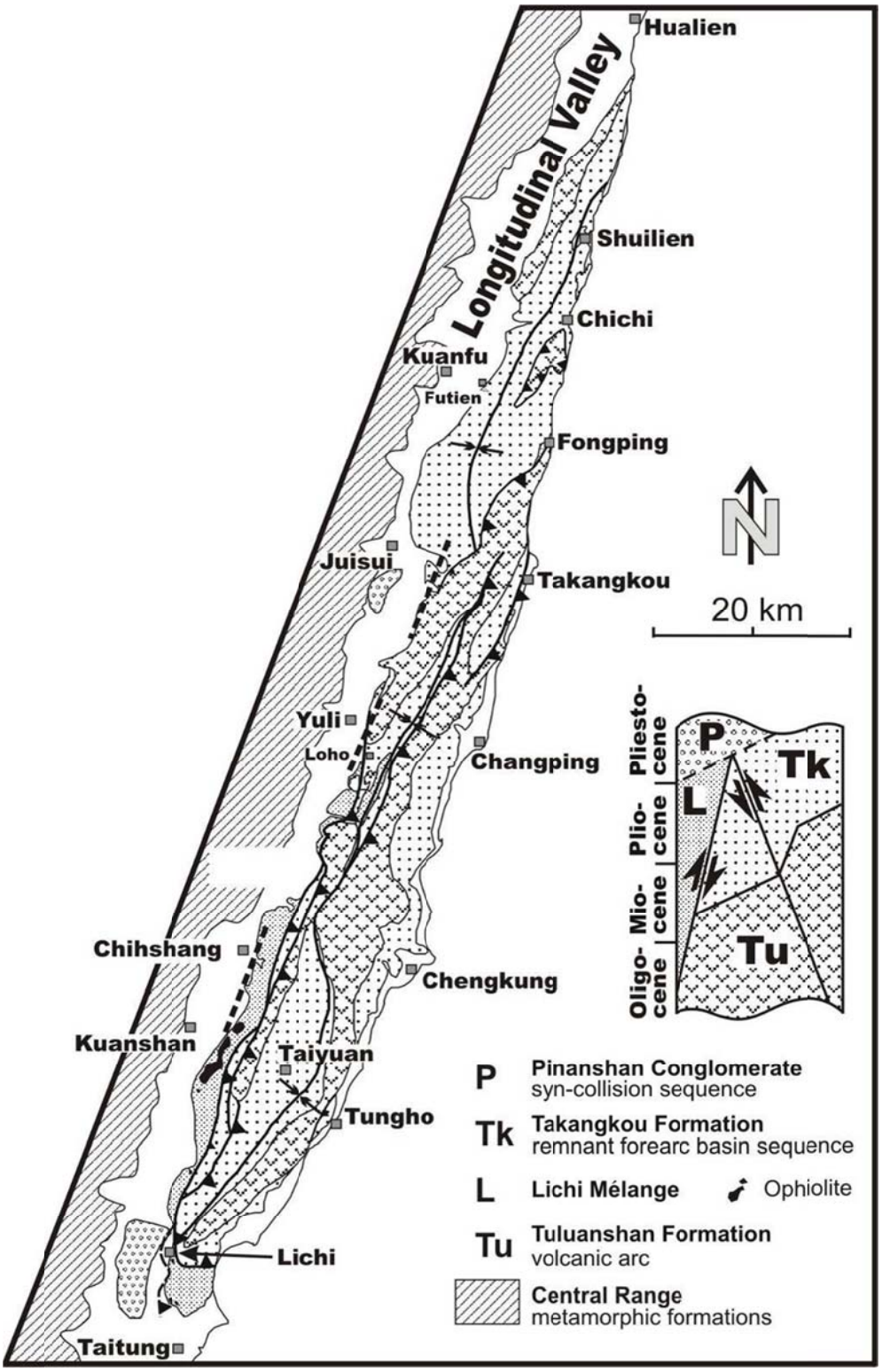

Fig. 2-5. Geological structures and stratigraphy of the Coastal Range (from Chang et al., 2003 and references therein).

3. Stratigraphy and tectonic development of the Hengchun Peninsula

The Hengchun Peninsula at the southern tip of Taiwan represents the accretionary prism of the Manila subduction system (Fig. 3-1). With elevation less than 1000 m, the peninsula is primarily composed of N-S oriented Middle-Late Miocene turbidites. It lies between the offshore North Luzon arc-forearc to the east and the offshore fold-and-thrust belt of the Kaoping Slope to the west. To the north of the peninsula, there is the Early-Middle Miocene slate belt and the Eocene meta-sandstones and the Paleozoic-Mesozoic metamorphic rocks (underthrust Eurasian Continent) of the Central Range.

The Hengchun Peninsula consists of three distinct geological units (Fig. 3-1): the Middle-Late Miocene deep-sea turbidites of the Mutan Formation (east of the Hengchun Valley), the Plio-Pleistocene shallow marine sequences (in the West Hengchun Hill), and the sheared Kenting Mélange along the Hengchun Valley (Chang, 1965, 1966; Cheng and Huang, 1975; Huang, 1984a; Sung, 1991; Chang et al., 2002).

The Miocene Mutan Formation and Loshui Sandstone

The Mutan Formation (Sung, 1991) is mainly composed of alternated sandstones and shales intercalated sporadically with lenticular bodies of sandstones and conglomerates. These lenticular units consist of the Shihmen Conglomerate, the Loshui Sandstone, the Lilongshan Sandstone and the Shitzutou Sandstone. They represent the deposits of submarine channels or canyons and deep-sea fans from the continental slope to the base of the slope. The turbidites are derived from SE Asian continent (Cheng et al., 1984).The turbidites were originally deposited on the passive Asian continental slope, but accreted into an accretionary wedge since latest Miocene at around 6-5 Ma. Various turbidite facies are observed in the Hengchun Peninsula, including fluxoturbidites of the feeder channel (Shihmen Conglomerate), thick mid-fan sandstones (Loshui Sandstone and Lilongshan Sandstone), as well as classic sandy and muddy proximal turbidites fan facies, and basin plain mudstone (Huang, 1984b; Cheng et al.,1984; Sung and Wang, 1986; Sung, 1991). Petrofacies analyses suggest that the Mutan and Loushui Formation sediments were derived mainly from low grade metamorphic terrane as well as magmatic arc, most likely in SE China (Sung and Wang, 1986).

Based on the studies of facies associations and paleocurrent distribution, the sandstone deposits of the Hengchun peninsula belonged to two major submarine fan systems, the Mutan fan to the north and the Loshui fan to the south (Cheng et al., 1984; Sung and Wang, 1986). Paleocurrent measurements indicate that sediments of the Mutan Formation were transported from the north or northwest (Fig.

3-3)(Huang, 1984; Chen et al., 1985; Sung and Wang, 1986). In contrast, flute casts in the Loshui Formation indicate sediment transportation from southeast to northwest (Fig. 3-3) (Cheng et al., 1984).

Two possible explanations for this contrasted paleo-current have been proposed: (1) there was a landmass or ridge existing in the south of the present Hengchun Peninsula, and from this now submerged landmass or ridge, it developed a northward-extending deep-sea fan (the Loshui Sandstone); (2) Rocks of the Hengchun peninsula (the Hengchun block) have undergone both tilting and counterclockwise rotation of about 90°. The structural boundaries of this rotated Hengchun block are: the Kenting Melange zone in the southwest, the Fongkang Fault in the north, and a submarine backthrust in the east (Chang et al., 2003).

Because there could not have existed continent to the south of the Hengchun Peninsula to serve as sediment source, the contrast in paleocurrent direction is probably the result of either clockwise rotation of the Loshui Sandstone relative to the hosting Mutan Formation, or the Peninsula has been rotated (based on some paleomagnetic measurements) along major faults (Fig. 3-3) (Chang, 2001).

Kenting Mélange (or Kenting Formation)

The Kenting Mélange is a mega-shear zone where sheared millimeter to hundred meter-size polygenic clasts are embedded in a dominantly argillaceous matrix (Tsan, 1974). It crops out in low hills southwest of the mountainous Miocene Mutan Formation turbidites. The shearing is so pervasive that no stratification is discernible. Contrasting to the N-S structural grain found in the Mutan Formation, the Kenting Mélange orients NW-SE, parallel to the trend of West Hengchun Hill and the Hengchun Valley.

The Paoli profile about 3 km north of Hengchun presents the best exposure of the Kenting Mélange (Fig. 3-5). It exhibits a typical badland topography. Centimeter-wide fault gouges in the argillaceous matrix are generally parallel to the shearing planes. Quartzose sandstone, conglomerates and basalt blocks found in the mélange are mostly angular and sheared throughout. All rock types present in the Kenting Mélange, except chromitite, can also be found in the Mutan Formation. Chromitite blocks rich in chromium spinel (> 90%; Chu et al., 1988) found in the Kenting Mélange are also highly sheared, and are believed to originate from lower crust or uppermost mantle of the South China Sea.

Various models for the tectonic setting, mechanism, and age of the Kenting Mélange have been proposed. For example, Tsan, (1974); Pelletier and Stephan (1986); and Sung (1991) suggested a Late Miocene slumping-on-passive-continental-margin model (olistostrome), while Page and Lan (1983); Byrne (1998) proposed a

similar phenomenon on inner trench slope of an accretionary prism. Even for the olistostrome model, two different settings were suggested. Page and Lan (1983) interpreted that the mafic igneous pebbles were derived from the South China Sea oceanic crust that had been exposed earlier in an accretionary wedge (formed by subduction or obduction) beside the Luzon arc. They thought that the igneous pebbles were first accumulated on slope basin in the accretionary prism, but then slumped westward into Manila Trench, indicating little tectonic shearing.

In comparison, Pelletier and Stephan (1986) also proposed a sedimentary model. They suggested that the mélange materials were deposited in Late Miocene by submarine slumping on a passive Asian continetal margin, but were later thrust and sheared. On the other hand, the Kenting Mélange has been considered a tectonic subduction mélange developed east of the Manila Trench in an accretionary wedge in the Plio-Pleistocene (Biq, 1977) or Late Miocene (Lu and Hsü, 1992). All the models proposed above however, shared a common deficiency in that they lacked observations on the active arc-continent collision now operating offshore in southern Taiwan in 21o 20'N-22 o 40'N. Nor they made comparison between the modern tectonic environment and that in which the Kenting Mélange was formed (Huang et al., 1997, 2000). In addition, controversial Late Miocene or Plio-Pleistocene ages of the Kenting Mélange were recommended because different mechanisms and settings were preferred in previous studies. Geological role of the Kenting Mélange is further complicated if the Lichi Mélange in the Coastal Range, eastern Taiwan, is analyzed in a regional scale (Ho, 1986).

The Lichi Mélange in the Coastal Range was considered a subduction complex in the Manila Trench system (Biq, 1973, 1977; Teng, 1985, 1990). If this is the case, since the Kenting Mélange in the Hengchun Peninsula is located far away from the Luzon arc and appears unrelated to subduction, its origin has no alternative but being part of a olistostrome developed on the passive Eurasian continental margin Tsan, 1974; Pelletier and Stephan, 1986). However, field study and recent marine survey indicates that the Lichi Mélange is most likely a sheared forearc sequences developed in the collision complex east of the Hengchun accretionary wedge (including the Hengchun Peninsula and the Hengchun Ridge)(Liu et al., 1999; Huang et al., 2000, 2001; Chang et al., 2000). The mafic blocks found in the Lichi Mélange could be thrust slices derived presumably from the Luzon arc basement instead of the South China Sea as it was thought previously (Huang et al., 2000; Chang et al., 2000).

Plio-Pleistocene strata

The Maanshan Formation is manly composed of quartzose siltstones deposited in slope basins in an accretionary wedge. In late Miocene, the Luzon arc began to collide with the Chinese continental margin and, subsequently, the sediments of passive-margin sequence was uplifted and partly eroded to form the proto-Hengchun Peninsula. During the Pleistocene, the shallow-marine Hengchun Limestone was developed unconformably on top of the deformed Miocene to Pliocene, deep-water sequence. Finally, the Oluanpi Formation was deposited as fluvial facies. Quaternary uplifting has since resulted in the tilting and the development of reef terraces.

The West Hengchun Terrace and the O-Luan-Pi Terrace are the most spectacular landform in the southern part of the Hengchun Peninsula. They both underlain by raised reef limestones with covers of lateritic beds consisting of sands and pebbles (the so-called LH surface). These Quaternary terraces were formed near the sea-level and subsequently uplifted, tilted or warped by recent tectonic activities to a height of up to 300 m above sea level (i.e. at the Ken-Ting Park).

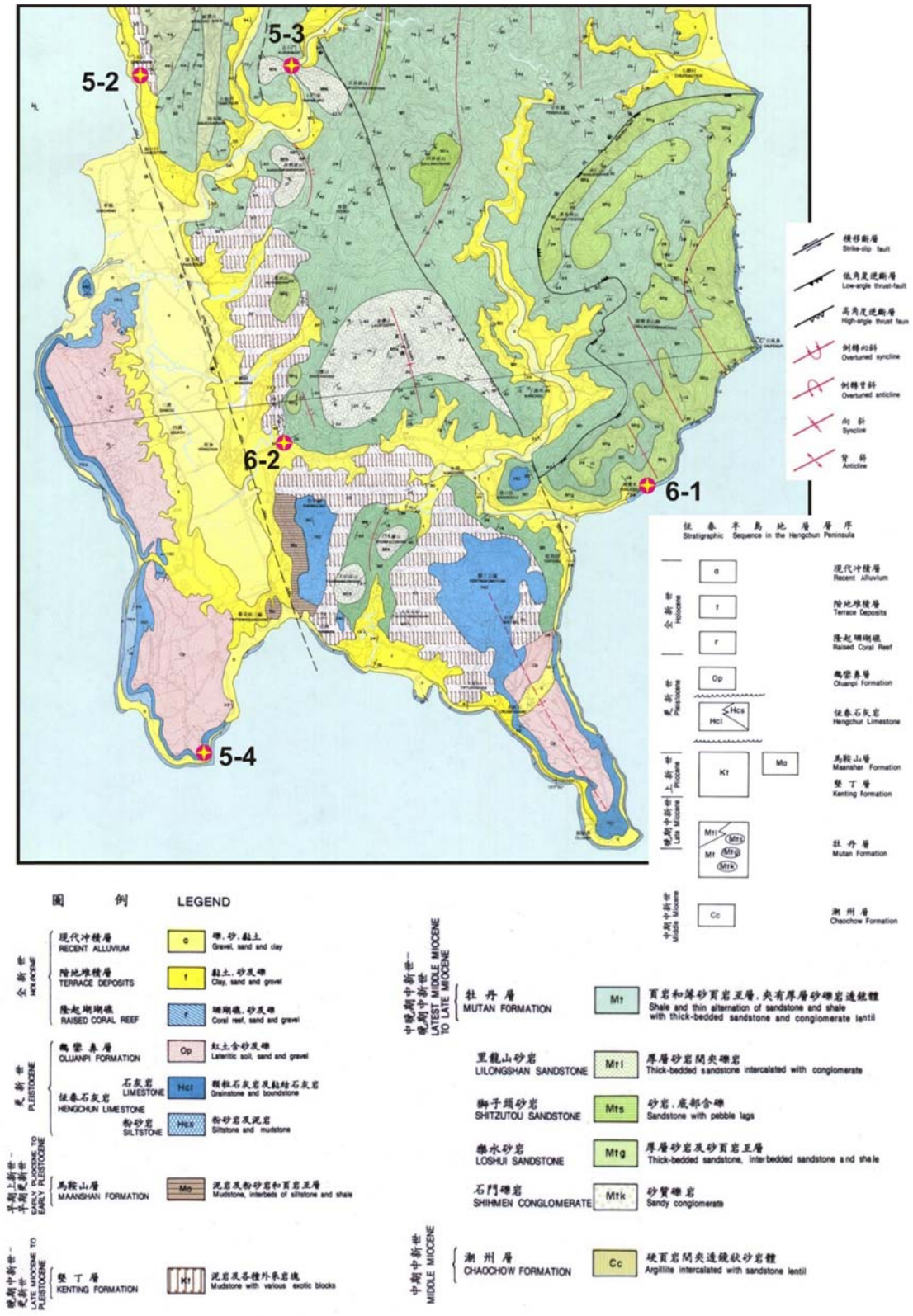

Fig. 3-1. Geologic map of the Hengchun Peninsula and field stops (after Sung, 1991).

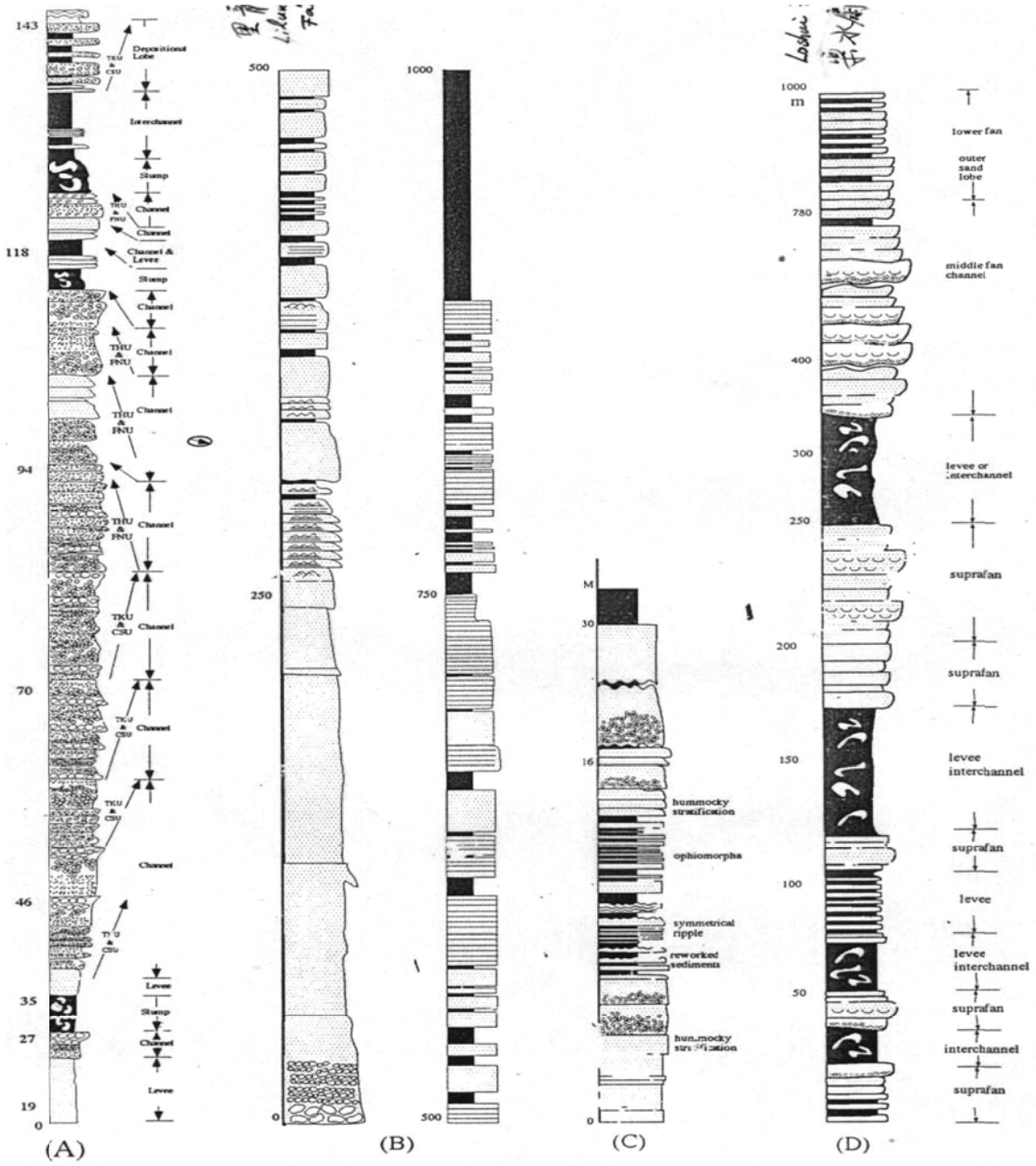

Fig. 3-2. Turbidite facies observed in the Hengchun Peninsula: A) Feeder channel conglomerates Shihmen Conglomerate) exposed along the Shihmen Gorge; B) Mid-fan sandstone facies of Lilungshn Sandstone; C) Upper fan conglomerate and mid-fan facies of the Shihtzutou Sandstone, and D) Middle fan and slump facies of the Lohsui Formation (Huang, 1984).

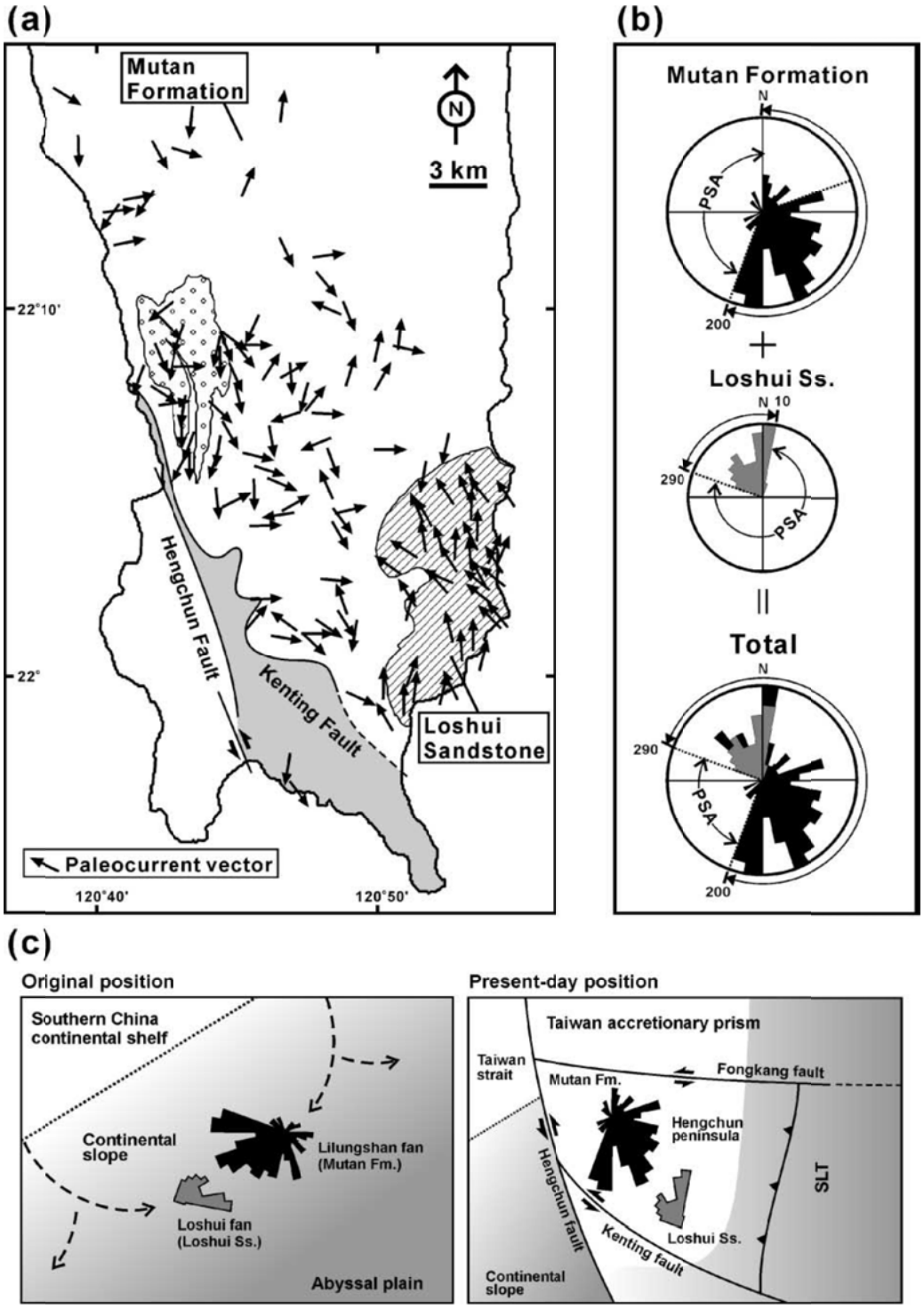

Fig. 3-3. (a) Paleocurrents (thin arrows) measured in the Miocene turbidites of the Hengchun peninsula (data compiled after Cheng et al., 1984; Sung, 1991). (b) Rose diagram of paleocurrents in the Mutan Formation and the Loshui Sandstone. PSA= possible source area. (c) Reconstruction of the paleocurrent distribution recorded in the Hengchun peninsula domain, before and after the tectonic rotation. SLT= southern Longitudinal Trough (Chang et al., 2003).

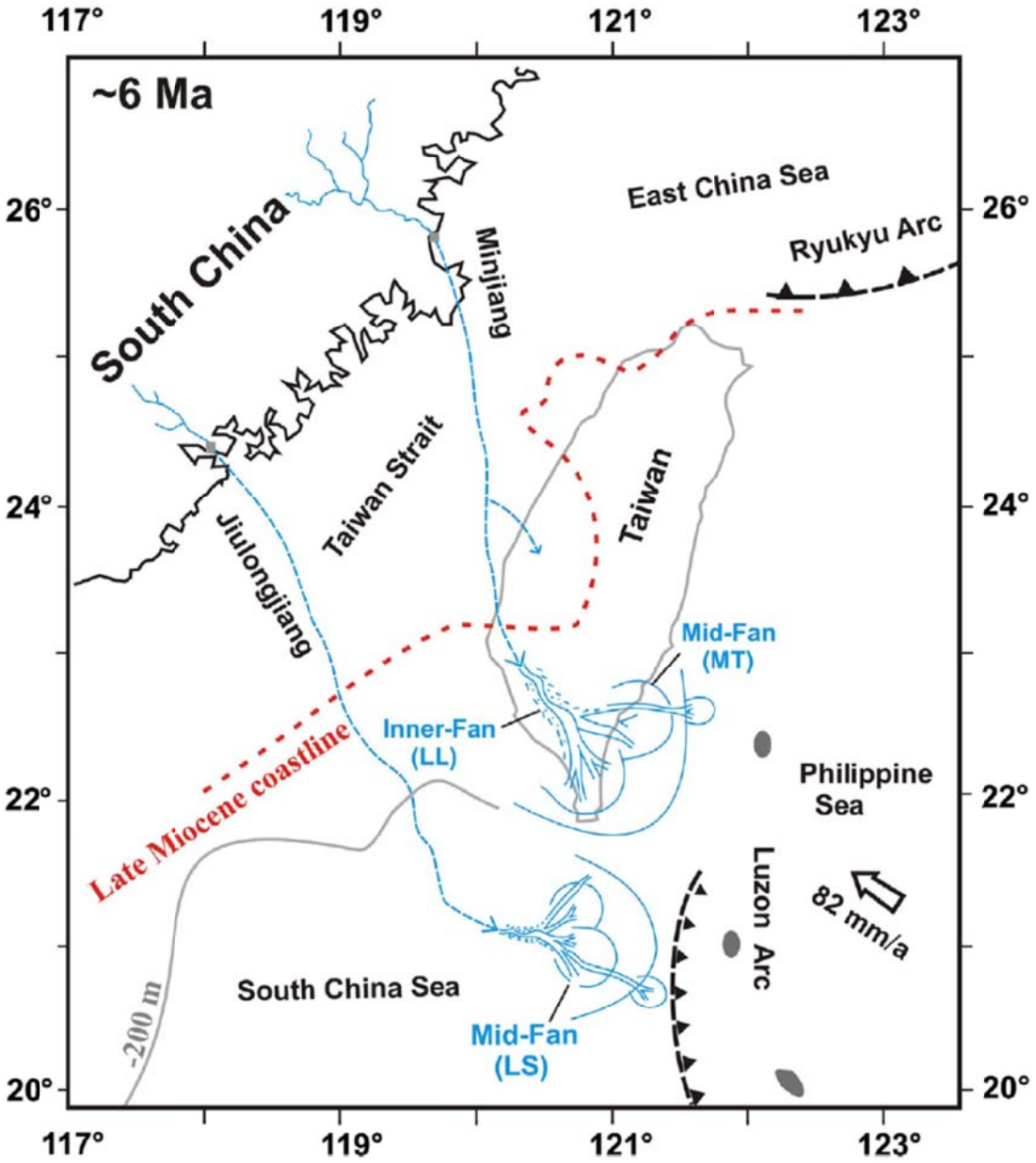

Fig. 3-4. Schematic map of the paleogeographic of the SE China in Late Miocene, black dashed line represent the NW Fujian province and SW Zhejiang province; red dashed line and blue line represent the paleo-coastline and the paleo-transport path, respectively (LL-Lilungshan Formation; LS-Loshui Formation; MT-Mutan Formation). (Zhang et al., 2014).

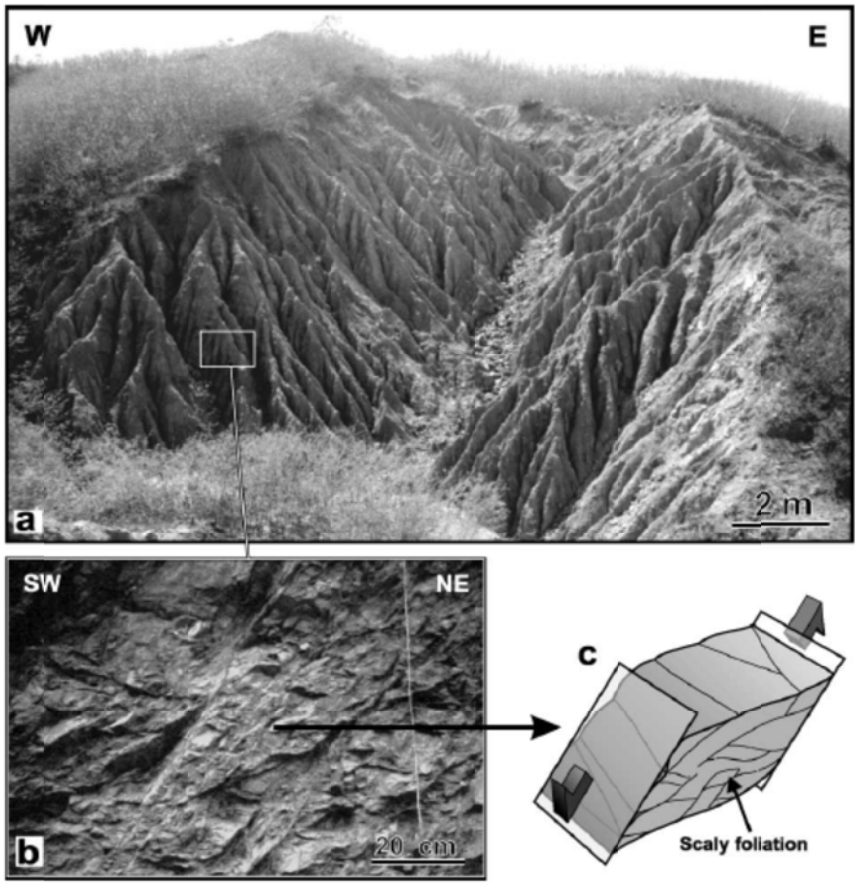

Fig. 3-5. (a) Typical outcrop of the Kenting Mélange. (b) Scaly foliation associated with shear deformation in the argillaceous matrix. (c) The sigmoid shape of the scaly foliation indicates the shear sense (Chang et al., 2003).

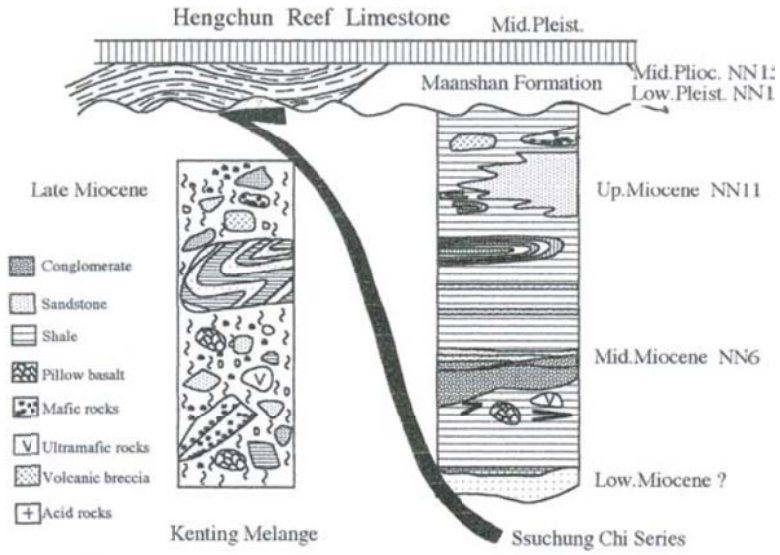

Fig. 3-6. The Kenting Melange was interpreted as a mega-thrust on the passive continental margin by Pelletier and Stephan (1986).

4. Stratigraphy of the Coastal Range

The sequences of the Coastal Range comprise about 6000~8000 m of marine and fluvial sedimentary and volcanic rocks of Neogene-Quaternary age (Hsu, 1956, 1976; Chang, 1967, 1969). These rocks may be divided into four rock-stratigraphic units: (1) the Miocene volcanics of the Tuluanshan Formation; (2) Pliocene-Pleistocene deep-sea turbidites of the Takangkou Formation; (3) the Lichi Mélange; and (4) the Pinanshan Conglomerate (Fig. 4-1). The Takangkou Formation is further divided into Fanshuliao Formation and Paliwan Formation (Teng, 1979; 1982). Here we review the stratigraphic scheme (Fig. 4-1) of the Coastal Range as summarized in Teng and Chen (1988).

4.1 Tuluanshan Formation

The Tuluanshan Formation represents the remnant Luzon arc massif. Dated materials in the Coast Ranges (Yang et al., 1988; Yang et al., 1995) reveal that the northern Luzon arc eruption began at ca. 16-15 Ma. The Tuluanshan Formation consists of a variety of volcanic and volcaniclastic rocks that underlie a great part of the range. Pyroclastic rocks, such as breccias, lapilli tuffs, and tuffs make up the bulk of the volcanics with a minor amount of lava. Most of the volcanics are andesite, some are basalt and dacite. Thin volcaniclastic reefal limestones are often intercalated with the volcanics near the top (Cheng and Wei, 1983; Teng and Lo, 1985). The age of the volcanics ranges from late Oligocene to early Pliocene and that of the limestones from late Miocene to late Pliocene (Chang, 1967, 1968, 1969; Chi et al., 1981; Chi and Chu, 1982; Cheng and Wei, 1983; Juang and Bellon, 1984; Richard et al., 1986).

4.2 Fanshuliao Formation

The Fanshuliao Formation, conformably overlying the Tuluanshan Formation with a slightly transitional contact, is dominated by fine-grained turbidites. Slump beds and slide blocks whose dimension ranges from less than a meter to hundreds of meters are very common (Chen, 1997b; Teng et al., 2002). Sedimentary features indicate that the Fanshuliao beds are mass-flow deposits laid down in a base-of-slope setting (Teng, 1980a, Teng et al., 2002). The Fanshuliao Formation may be regarded as an olistostrome as it is dominated by submarine slump deposits according to Teng et al. (2002). The Fanshuliao sandstones are characterized by abundant volcanic detritus and fossil fragments and quartzo-feldspathic grains (Teng, 1979). In the field, the presence of whitish calcareous sandstones allows clear identification of the Fanshuliao sequences. The age of the Fanshuliao Formation roughly spans the late

Miocene and early Pliocene (Chang, 1967; Chi et al., 1981; Wei and Cheng, 1982)

4.3 Lichi Formation

The Lichi Formation, exposed around the southwestern verge of the range, is composed of chaotic mudstones that contain numerous exotic blocks of various sizes and lithologies. The stratigraphic relationship between the Lichi Formation and other rock units is not clear, and both fault and conformable contacts have been suggested (Hsu, 1976; Page and Suppe, 1981; Barrier and Muller, 1984; Chang et al., 2000). The exotic blocks include ophiolitic rocks, a few andesites, and various kinds of sedimentary clasts. Both the mudstone matrix and enclosed blocks are often cut by penetrative shearing and display the disorganized features of a mélange (Hsu, 1976; Teng, 1981; Page and Suppe, 1981). Fossils indicative of Eocene to Pliocene age are found, in which Miocene fossils dominate (Chang, 1967, 1969; Huang, 1969; Chi, 1982). In terms of the fossil assemblage, Teng and Lo (1985) proposed that the Lichi deposits were accumulated continually from the late Oligocene to early Pliocene.

4.4 Paliwan Formation

The Paliwan Formation consists of various facies of turbidites that overlie both the Tuluanshan and Fanshuliao Formations with apparently coherent contacts. In general, conglomeratic facies dominates in the north, sandy facies in the middle, and shaly facies in the south (Teng, 1982). Pebbly mudstones and sandstones associated with contorted beds are widely distributed in the Paliwan sequences. Sub-metamorphic rock fragments, such as slate and metasandstone, dominate in the Paliwan deposits and serve as a lithological characteristic distinctive from the Fanshuliao sequences (Teng, 1979; 1982). The conglomeratic facies is also termed the “Shuilien Conglomerate” as a member in the Paliwan (Usami, 1939; Teng, 1982). The remaining sandy to shaly facies is included in the Taiyuan Member. The age of Paliwan is assigned to late Pliocene to early Pleistocene (Chang, 1967, 1968, 1969; Chang and Chen, 1970; Huang, 1969; Chi et al., 1981).

4.5 Pinanshan Conglomerate

The Pinanshan Conglomerate includes a number of molassic deposits disseminated in the Longitudinal Valley. The stratigraphic relationship between the Pinanshan rocks and other rock units is unknown on account of the lack of stratigraphic contacts. The only visible contact between the Pinanshan Conglomerate and the Lichi Formation is generally interpreted as a fault (Page and Suppe, 1981). The conglomerates exposed near Hualien are also termed the “Milun Conglomerate” (Usami, 1939). Compositionally all the Pinanshan strata are dominated by

metamorphic rock fragments such as marble, schist, gneiss, and amphibolite, with some slate and metasandstone. Most of the Pinansahn rocks are devoid of marine fossils except some reworked specimens, but indigenous nannofossils indicative of NN20 were found in the Milun Conglomerate (Chang, 1967, 1969; Chi et al., 1983). The age of the Pinanshan is believed to be middle to late Pleistocene (Chi et al., 1983; Teng, 1987).

4.6 Origin of the Lichi Melange

The Lichi Mélange is widely distributed along the southwestern flank of the Coastal Range, which is composed of chaotic mudstones intermixed with "exotic" blocks of various size and lithology. The most characteristic lithological feature of the Lichi Mélange lies in the presence of intensely sheared mudstones without distinctive stratification and the most common mesoscopic structure is the scaly foliation. The curviplanar surfaces of this penetrative scaly foliation are generally polished and bear aligned minerals and slickensides (Hsu, 1976; Teng, 1981; Chen, 1991, 1997; Chang et al., 2000). However, some layers of pebbly mudstones and coherent stratification have been locally reported (Chang, 1969; Liou, Suppe & Ernst, 1977; Page, 1978; Page & Suppe, 1981; Barrier & Muller, 1984). The blocks inside the mélange may reach kilometric size and are generally angular in shape. Most small blocks (decametric or smaller) are heavily sheared and polished, but many large blocks appear almost undeformed (Teng et al., 1988). In terms of lithology, the blocks considered as "exotic" belong to three main types; (1) ophiolitic rocks, including basic to ultrabasic rocks; (2) sedimentary rocks, including sandstones, sandstone/shale interbeds, shales, and limestones; and (3) andesitic rocks, including volcanic breccias, tuffs, and volcaniclastic turbidites (Hsu, 1976; Liou, Lan & Ernst, 1977; Page & Suppe, 1981).

Micropaleontological analyses demonstrated a chaotic mixing of fossils indicative of Miocene to Pliocene ages, and the definite biostratigraphic sequence is difficult to identify (Chang, 1967, 1969; Huang, 1969; Chi, 1982). Ho (1977) advocated that the Lichi Mélange was emplaced in Pleistocene time and thus assigned the Lichi Mélange to Plio-Pleistocene in age. Page & Suppe (1981), putting emphasis on the youngest age shown by the fossil assemblages, concluded that the Lichi Mélange was deposited in Late Pliocene time. Teng & Lo (1985) proposed a continued mixing from Oligocene to Late Pliocene time, based on consideration of various fossil ages inside the Lichi Mélange.

The estimation of the thickness of the Lichi Mélange is based on the log of a Chinese Petroleum Corporation well near Houtzeshan in the southernmost Coastal Range (Meng & Chiang, 1965). The well penetrated 1,056 m without reaching the base, which shows that the thickness of the Lichi Mélange, whether truly stratigraphic or

actually tectonic, is at least 1000 m. The well penetrated a number of slabs of basalt and other basic rocks embedded in the muddy matrix, demonstrating that they are exotics at depth as well as at the surface (Hsu, 1976). The contact between the Lichi Mélange and other rock units of the Coastal Range is observed to be mostly faulted (Hsu, 1976), but there is local interfingering with strata of the Takangkou Formation (Page & Suppe, 1981; Barrier & Muller, 1984; Chang et al., 2000 ; Chang et al., 2001). The best evidence for stratigraphic interfingering is cropped out in the area of Muken River, between the Lichi Mélange and the lower Takangkou flysch, which is Early Pliocene in age (NN14~NN15 nannoplankton zones, M. Lee, unpub. MS thesis, Taiwan Univ., 1984).

The origin of the Lichi Mélange has been the subject of much controversy. Two main hypotheses are illustrated in Fig. 2-2. Because of the intense scaly foliation and the existence of the exotic blocks, many geologists think that the Lichi Mélange is a “subduction complex” (Fig. 2-2a) formed by tectonic processes as the South China Sea oceanic crust was subducted (Biq, 1971, 1973; Karig, 1973; Teng, 1981; Hsu, 1988; Chen, 1991, 1997). But because of the occurrence of well bedded units in the mélange, as well as coherent turbidites, many other geologists considered the Lichi Mélange as an “olistostrome” (Hsu, 1956; Wang, 1976; Ernst, 1977; Ho, 1977, 1979; Liou, Suppe & Ernst, 1977; Liou & Ernst, 1979; Page & Suppe, 1981; Barrier & Muller, 1984) that developed between the outer arc and a forearc basin (Fig. 2-2b). According to the model of subduction complex origin, the Longitudinal Valley fault is a relic of the former subduction trench and was an active major structure before and during arc-continent collision (Fig. 2-2a). In contrast, in the olistostrome model (Fig. 2-2b), the Longitudinal Valley represents a part of forearc basin, which was a relatively quiet region before the arc-continent collision.

The significance of the mélange is crucial in any reconstruction of the geological history of eastern Taiwan and especially of the Longitudinal Valley, the so-called "suture" between the Eurasian continental margin and the Luzon arc. The Lichi Mélange in the Coastal Range is therefore a key to the interpretation of the evolution of Taiwan orogenic belt. Recent study by Chang et al. (2001) suggested that the Lichi Mélange results mainly from the shearing of lower forearc basin sequences, rather than from a subduction complex or a mere olistostrome (Fig. 4-3).

4.7 Accreted volcanic islands of the Coastal Range

The oldest unit in the Coastal Range is the Tuluanshan Formation composed of dikes, andesitic flow, andesitic breccia and tuff, representing an island arc setting (Wang, 1976). The Tuluanshan Formation can be genetically and paleogeographically divided into three groups: the Yuehmei pyroclastics in the north, the Chimei igneous

complex at the middle; and the Chengkuangao igneous complex at the south (Fig. 4-3).

The Yuehmei pyroclastics represents part of a remnant collapsed volcanic island, which subsided in the arc collapse/subduction zone north of 20°N. The Chingshui fault scarp at 24°-24°30'N probably marks the boundary of the arc collapse. However, the Chimei and Chengkuangao volcanic islands are well preserved in the middle and southern part of the Coastal Range. These independent volcanic islands can be identified by their characteristic location, age, geochemistry and the overlying reef limestone (Huang et al., 1995).

The Chimei igneous complex in the north has been uplifted and deeply eroded to reveal its lateral and vertical changes in texture and lithology. A schematic north-south cross-section (Fig. 4-5) shows a nearly symmetrical facies change from a near-vent volcanic core facies (diabase intrusive, dikes and lava flow), through a proximal-medial volcaniclastics facies (predominant angular andesitic breccia deposited near the eruption center), to a distal volcaniclastic facies (fine tuff far away from the eruption center) (Song, 1990; Song & Lo, 2002). Such facies relationship strongly suggests that the Chimei igneous complex was an independent and unique offshore volcanic island prior to its accretion to the Asian continent.

The Chengkuangao igneous complex is not well exposed. However, the individuality of Chimei and Chengkuangao "volcanic islands" are supported by their different radiometric dates (Chimei: 17-5 Ma; Chengkuangao: 5-4 Ma; Yang et al., 1988; Chen et al., 1990; Lo and Onstott, 1993), distinct Nd isotope values (Chimei: +6.3 per mil; Chengkuangao: +2.1 to +4.5 per mil; Chen et al., 1990) and La/Yb ratio (Chimei: >6; Chengkuangao: <6; Lo,1989).

In addition, limestones deposited on Tuluanshan Formation of the Chimei and Chengkuangao igneous complexes are different. The Kangkou Limestion on the Chimei igneous complex (found from Shihtiping to Changyuan) (Figs. 4-4; 4-6) is 20-25 m thick, and composed of coral fragments, rhodoliths, mollusks and larger foraminifers of *Lepidocyclina* and planktic foraminifers (Fig. 4-6).

In contrast, the Tungho Limestone exposed on the Chengkuangao igneous complex from Wushihpi to Tungho (Fig. 4-6) is 30-50 m thick and dominated by fragments of coral, rhodolith and larger foraminifers of *Gypsina* and *Amphistegina* but devoid of *Lepidocyclina*. Furthermore, the age of Kangkou Limestone is about 5.2-5.1 Ma (Zone N18, Huang et al., 1988), considerably older than the Tungho Limestone (2.9 Ma, Zone N21, Chang, 1967, 1969; Huang and Yuan, 1994). Their differences in age, lithology and fossil forms suggest that the Kangkou and Tungho Limestones were deposited separately on two distinct eruption centers, namely, the Neogene Chimei and Chengkuangao volcanic islands.

The two offshore late Pleistocene Lutao and Lanhsu volcanic islands serve as good modern analogues of the two onland volcanic complexes. The modern islands, although separated by a 3000 m-deep Lutao-Lanhsu Trough (part of a deformed forearc basin), are both fringed by latest Pleistocene-Holocene coral reefs (Lin, 1967; Huang, 1993). A similar paleogeographic configuration ,i.e., two volcanic islands each fringed by reef limestones and separated by a deep trough, presumably also existed in late Neogene, when the Chimei and Chengkuangao volcanic islands were capped by Kangkou and Tungho Limestones, respectively, and separated by the Loho forearc sequence (Huang, 1992, 1993). Huang et al. (2006) proposed a sequential development of the accreted volcanic arc that is shown in Fig. 4-7.

4.8 Sequential developments of volcanoes and volcaniclastics

The Neogene volcanic rocks in Eastern Taiwan's Coastal Range (CR) extend for approximately 140 km between the cities of Hualien and Taitung. Eruption of these rocks began in a submarine environment because of eastward subduction approximately 17 to 35 Ma ago (Taylor and Hayes, 1983), with volcanic edifices rising from deep to shallow water, and even to the subaerial surface (Fig. 4-8) (Song and Lo, 1987, 1988, 2002). Volcanism ceased, and the volcanoes deformed during arc-continent collision, and accreted onto the Asian continental margin to form the main body of Eastern Taiwan's CR.

The volcanoes in Eastern Taiwan's CR were formed using the same processes as the volcanic islands found offshore, between Taiwan and Luzon Island. These volcanoes were produced by the subduction of the South China Sea lithosphere beneath the Philippine Sea Plate. Volcanic rocks erupted and formed seamounts that grew from the deep sea to become subaerial volcanoes, ending with a collision and subsequent accretion into the CR. The study (Lai et al., 2013) identified four volcanic bodies in the accreted arc on land, which shows varying levels of erosion from deep-seated centres to the outer skin of volcanoes. These variations suggest that the four volcanoes were uplifted in different periods. Erosion increased from the south to the north, with Yuemei being at least partially subducted beneath the Eurasian Plate.

In summary, the evidence for the volcanic territories of four volcanoes in the northern Luzon Arc was identified by the distribution of volcanic facies associations and isotopic rock ratios. A model for the evolution of volcanoes in an oceanic island arc setting, from their creation to extinction, can be established (Fig. 4-9). In the first stage, magmas were produced by subduction and erupted to form seamounts rising from the deep sea to the subaerial surface. In the northern Luzon Arc, active volcanoes such as Batan and Babuyun represent this stage (Richard et al., 1986; Defant et al., 1989, 1990; Yang et al., 1996). In the second stage, the volcanoes

moved with the Philippine Sea Plate but ceased their eruptions as arc-continent collision commenced. The volcanic islands located offshore of Eastern Taiwan, Lutao and Lanyu, are at this stage. The volcanic extinction dates progressively younger from the north to the south (Yang et al., 1996). The last recorded eruption near Lanyu's ocean floor was in 1858 A.D. (Chen and Shen, 2005), and may be the boundary between active and extinct volcanoes. In the third stage, the volcanic islands were uplifted and accreted to the CR by an oblique arc-continent collision and suffered varying degrees of erosion and crustal exposure during different periods on land. That the Chimei, Chengkuangao and Tuluanshan volcanoes show the near-vent facies association with distinctive internal lithofacies is powerful evidence of the gradual uplift and erosional processes in this stage. Finally, in the last stage, a volcano is being subducted beneath the Eurasian Plate at the northernmost end of the Luzon Arc along with the western Philippine Sea Plate. The cryptic volcanic centre of Yuemei may have been subducted underneath the Eurasian Plate, documenting this stage.

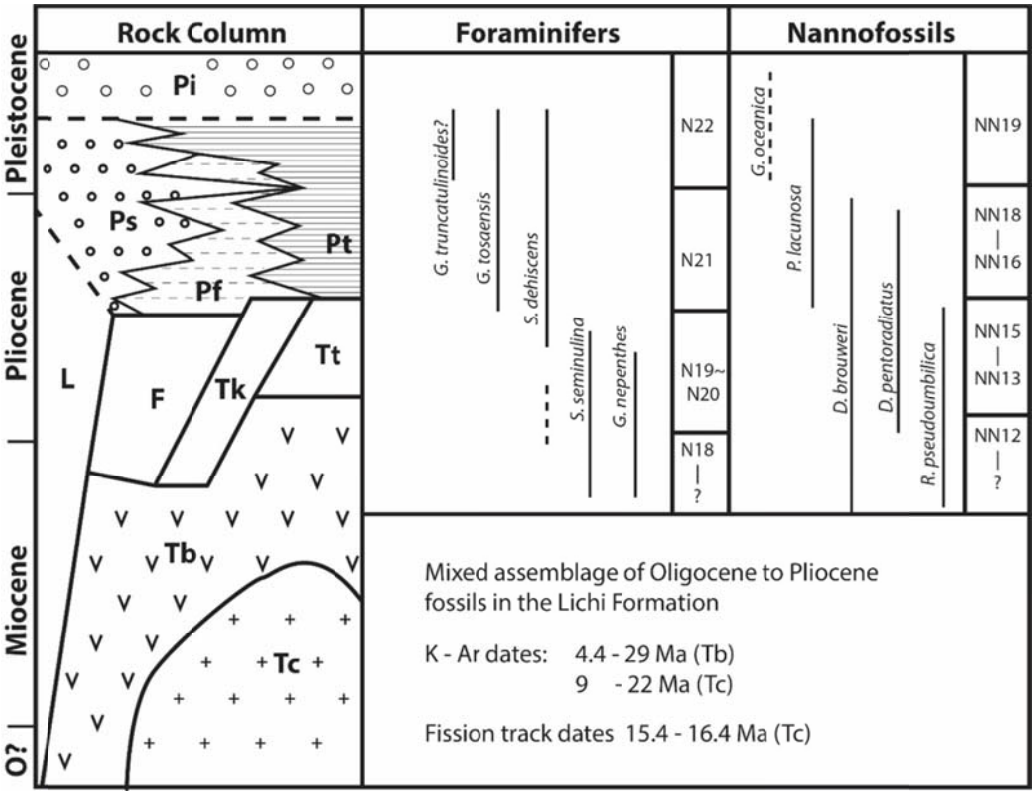

Fig. 4-1. Biostratigraphy and chronostratigraphic units of the Coastal Range. (Redrawn from Teng et al., 1988). L: Lichi Formation; Tx: Tuluanshan Formation (Tk: Kangkou Limestone; Tt: Shihtiping Tuff; Tb: Shihmen Breccia; Tc: Chimei Andesite); Px: Paliwan Formation (Ps: Shuilien Conglomerate; Pt: Taiyuan Member; Pt: Futien Member); F: Fanshuliao Formation; Pi: Pinanshan Conglomerates.

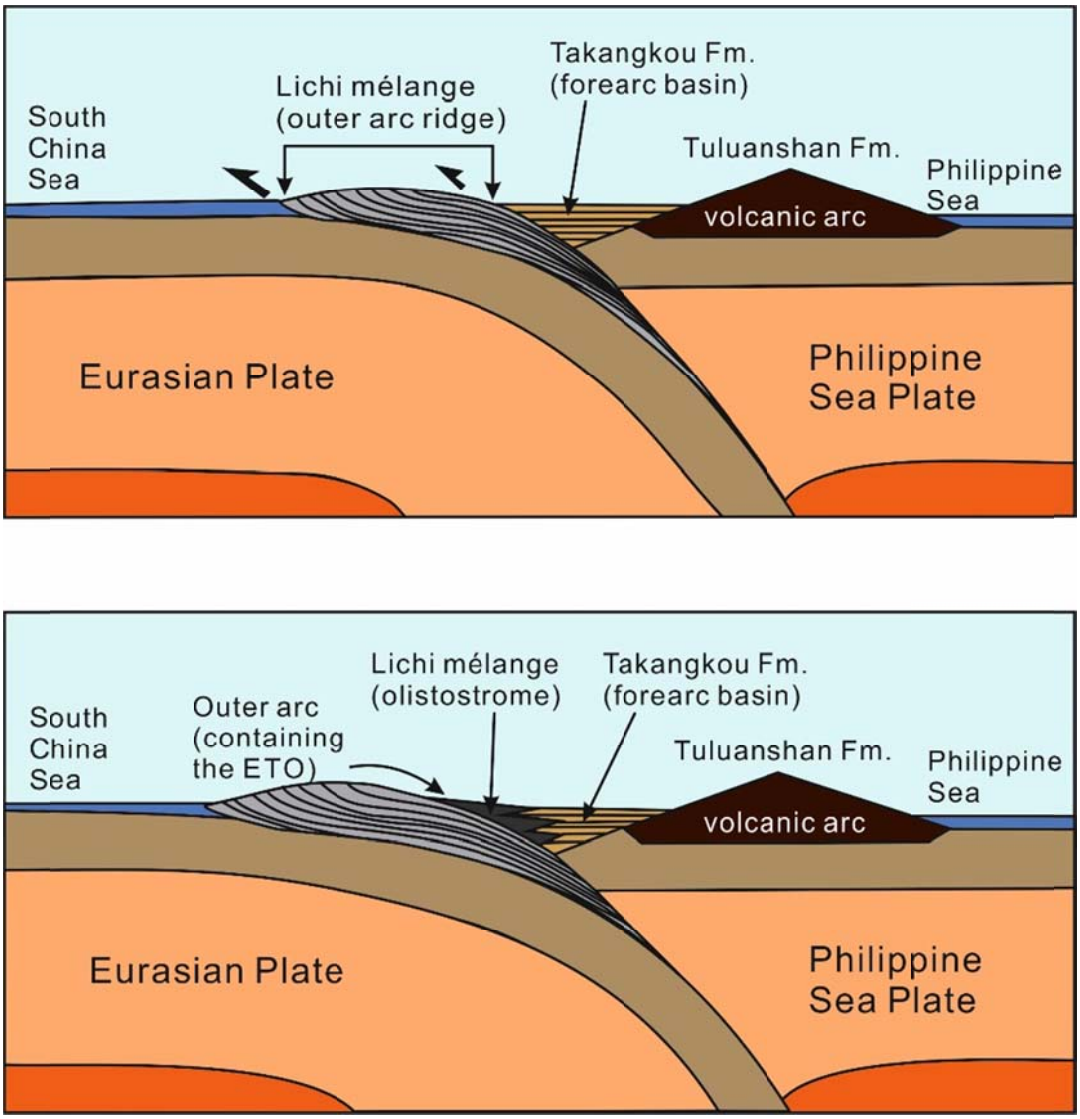

Fig. 4-2. Comparison of the origin of the Lichi Mélange (from Chang et al., 2001). (a) Hypothesis of "subduction complex" origin. In this model, the Lichi Mélange is the relic of the subduction complex, composed of scrapped oceanic sediments and upper crust material of the South China Sea oceanic crust ; the Longitudinal Valley is the proto-Manila trench. (b) Hypothesis of "olistostrome" origin. In this model, the Lichi Mélange is an olistostrome deposited in the eastern forearc basin, its source being the eastern flank of the outer nonvolcanic arc (accretionary prism).

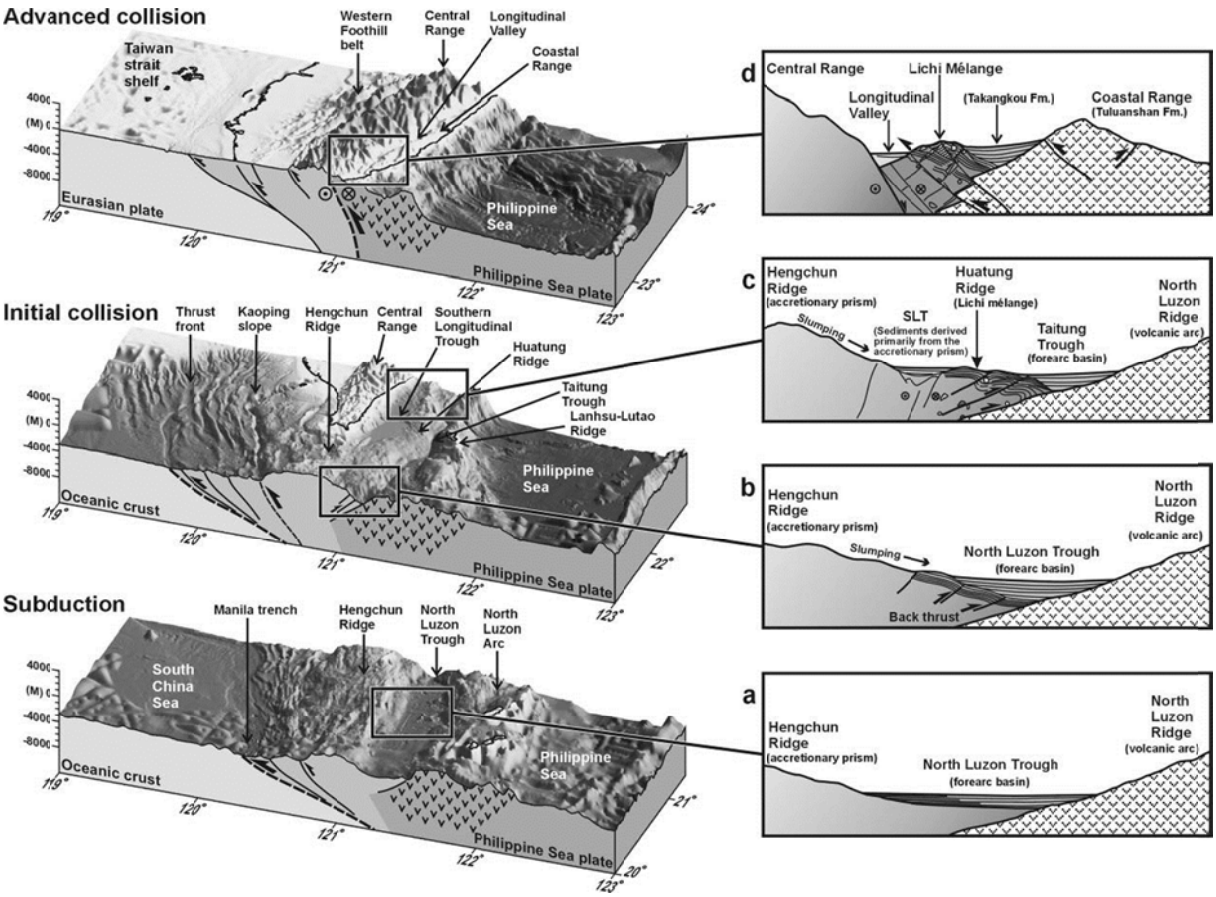

Fig. 4-3. Tectonic evolution of the Taiwan island and the Lichi Mélange (Chang et al., 2001). The block-diagrams show the general morphology and main crustal structure of the subduction, the initial collision and the advanced collision stage of Taiwan area. a, b, c, d, cross-sections summarizing the evolution of the North Luzon Ridge (volcanic arc) and Hengchun Ridge (former accretionary prism) into the Coastal Range and Central Range of Taiwan (respectively), with evolution of intermediate basins and ridges.

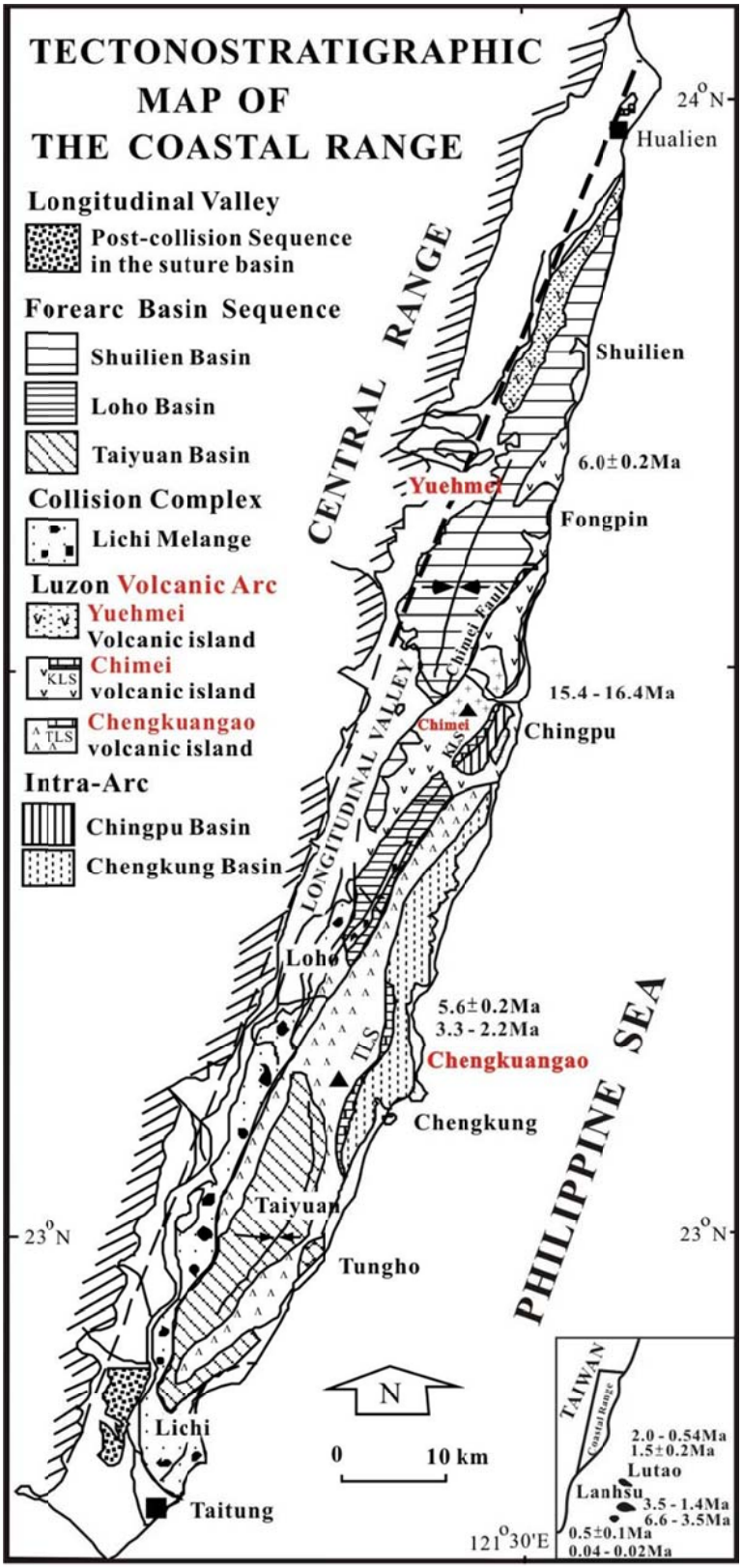

Fig. 4-4. Tectonostratigraphic map of the Coastal Range, showing three accreted volcanic islands, three remnant forearc basins, two intra-arc basins, and the Lichi Mélange (Huang et al., 2006). Age data on the volcanic sequences compiled from Chen et al. (1990), Yang et al. (1988), and Lo et al. (1994).

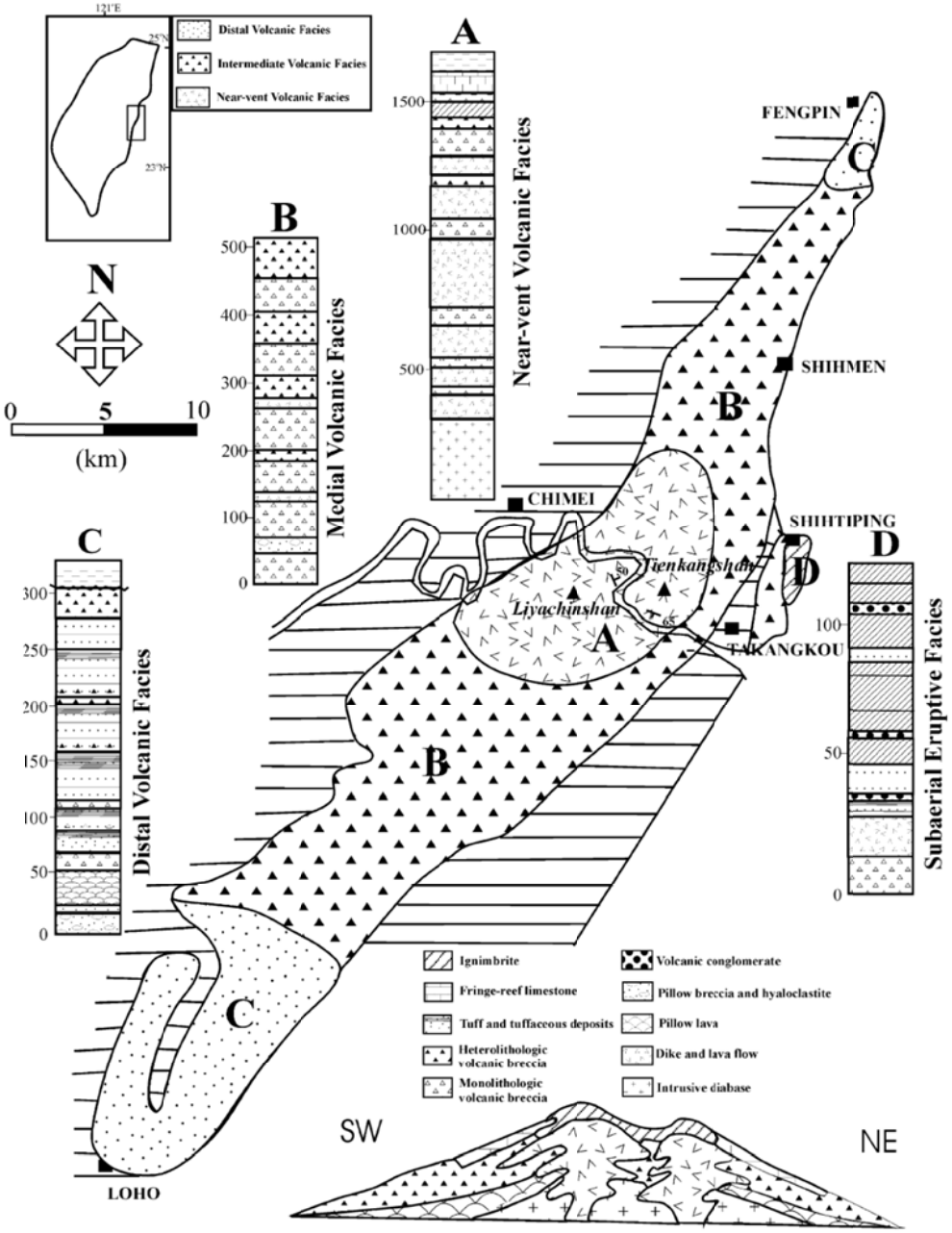

Fig. 4-5. Lithofacies of the proposed Miocene Chimei volcanic island and Chinpu intra-arc basin. Also shown are schematic east-west and north-south cross sections of the Chimei volcanic island (Song & Lo, 2002).

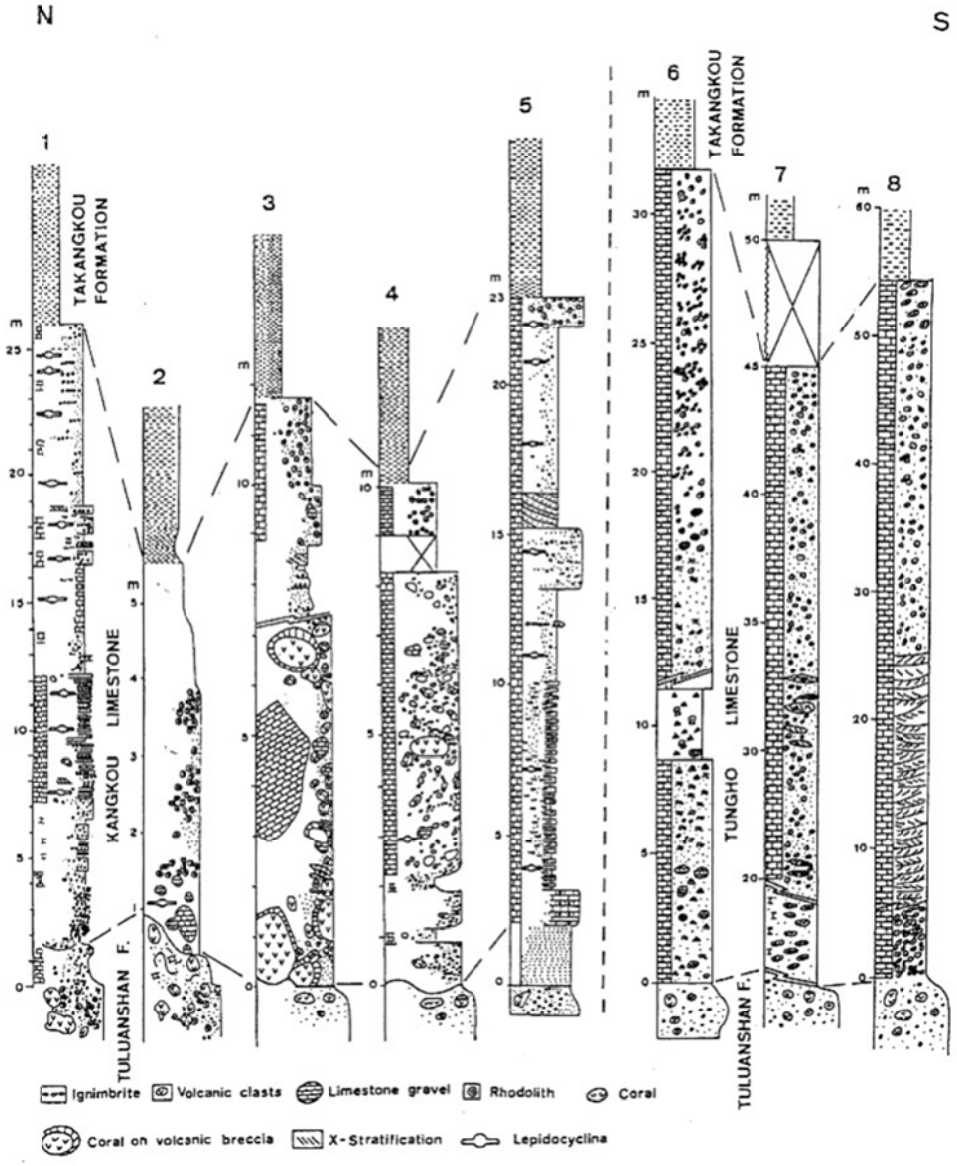

Fig. 4-6. Lithologic columns of the Kangkou Limestone (left) and Tungho Limestone (right) in the Coastal Range (after Huang et a l., 1995).

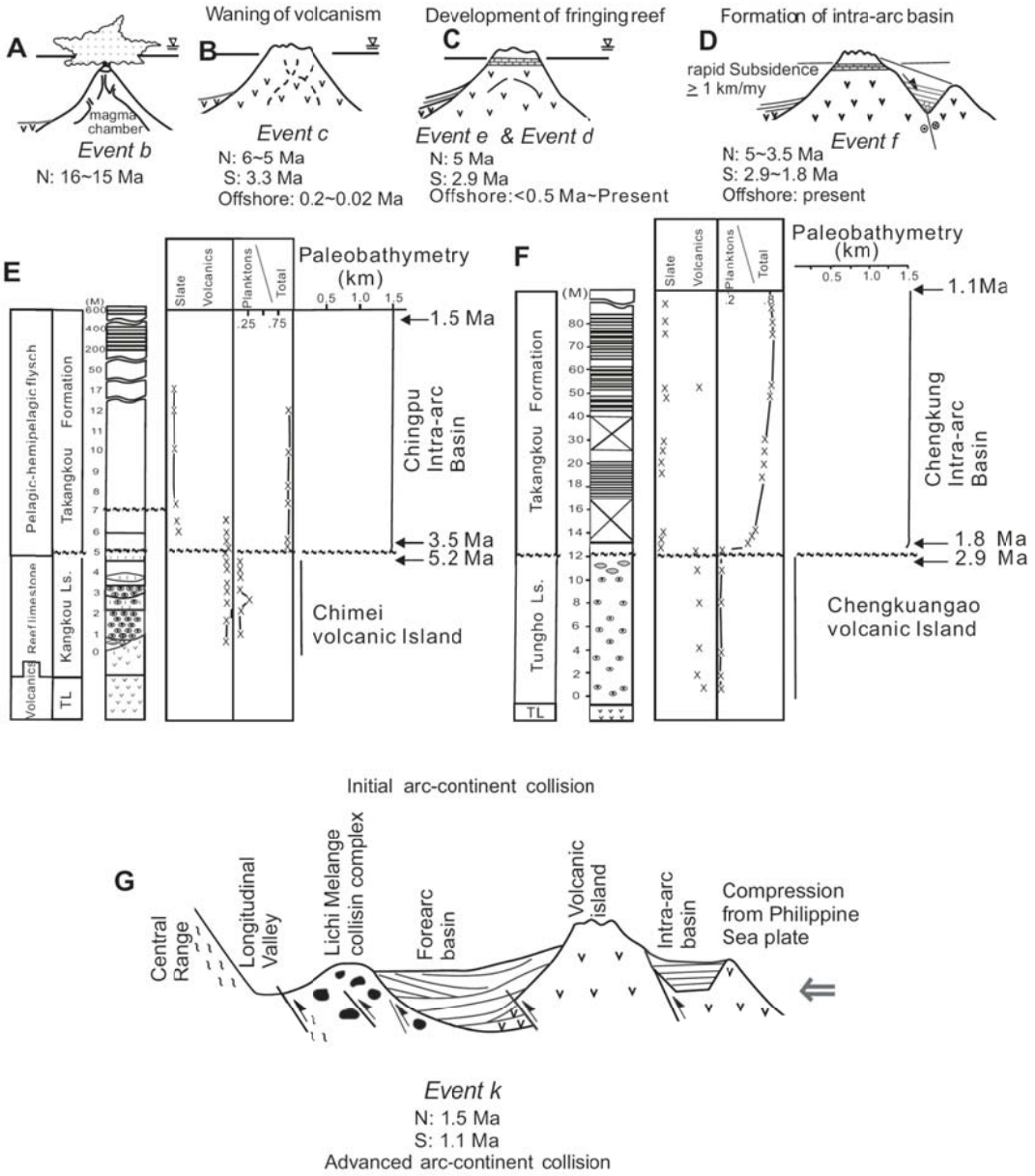

Fig. 4-7. Stratigraphic sequence recording the (A) active volcanism (event a) during intra-oceanic subduction, (B) waning of volcanism (event c), (C) sedimentation of forearc basin (event e) and development of fringing reef (event d), (D) arc subsidence (event f) and infilling of intra-arc basin with deep-marine flysch overlying shallow-marine fringing limestone in (E) Chingpu intra-arc basin and (F) Chengkung intra-arc basin during initial arc-continent collision, to finally (G) westward-landward thrusting and accreting of the arc-forearc onto the exposed underthrust Eurasian continent (eastern Central Range) (event k) along the collision suture of Longitudinal Valley during advanced arc-continent collision. From Huang et al. (2006). N—north; S—south.

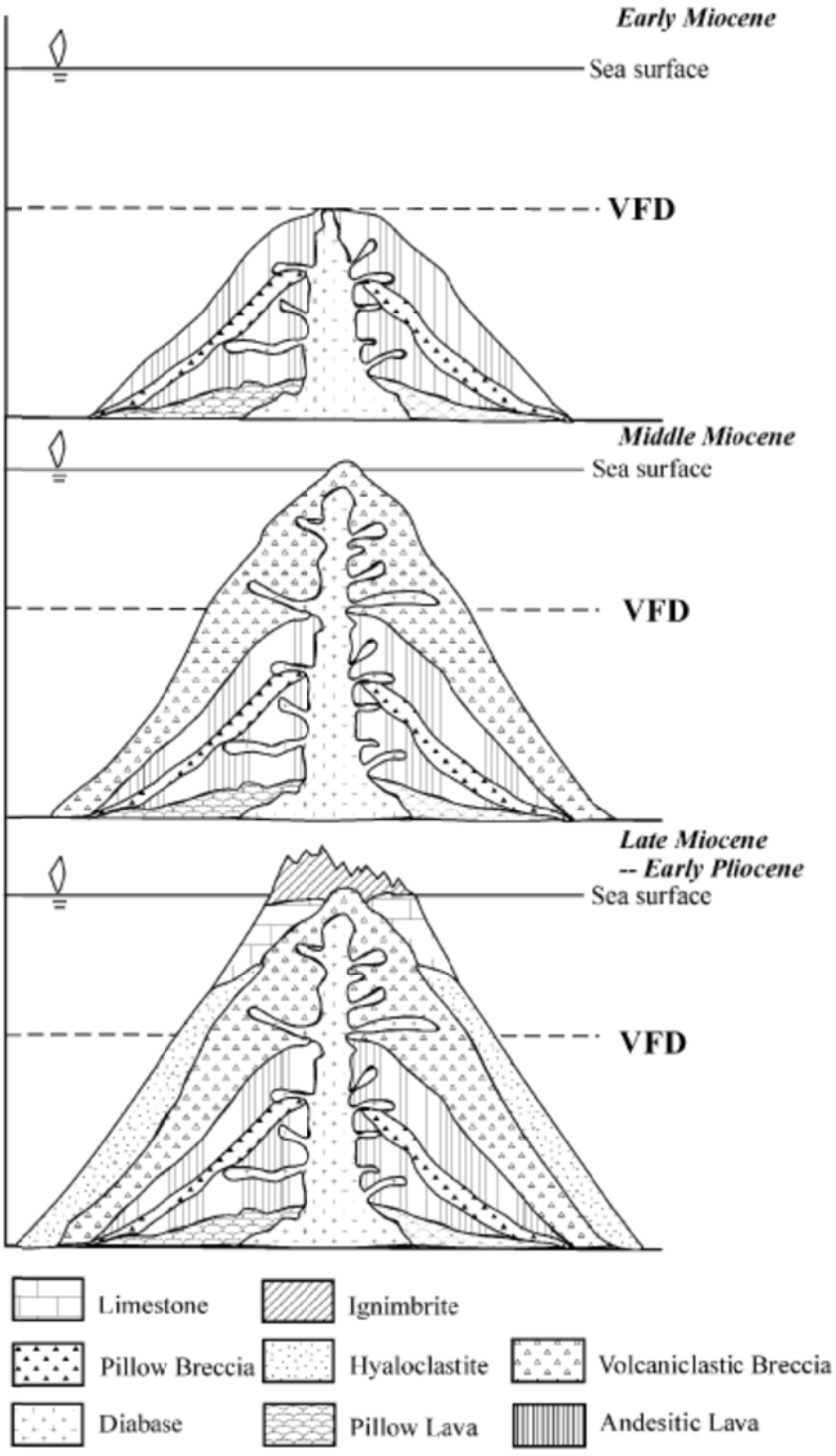

Fig. 4-8. Model for the evolution of volcanism of the central Coastal Range, eastern Taiwan. VFD: volatile fragmentation depth, generally shallower than 500 m. The volcano commenced eruption in deep-water environment in early Miocene, then evolved to shallow marine in middle Miocene, finally erupting in subaerial conditions in late Miocene to early Pliocene.

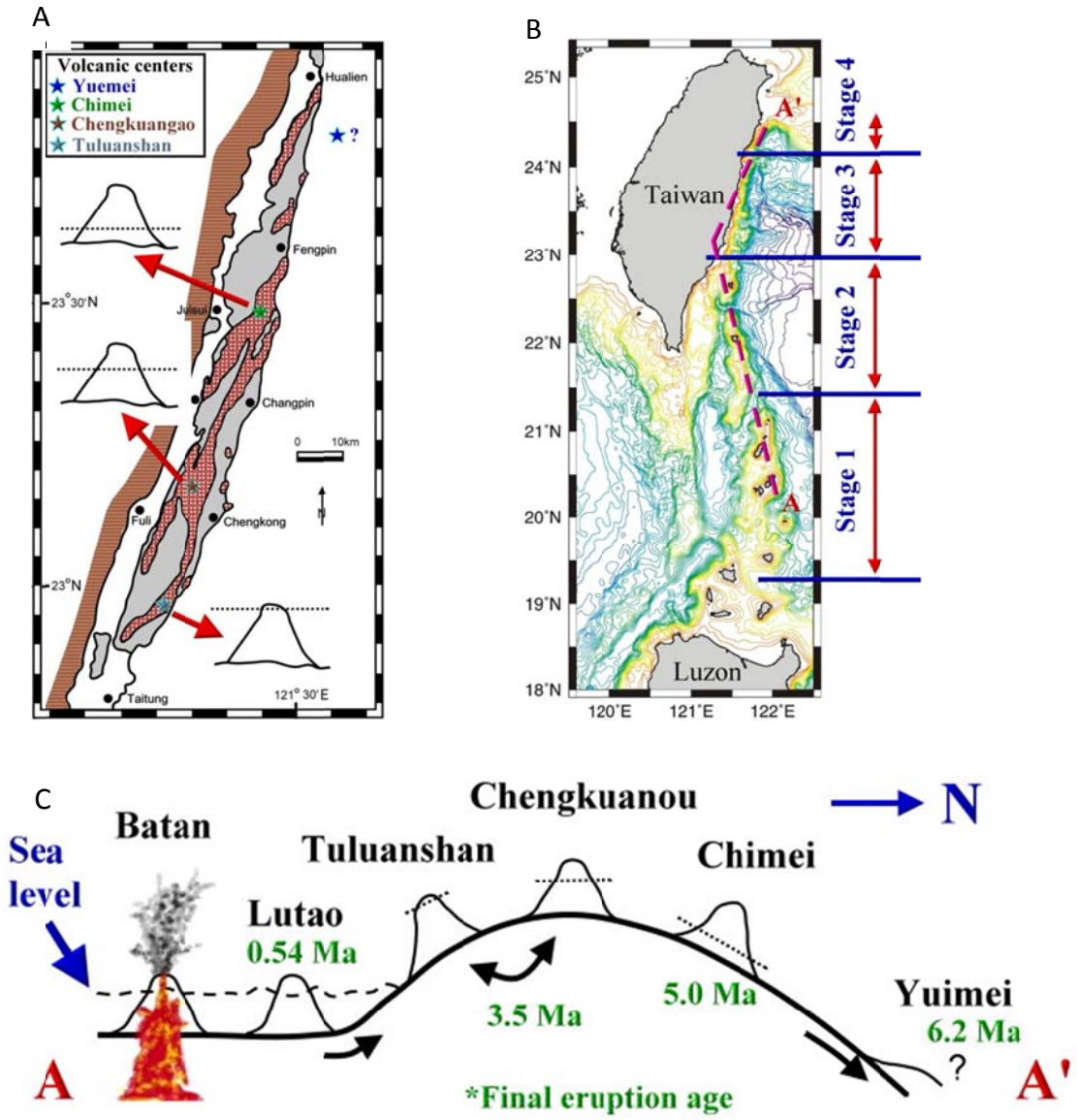

Fig. 4-9. (A) Different degrees of erosion inside the volcano edifices of the Chimei, Chengkuangao and Tuluanshan volcanoes; (B and C) the volcanoes' evolution model in four stages. Volcanic islands are still active in the first stage, while they moved and ceased in the second stage. They uplifted, accreted and suffered different degrees of erosion to form a part of Taiwan in the third stage. Finally, in the last stage a volcano is subducted beneath the Eurasian Plate. Section A - A' shows the volcanoes' detailed evolution from birth to extinction in 7B. The final eruption ages were from Yang et al. (1992) and Song and Lo (2002).

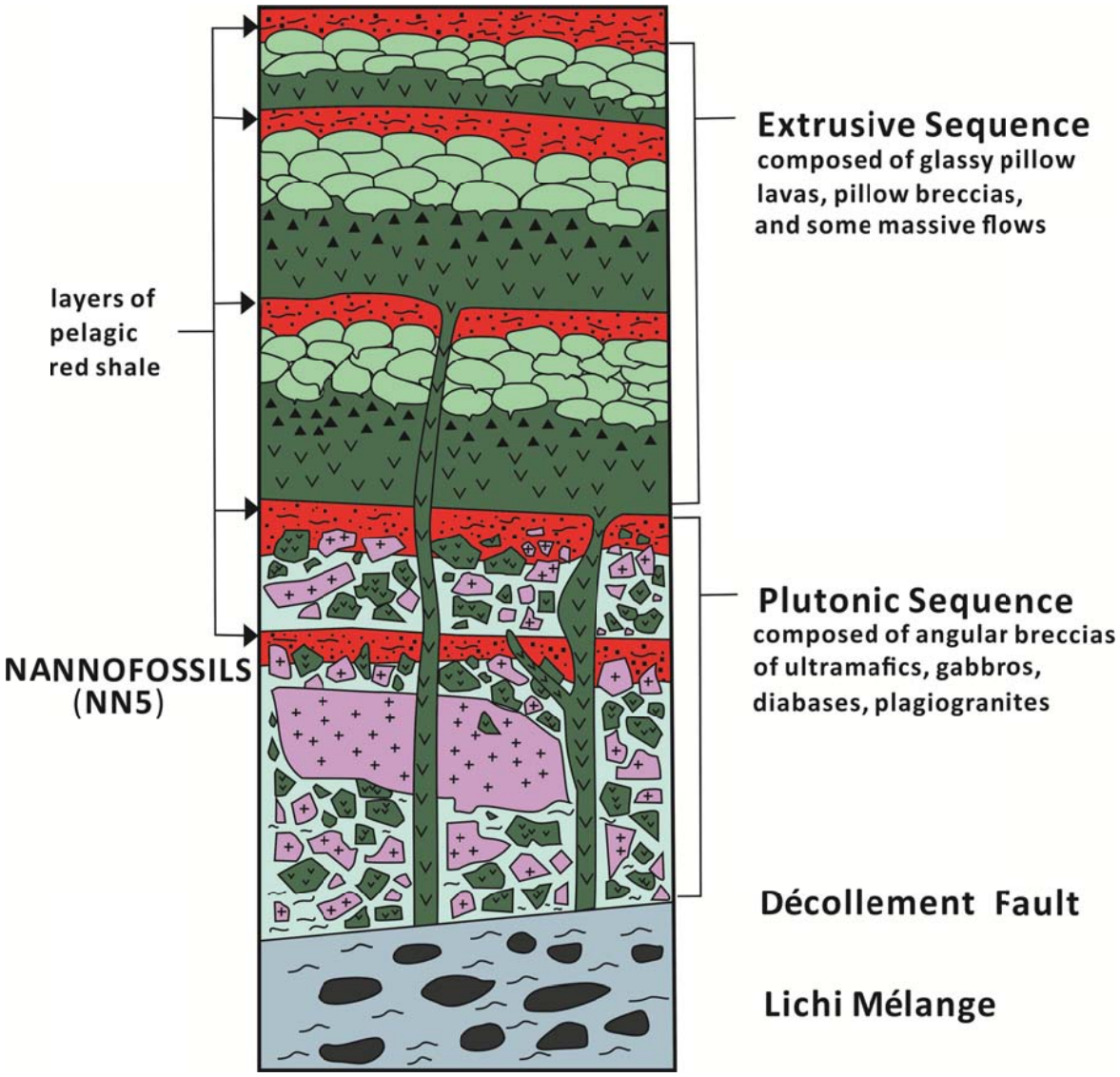

Figure 4-10. Schematic stratigraphic section of the ETO (after Liou et al. 1977).

5. Field-Trip Stops

Day 1: Late Paleozoic and Mesozoic metamorphic rocks in the Central Range along the Central Cross-Island Highway

Tectonic Models for Mesozoic evolution

The Mesozoic tectonic evolution of the basement has been debated for years due to the limited number of constraints. Two types of tectonic model have been proposed: a subduction type (Yui et al., 1988; Fig. 5-6A) and a collision type (Wang-Lee and Wang, 1987; Fig. 1-6B).

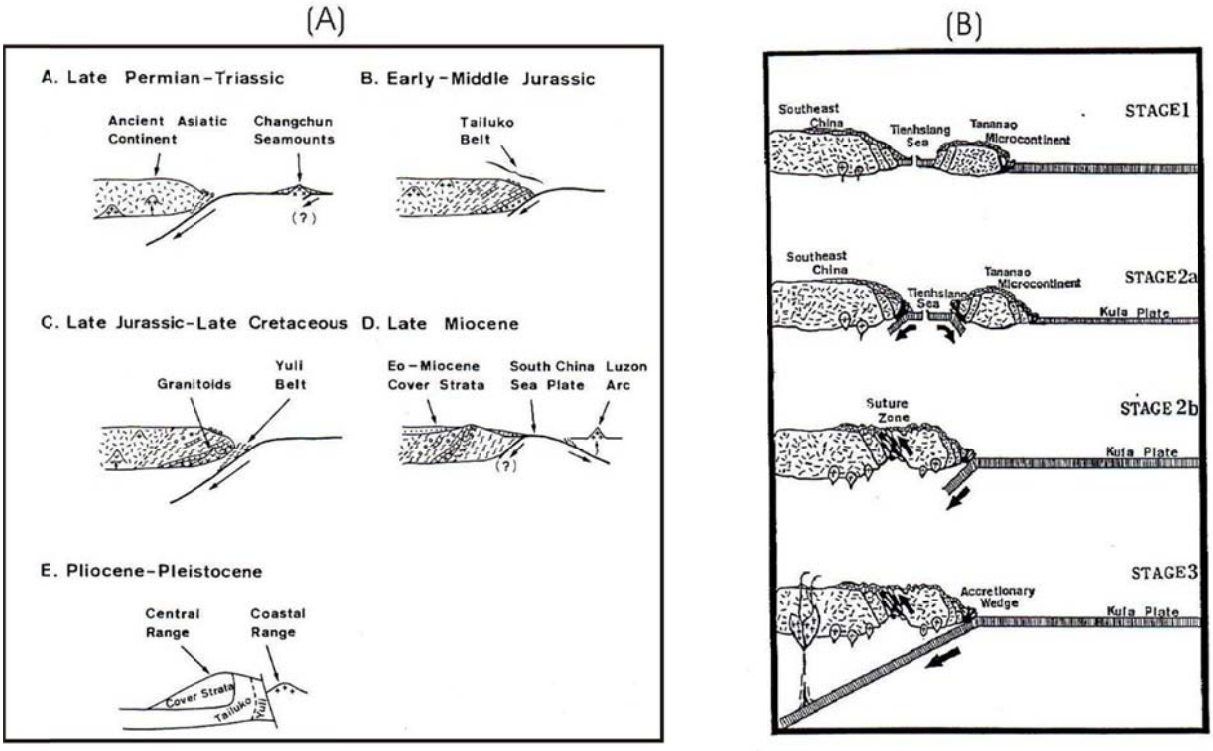

Fig. 5-1. Two proposed tectonic models for the evolution of the Tananao metamorphic complex. (A) subduction model of Yui et al.(1988) and (B) collision model of Wang-Lee and Wang (1987).

Cenozoic Exhumation Model

The basement complex was covered by young sediments during the Cenozoic rifting. Due to the arc-continental collision (or the accretion of the Luzon arc) since the Plio-Pleistocene, the basement rock began to be exhumed. Several mechanisms have been postulated to account for the exhumation (mountain building) process (Fig. 5-7): a critical wedge model (e.g., Davis et al., 1983), a discrete sequential thrusting model (Hwang and Wang, 1993), a lateral extrusion and normal faulting model (Byrne, 1995; Crespi et al., 1996), a lithospheric collision (Wu et al., 1997) and a subduction and extrusion model (Lin et al., 1998).

(A) Davis et al. (1983)

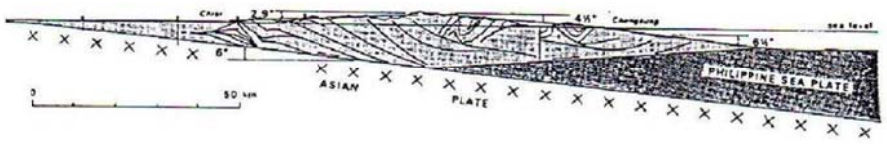

(B) Hwang and Wang (1993)

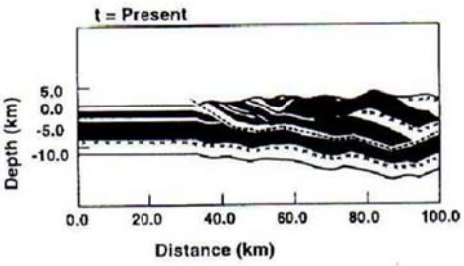

(C) Crespi et al. (1996)

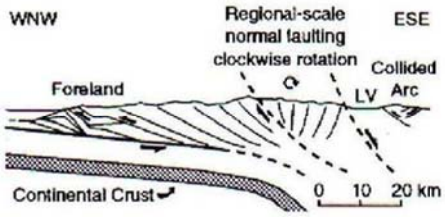

(D) Byrne (1995)

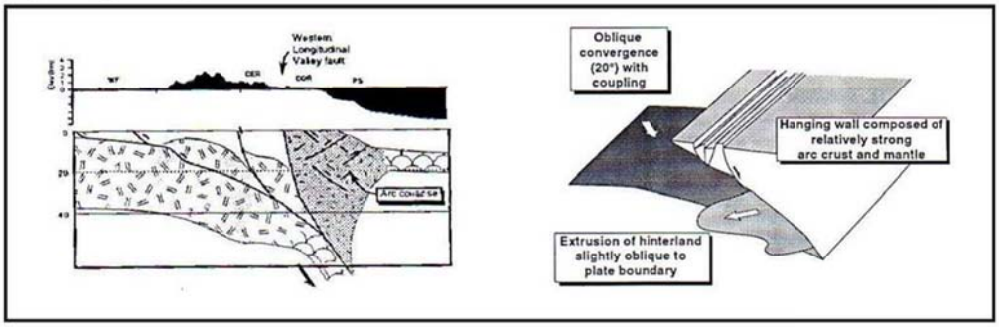

(E) Wu et al. (1997)

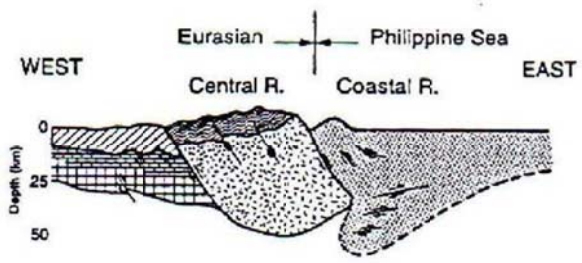

(F) Lin et al. (1998)

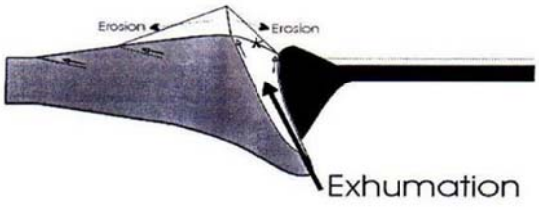

Fig. 5-2. Models for the regional tectonics of the Taiwan mountain belts.

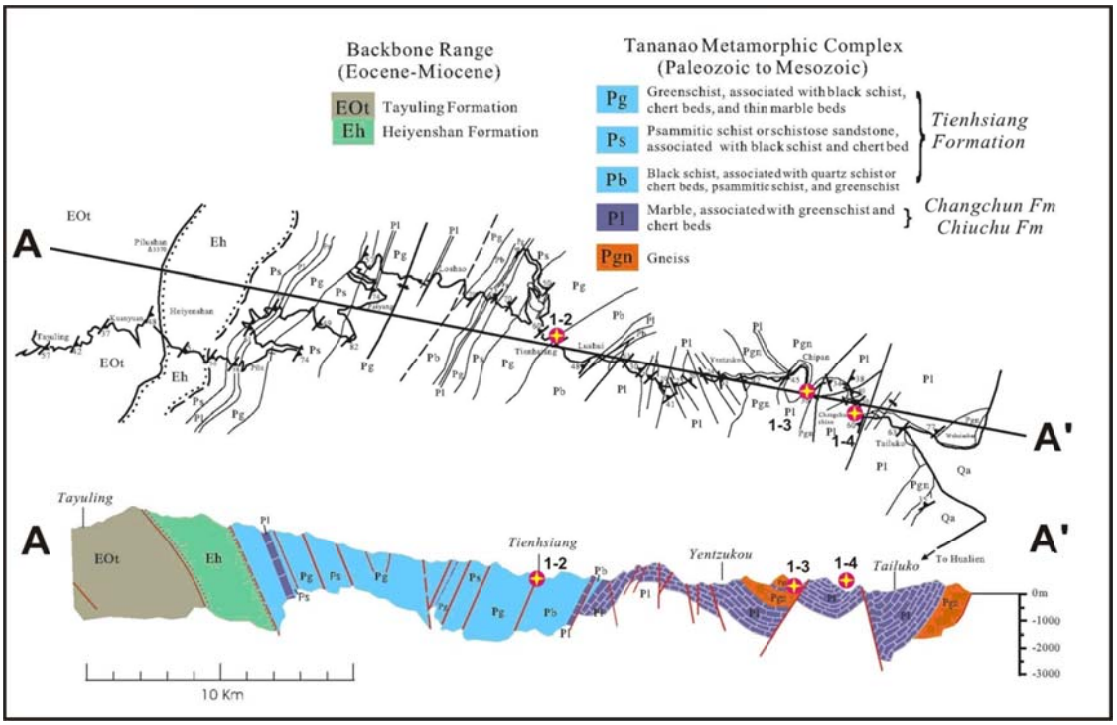

Fig. 5-3. Geological traverse map of the eastern Central Range along the Central Cross-Island Highway (after Chen, 1979). Trip stops are shown as red circles with numbers.

Stop 1-1 Schists of Late Paleozoic and Mesozoic metamorphic rocks: Chaoyang harbor

Chaoyang harbor is located in the eastern end of Ilan country road no. 56 at Nanao coast. The outcrop behind the northern harbor bank mainly exposes various kinds of schists, including quartz-mica schist, graphite schist and chlorite schist. Features of highly sheared zones are commonly found in those schists (Fig. 5-4.). Thus, some researchers even consider them as mylonite. Based on the finding of fossil *fusulinid*, the rock is inferred to be Permian in age, locally up to Mesozoic.

Figure 5-4. Augen structure and ϕ-type porphyroclasts in ductile shear zones.

Stop 1-2: Schists of Mesozoic metamorphosed mélange: Tienhsiang (170 km), Central Cross-Island Highway

Tien-hsiang, a famous recreation area within the National Taroko park, is located on a terrace at the intersection of Da-sa river and Takili river. Below the Chih-hui bridge, an outcrop of metamorphosed melange can be found. The metamorphosed exotic blocks here including marble, metasandstone, quartzite, metachert, and green schist are highly deformed and randomly distributed within strongly foliated quartz-mica schists. The quartz-mica schists could represent the metamorphosed mudstone and shale which usually constitute the main part of melange. Please note that the quartz-mica schists have suffered polyphase deformation and foldings which results in multi-schistosity developed within the rocks.

Fig. 5-5. Stop 1-2. Black schist with highly deformed white marble layers indicating the nature of a Mesozoic mélange.

1-3: Contact between marble and gneiss: Chipan, Baisha Bridge, Central Cross-Island Highway

A contact zone between granite and marble is observed near Baisha Bridge. Rocks near the granitic intrusions may contain amphibolite facies minerals. The P-T conditions as revealed by the Chipan granitic gneiss and Kainangang foliated gneiss indicate three episodes of metamorphism – the first stage at 2 kb and ca. 500°C, the second at 5-7 kb and 650-700°C, and the third stage at 4 kb and 450°C. Jahn et al. (1986) and Lan et al. (1996).

Fig. 5-6. Stop 1-3. (left) Fault contact between white marble on the lower right and granitic gneiss on the upper left. (right) A close up view of the contact zone.

1-4: Changchun Shrine (Eternal Spring Shrine)

The Changchun Shine (Eternal Spring Shrine) recognizes the personnel died during the construction of Central Cross-Island Highway. Rivers adjacent to the Changchun Shrine become the scattering falls, and the Highway Bureau named it after "Chanchun Falls" which is now the significant landmark on Central Cross-Island Highway.

Fig. 5-7. Changchun Shrine.

Days 2 & 3: Coastal Range

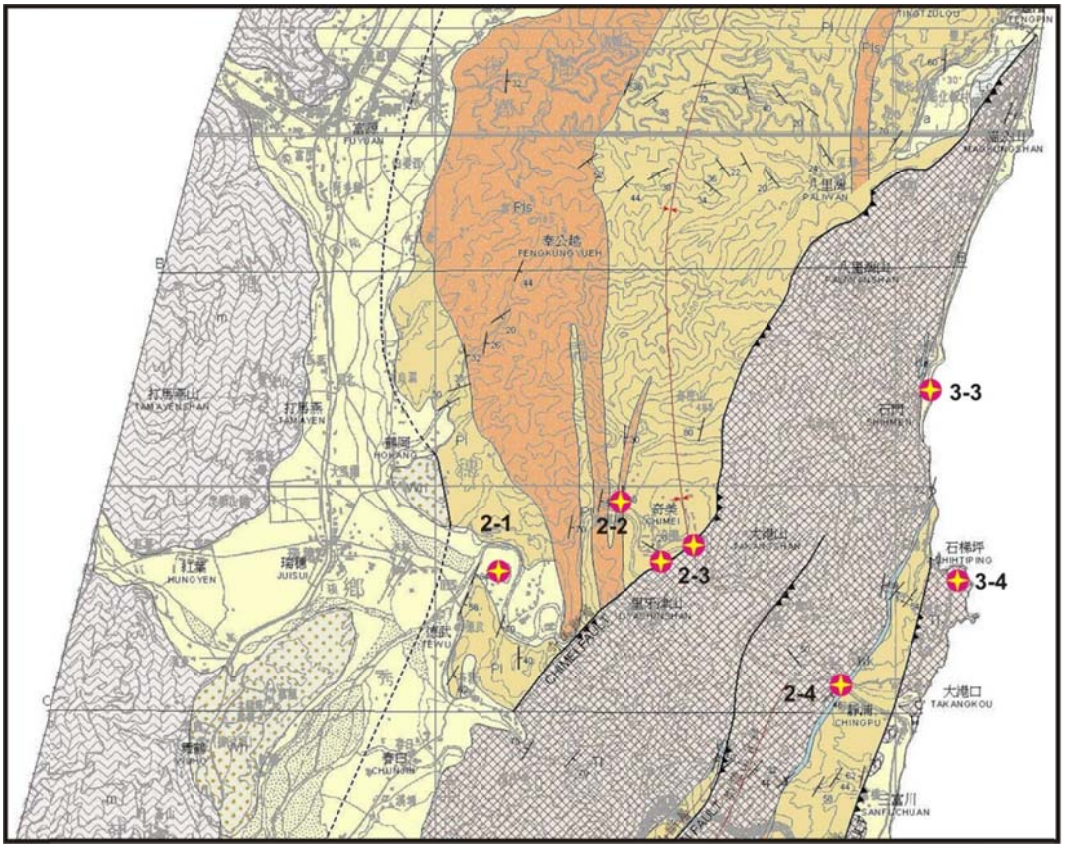

Fig. 5-8. Geological map of the north-central Coastal Range (from Wang and Chen, 1993) showing stop locations of 2-1, 2-2, 2-3, 2-4, 3-3 and 3-4.

2-1: Derwu River terraces

The Hsiu-ku-luan River, draining the eastern slope of the Central Range, is the only river that crosses the Coastal Range. The river is believed to be an anticedient one, existing long before the emergence of the Coastal Range, and has been capable of incising and checking the uplift of the range since its emergence. The river shows a magnificent meander pattern in the west where it cuts through soft mudstone (the Takangkou Formation). Progressive meander migration and cut-off, associated with downward incision, left flights of river terraces up to 150 m in height. These terraces are mostly of strath type, with capping fluvial sediments generally 5-7 m in thickness. The river valley narrows downstream of these terraces (east of the Chimei Fault) where hard volcanic rock (the Tuluanshan Formation) is exposed.

The multiple-step strath terraces west of the Chimei Fault have recently been studied by Shyu et al. (2005). Dating of the multiple terraces indicates that the bedrock incision rates are in the range 1-2 cm/yr, and may decrease to the east (Fig. 5-9).

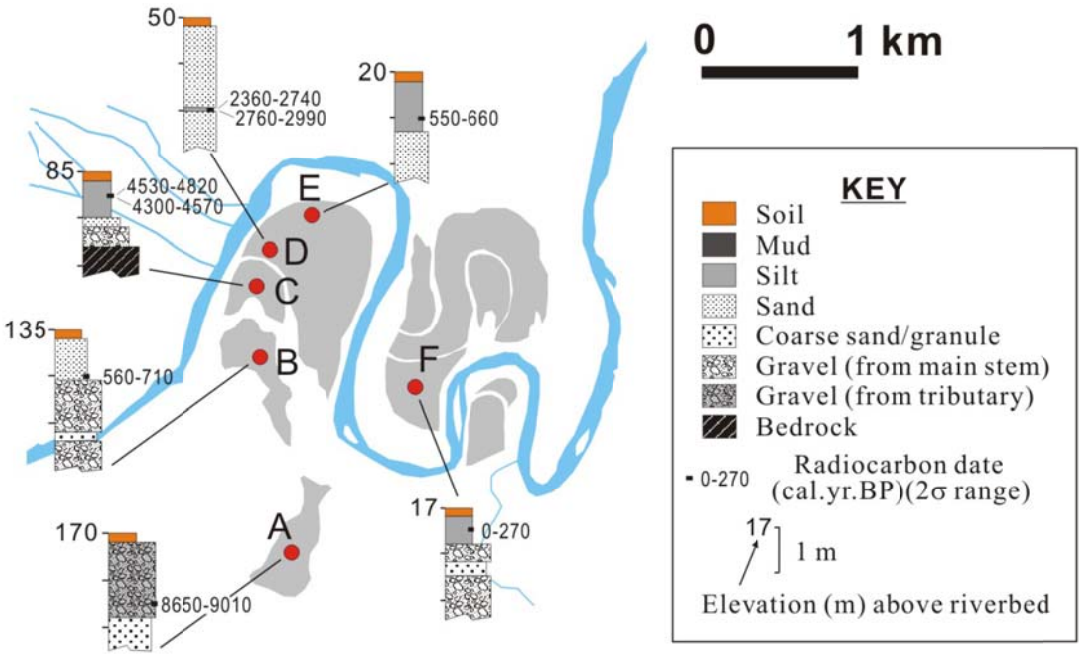

Fig. 5-9. Stop 2-1. Derwu River terraces (gray-shaded areas) with radiocarbon dates (from Shyu et al., 2005). Note that the ages of terraces A to F decrease northward toward the modern river course.

2-2: Channelized forearc conglomerates: 7.5 km, Chimei Bridge, Paliwan Formation

At this stop, conglomerates deposited in submarine canyons in the forearc basin are observed.

Fig. 5-10. Stop 2-2. Resedimented conglomerates by mass flows.

2-3: The Chimei Fault: Chimei Fault bringing Miocene arc massif (Tuluanshan Formation) on top of Pleistocene forearc turbidites (Paliwan Formation)

At this stop (see Fig. 5-8 for location), two major stratigraphic units: the Tuluanshan Formation and the Paliwan Formation of the Coastal Range are well exposed along the river bank of the Hsiukuluan River. The Miocene Tuluanshan Formation is the lowest stratigraphic unit of the Coastal Range and is composed of agglomerate, tuff, and tuffaceous sediments related to the andesitic arc volcanism. The Pleistocene Paliwan Formation is mainly consists of shale, sandstone, and conglomerate of turbiditic deposits. The Chimei Fault thrusts the Miocene andesite of the Tuluanshan Formation over the Pleistocene turbidites of the Paliwan Formation with a fault plane dips 70 degree towards southeast. Intense deformations with numerous minor reverse faults, folds, and slickensides could be observed in the sandstone and shale beds adjacent to the fault plane. Iron oxides, and sulphur deposits in both Formations in the fault zone exhibit hydrothermal activity.

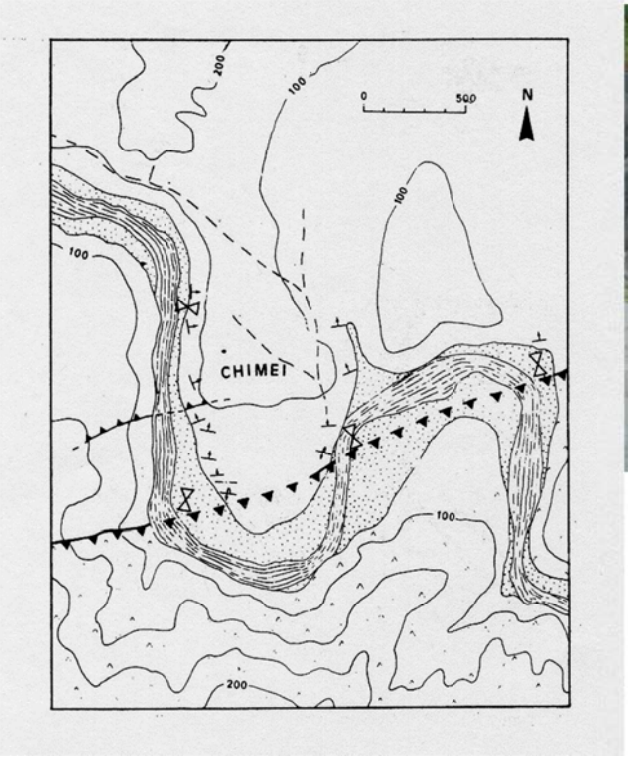

Fig. 5-11. (Left) Map showing the Chimei Fault thrusts the Miocene andesites of the Tuluanshan Formation over the Pleistocene turbidites of the Paliwan Formation (after Barrier and Chu, 1984). (Right) Outcrop photo showing the major tectonic contact between the pyroclastic rocks of the Miocene Tuluanshan Formation (light-colored igneous rocks on the right) and the turbidite of the Pleistocene Paliwan Formation (dark-gray shale on the left) along the Hsiukuluan River bank. The former was over-thrusted onto the later with vergence towards WNW. The shear zone with crenulation cleavages is well exhibited (see the left figure for outcrop location).

2-4: Agglomerates and Kangkou limestone: Changhung Bridge, Hsiukuluan River


都巒山層


港口石灰岩

Fig. 5-12. Stop 2-4.

3-1: Miocene pyroclastics: Lingting, northern tip of the Coastal Range

At Lingting in the northern tip of the Coastal Range (see Fig. 5-13 for stop location) it shows continuous coastal exposure of the volcano-pyroclastic rocks of the Miocene Tuluanshan Formation.

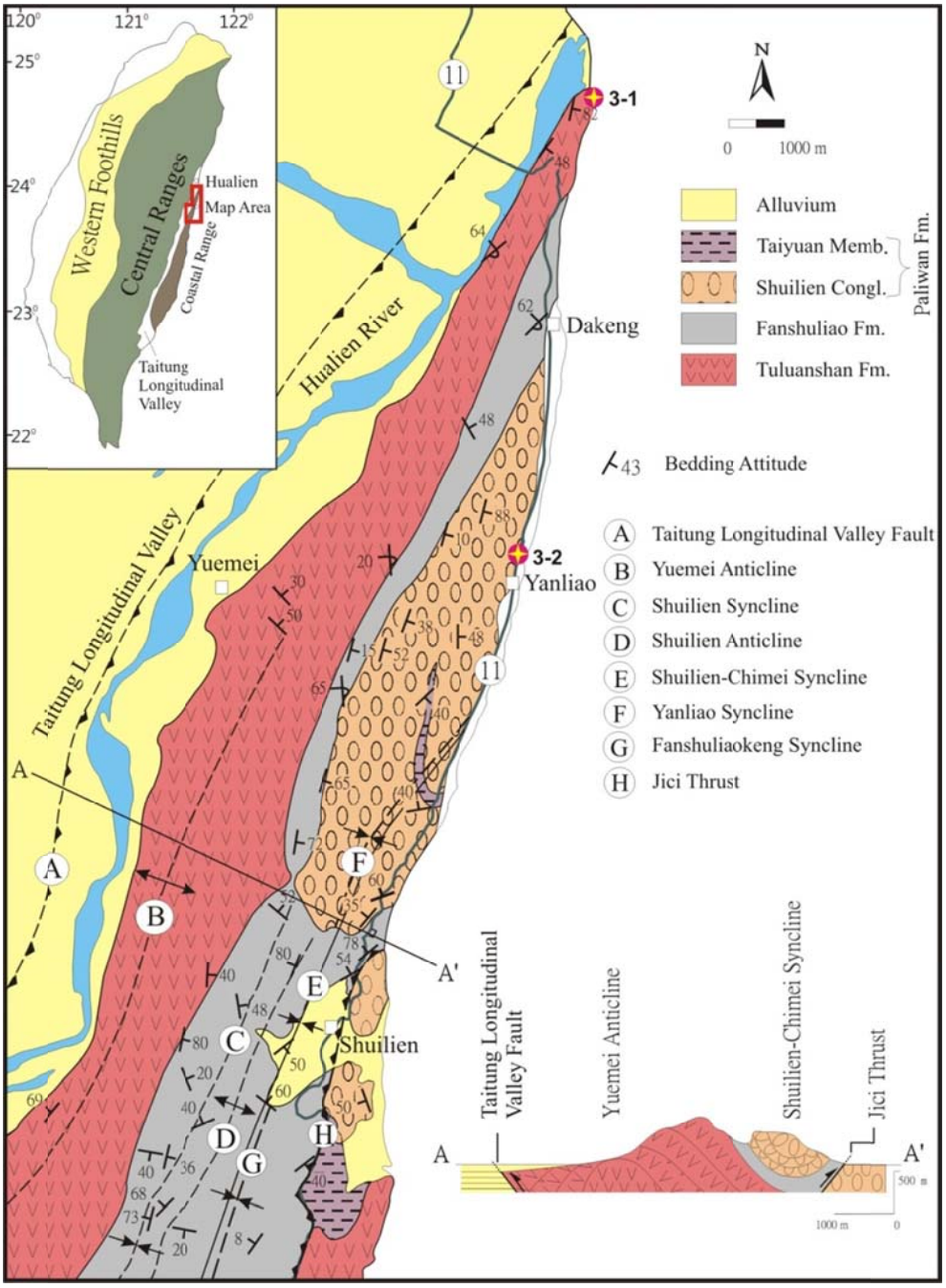

Fig. 5-13. Geological map of the northern Coastal Range (after Teng et al, 2002). A cross section (AA') is shown in the lower right corner featuring that the east-vergent Jici thrust brings Fanshuliao Formation on top of Paliwan Formation. Trip stops are shown as circles with numbers.

Fig. 5-14. Agglomerates of the Miocene Tuluanshan Formation exposed at the northern tip of the Coastal Range near Lingting.

3-2: Bridge no. 10 of Coastal Highway at Yanliao: Forearc coarse-grained turbidites

In the No. 10 bridge outcrop, Shuilien Conglomerates reaches 1km in thickness (Figs. 5-15). Thick-bedded conglomerate layers (belonging to the Pleistocene Shuilien Conglomerate Member of the Paliwan Formation) are well exposed along the river gorge wall.

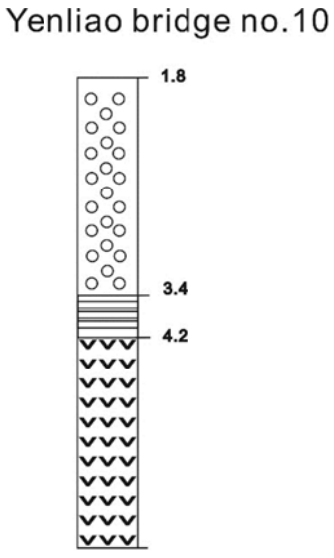

Fig. 5-15. (left) Thick conglomerates of the Shuilien Conglomerates exposed at stop 3-2. (right) Stratigraphic column at Stop 3-2. Age of the Fanshuliao Formation is around 3.4~4.2 Ma in this section, and the Shuilian conglomerates (of the Paliwan Formation) is approximately 1.8~3.4 Ma in age.

Stop 3-3: Shihmen: Shihmen Volcanic Breccia

Shihmen is located at the central Coastal Range, about 5 km north of the river mouth of Hsiukulanchi. Outcrop exposed in this location is characterized by the presence of monolithologic and polylithologic blocks with huge boulders, which named as “Shihmen Volcanic Breccia”. Monolithologic breccias may have been deposited directly from volcanic activity, while the polylithologic breccias may be derived from lahar or epiclastic processes.

The monothologic breccia is clast-supported or matrix-supported with poorly- to well-sorted tuffs as matrix, consisting of angular to subangular blocks with cooling prismatic fractures. These blocks vary from black to gray, and range from 5 to 50 cm in diameter. Plagioclase and pyroxene predominate in the phenocrysts. Massive breccias with a little matrix may have formed through dome collapse pyroclastic flow deposits.

Polylithologic breccias are widely exposed interbedded with monolithologic breccias in the Coastal Range. They often form massive, matrix- to clast-supported breccias with various types of blocks containing a mixture of gray, black, green, and red0. The subangular and subrounded blocks range from 5 to 100 cm in diameter with a columnar-jointed huge boulder, named as megablock in this location. Most of these breccias are thick but poorly bedded, or are partially interbedded with monolithologic breccias, ignimbrites, or tuffs. Epiclastic blocks, such as peperites, limestones, and ignimbrites, are also found in these breccias in the outcrops. According to the lithologic variety of breccias and epiclastic detritus, the polylithologic breccias blocks were eroded from older deposits of volcanic edifices. Reddish blocks, which resulted from thermal oxidation in subaerial environments, are contained at the top of this sequence.

The presence of megablock, brecciated devris and polylithologic blocks in the Shihtiping suggest that they were the volcanic debris avalanche deposits generated by the slumping of volcanic edifice. This debris avalanche may run from the southwest to the northeast of Shihmen as inferred from the decrease of the block sizes and block/matrix ratio in this direction. The location of avalanche within volcanic edifice or the flow direction of volcanic debris avalanche deposit often show a preferred orientation normal to the dominant direction of maximum horizontal compression, which is often displayed by orientation of dike swarm. The preferred orientation of the dike swarm in the Chimei area, a potential volcanic center in central Coastal Range, is northwestern and is normal to the flow direction of Shihmen volcanic debris avalanche deposits (Fig. 5-16). It, thus, is possible that the Chimei area is the most potential source for the Shihmen volcanic breccias.

The area also is geomorphically interesting for its gate-like sea cave cutting into

the volcanic rock. On the wall of this cave, an assemblage of barnacles, oysters, calcareous algae, and other intertidal shells occurs as a horizontal band up to 1.2 m in width (Fig. 5-17). The barnacles and oysters are generally concentrated in the upper portion of this fossil band and their lower boundary may roughly define the former mean sea level, which is ~5.2 m above the modern level. This fossil band is believed to have been stranded (and killed) during coseismic uplift. An intertidal shell in this band has been dated ~0.9 ka cal BP. The same dates (with their uncertainties significantly overlapped) also are revealed from other 3 sites on the coast (Hsieh and Rau, 2009). Imagine how big the earthquake, and its associated uplift, was ~0.9 ka ago to cause the mass mortality of intertidal organisms on the coast.

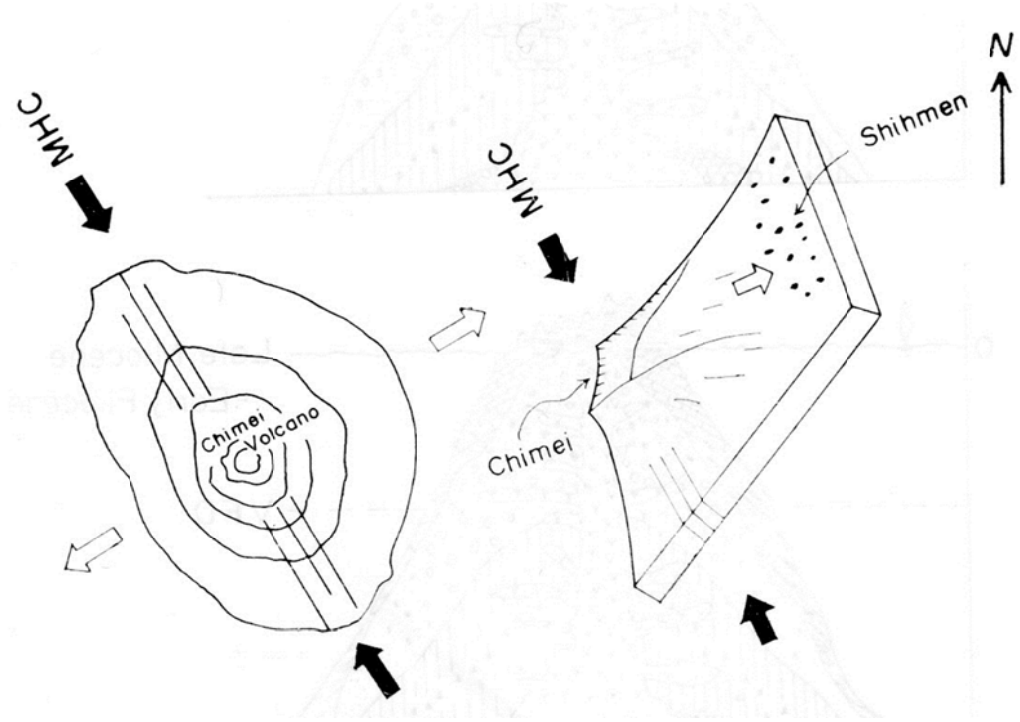

Fig. 5-16. Sketch map illustrating the emplacement of dikes in a direction parallel to the maximum horizontal compression (MHC), and showing the collapse of volcanic cone to produce the debris avalanche in a direction normal to the MHC.

Fig. 5-17. Shihmen Volcanic Breccia. A view of a horizontal band of intertidal communities, including barnacles, oysters, calcareous algae, and shells, affixed on the wall of a sea cave at Shihmen, north part of the Hua-tung Coast. Dotted lines approximate the upper and lower bounds of this fossil band. An intertidal shell in this band has been dated ~0.9 ka cal BP.

Stop 3-4: Shihtiping: White tuff of a topmost volcanic arc

The Shihtipuing is located at the central Coastal Range, about 3 km north to the mouth of Hsiukulanchi. Outcrop exposed in this location is characterized by the presence of lava flows, white ignimbrites, agglomerates with plastic deformation, tuffs and tuffaceous sandstones and conglomerates from lower to upper sections, which is named as “Shihtiping White Tuff”. It is about 100 meters in thickness and overlies the poorly columnar-jointed lavas of the Shihmen volcanic breccias (Fig. 5-18). Deposition of the Shihtiping White Tuff is later than late Miocene as indicated by the fossil age of the sediments at its base.

Both glass-rich and crystal-rich tuffs have been identified. They are the products of ash-fall, surge and pyroclastic flows. The ash-fall tuffs are thinly-bedded with fine-grained glasses and crystals in alternations and are well-sorted. The volcanic surge deposits, the base surges, are represented by the coarse-grained tuffs and lapillistones with massive, planar and dune-like sedimentary structures. It is

associated with ignimbrites containing juventile fragments, ranging from vesiculated to non-vesiculated cognate lithic clasts and ashes, and crystals.

The ignimbrites are pyroclastic flows with highly pumiceous and vesiculated glassy materials. About 36 meters in thickness occurred in Shihtiping are predominantly composed of white vesiculated glassy shards and pumices with eutaxitic texture. Except “standard sequence”, they also include massive lapillistones, and lenticular lithic breccias. Many sedimentary structures such as cross bedding, parallel lamination, normal and reserve graded beddings, impacted sag blocks, plastic deformations and erosion surface can be observed in the outcrops. Optical and scanning electron microscopic studies show that they are highly vesiculated and slightly welded.

White volcanic bombs are andesitic to dacitic, and consist of plastic, welded, and impacted structures in the outcrops. These deformed structures show that the pyroclastic flows were still high in temperature during transportation and deposition. This evidence suggests that these pyroclastic flows erupted and were deposited in a subaerial environment (Song and Lo, 1988). In some sections, peperite formed inside the white volcanic bombs because of the hot flow mingling with water or wet unconsolidated sediments. White volcanic bombs and pumice contain abundant vesicles with various shapes because of subaerial explosions. Lithic fragments in the ignimbrites are blackish, greenish, and reddish, and subangular to angular. The essential mineral constituents of the Shihtiping White Tuff are plagioclase, hornblende, hypersthenes, augite and magnetite listed in decreasing amount. The phenocrysts or crystal fragments are less than 50 percent, and the matrix is mainly glassy. Xenolithes of pyroxenite and hornblende gabbro can also be found in the Shihtiping.

Deformation bands, one kind of tabular structures, pervade in the Shihtiping where N14°E-trending syncline crops out (Fig. 5-20). The bands are commonly exposed as cluster zones and can be traced easily because they are commonly protruding on the ground surface (Fig. 5-21). The cluster zones range from 0.1 to 15 cm in width, up to 10 m in length and from 1 to 20 cm in total separation. Two sets of conjugate deformation bands with orientations of ENE and NW are widely distributed while those with orientations of NS and WE are locally found (Figs. 5-20 and 5-22). The dip angles of all sets range from 50° to 90°. The porosities of host rock and deformation band are, respectively, 16.3% and 5.0% calculated from image analysis of thin sections. Through permeability test, conductivities in deformation bands of two samples are 0.22 and 0.52 md, respectively, which reduce 2 to 3 orders. Minerals in the deformation bands usually contain plagioclase, hornblende and augite as in host rock but grains in the bands are relatively smaller and without

fracturing. It suggests that deformation bands in Shihtiping were formed by compaction, shearing and cataclasis. They can be classified as compactional shear and cataclastic bands in terms of kinematics and mechanism, respectively. They reflected the regional paleostress but were not genetically associated with any structure.

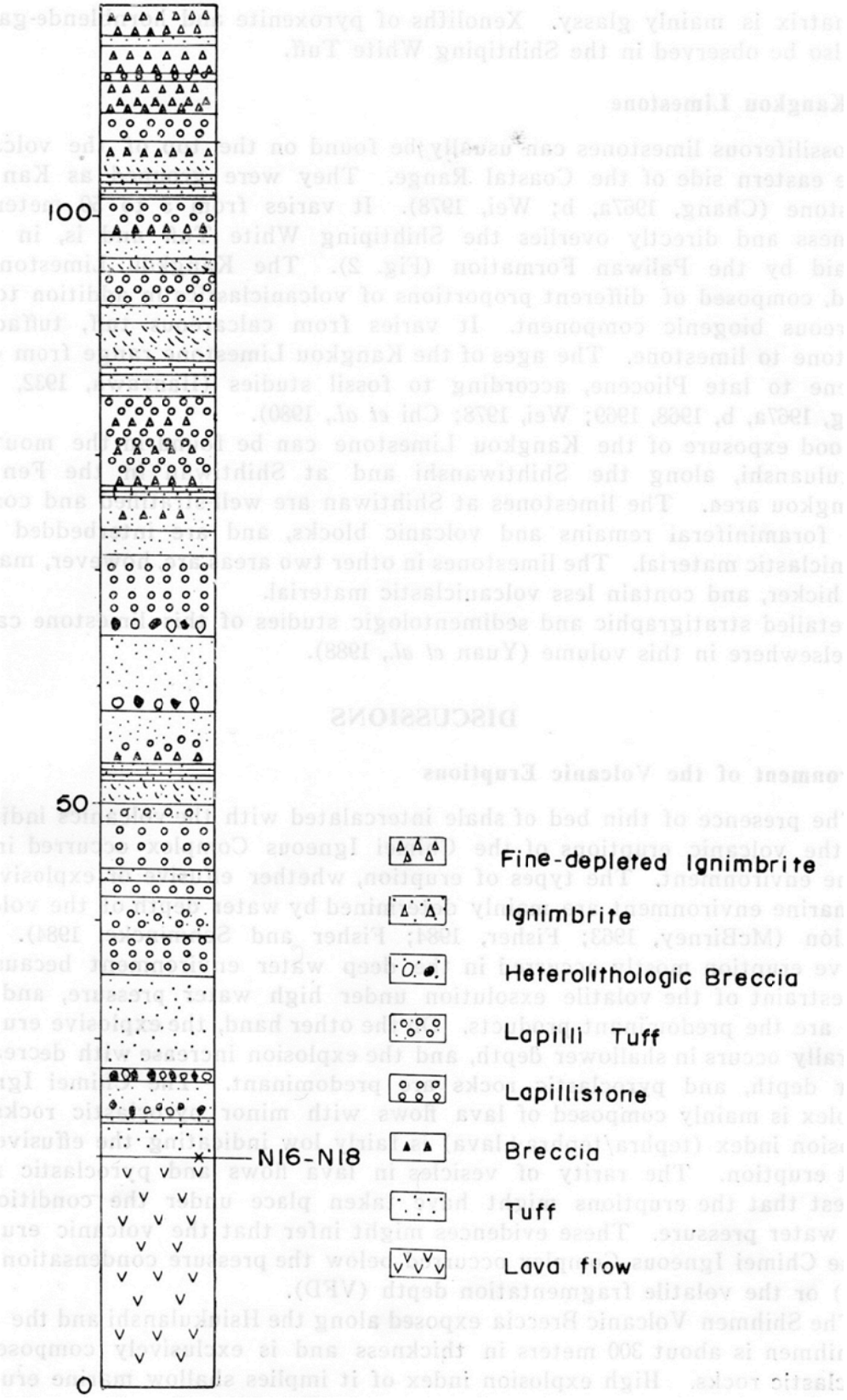

Fig. 5-18. Detailed lithologic column of the Shihtiping White Tuff in the Shihtiping area.

Fig. 5-19. Stop 3-4. White intermediate to acid tuff composed of welded volcanic glass shards and mafic minerals of pyroxene, hornblende, and opaque minerals at Shihtiping.

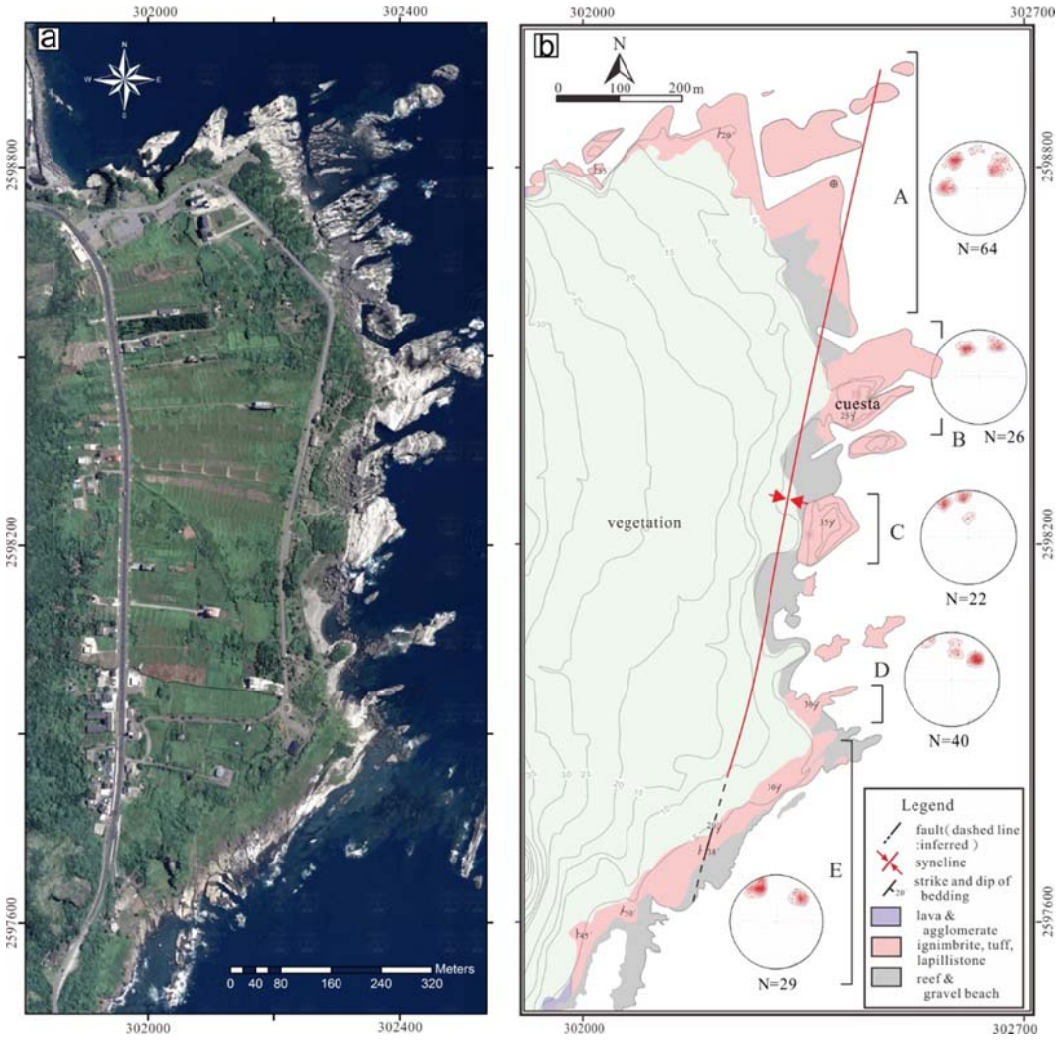

Fig. 5-20. (a) Aerial image of Shihtiping from Safe Taiwan. (b) Distribution of pyroclastic rocks and deformation bands in Shihtiping. N is the amount of measured deformation bands.

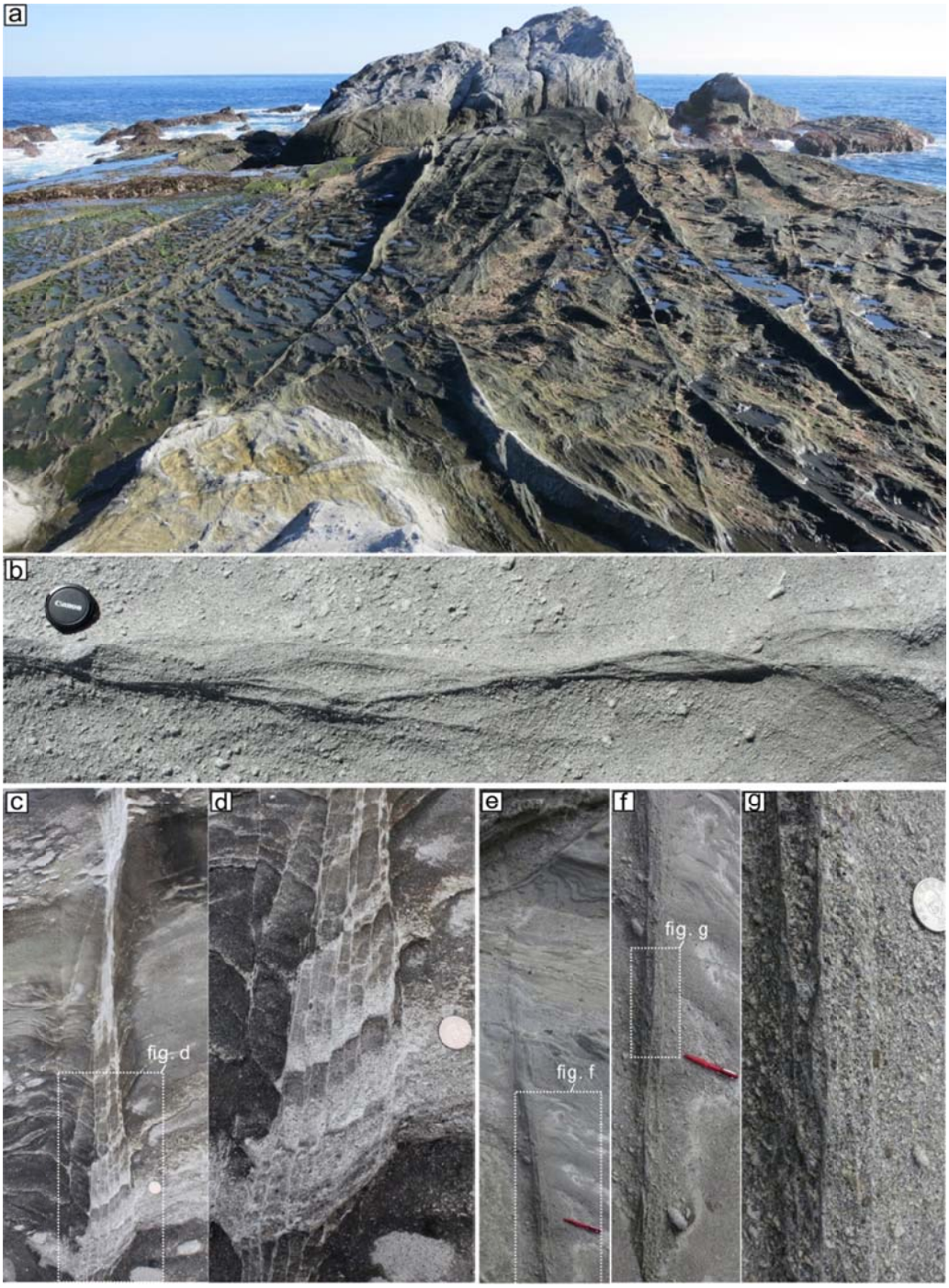

Fig. 5-21. Occurrence of Deformation bands in Shihtiping. All pictures were taken in zone B showed in Fig. 5-20. (b) & (e) are nearly flat ground. (c) is on a slope of >60°.

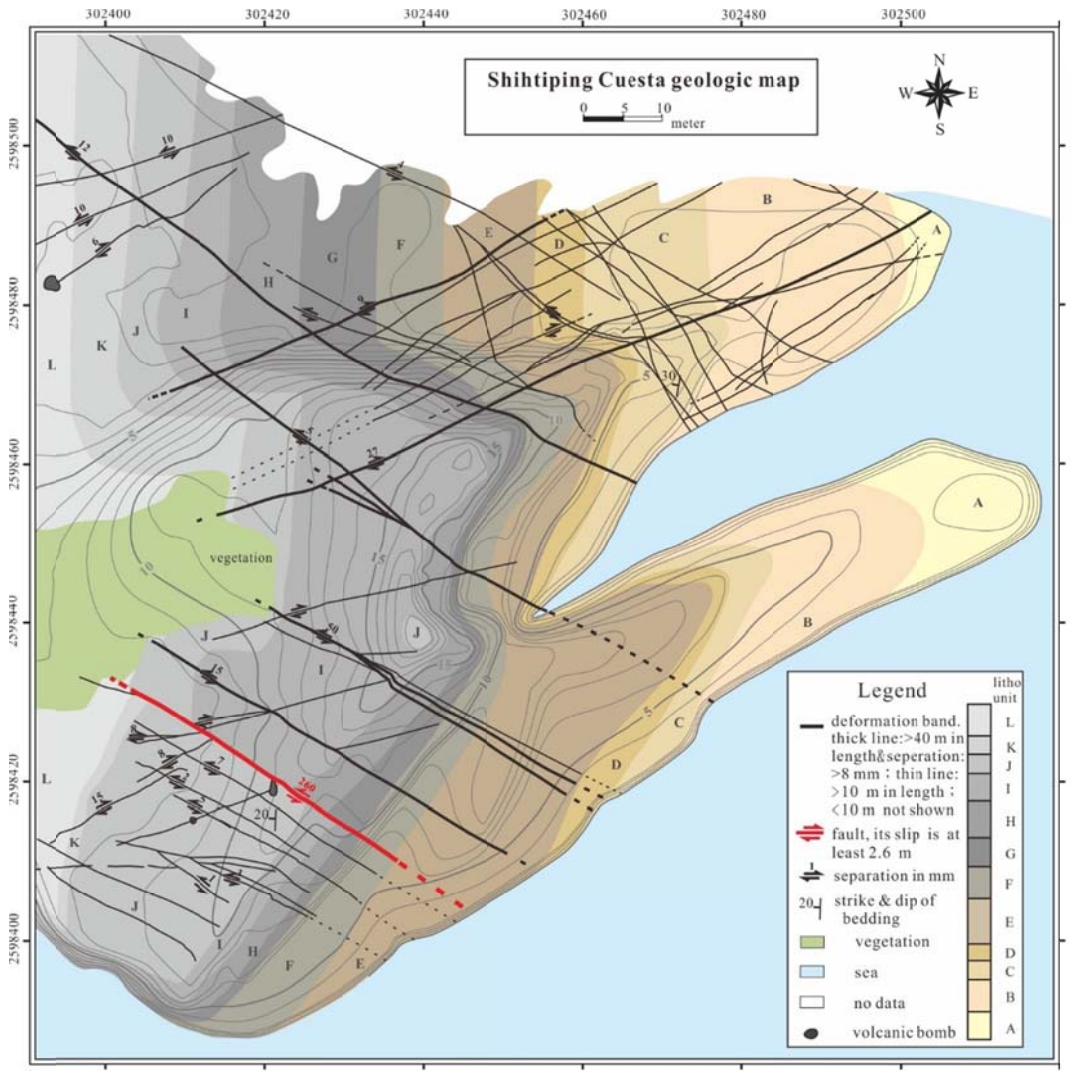

Fig. 5-22. Shihtiping Cuesta geologic map. A conjugate set of deformation bands are exposed on the cuesta located in zone B shown in Fig. 5-20b.

Stop 3-5: Wushihpi: A huge slided block of volcanic arc in contact with upper forearc sediments (Paliwan Formation)

Wushihpi is located at southern Coastal Range, about 15 km north of Chengkung, Taitung County. The rock outcropped in this location is the basaltic andesite, which occurs as columnar lava flows and volcanic breccias with abundant white veinlets and muddy sediments filled in columnar joints and fissures. The andesitic rock is light grey or yellow on the weathered surface and is dark on a fresh one. Columnar joints with four, five and six sided columns are well developed in massive lavas, which are the huge blocks distributed in the matrix of volcanic breccias. Different orientation of columnar joints also suggests that they are exotic blocks and derived from different cooling lavas. Volcanic breccias are predominantly

composed of monolithologic blocks with subsidiary matrix. They are also basaltic andesites and consist of augite, hypersthenes and plagioclase as phenocrysts. Fission-track age dates of those volcanic rocks range from 2.2 Ma to 3.3 Ma (Yang et al., 1995).

Many thin layer veins and geodes occur in the columnar joints, shearing planes and fractures. Mineral constituents filled in those geodes and veinlets are the analcime, prehnite and apophyllite, which were the low hydrothermally alteration products. Many fine grained muds with calcareous nannofossils are filled in the joints of columnar andesites and fissures or grain boundary of volcanic blocks. The nannofossil is NN15 which is equivalent to the middle Pliocene in age (Chi and Chu, 1982).

Volcanic formation occurred in Wushihpi is characterized by a huge block surrounded by shale of Paliwan Formation. This block, thus, may be a block of Tuluanshan volcanics slided into the forearc basin sediments (Paliwan Formation) during the arc-continent collision.

Fig. 5-23. Basaltic andesites with columnar joints exposed at Wushihpi.

Actively evolving Hua-tung coast

The Hua-tung Coast, located between Hualien and Taitung cities, is the coast fringing the Coastal Range in eastern Taiwan. In contrast to the straight (and somewhat monotonous) coasts to the north and to the south that bound on the Central Range, the Hua-tung Coast exhibits series of terraces with various origins and morphology controlled by bedrock lithology, tectonic uplift rate, global sea-level fluctuations, and episodic flux of coarse sediment from local rivers and hillslopes (Fig. 5-24).

The terraces along the Hua-tung Coast have been dated to <20 ka (e.g., Hsieh et

al., 2004; Yamaguchi and Ota, 2004; Hsieh and Rau, 2009), based on which the long-term uplift rates of the coast have been estimated generally 5-10 mm/yr (Hsieh and Rau, 2009). A part of this uplift is apparently coseismic, as evidenced by the occurrence of emerged wave-cut notches on resistant rock surfaces (Fig. 5-25), and by the presence of intertidal-fossil bands stranded above the sea level (Fig. 5-26). The most recent great uplift event, with amounts up to 3-6 m and influencing at least 70 km of the northern-middle part of the coast, has been dated ~0.9 ka (Hsieh and Rau, 2009). Notably, much of this part of the coast is currently undergoing subsidence, according to the leveling data (Ching et al., 2011).

Adjacent to the active Coastal Range, almost all the terraces along the Hua-tung Coast are either capped or entirely constituted by debris-flow and/or fluvial gravels, many of which formed distinct alluvial fans or fan-deltas (Hsieh et al., 2011) (Fig. 5-24). Hsieh and Rau (2009) linked the genesis of these landforms, which record the episodic great flux of sediment from the mountain, to periodic large earthquakes by finding the synchronism between the growth of the landforms and the mass mortality of intertidal organisms probably stranded by coseismic uplift. This episodic sediment flux is believed to have influenced the centennial to millennial advance/retreat of the shoreline. For example, the recent stability of the coast could result in the intense retreat (>1 m/year over the past 50 years) along many segments of the coast, even under the condition of rapid tectonic uplift (Fig. 5-24).

Fig. 5-24. A view to the coastal terraces around Chenggong, south part of the Hua-tung Coast. The terraces in the background (F) originated from a gigantic alluvial fan dated ~15 ka cal BP by radiocarbon methods. This part of the coast has undergone >100 m retreat in the past 50 years.

Fig. 5-25. Modern and uplifted wave-cut notches carving into volcanic rock (Tuluanshan Formation), south of Ching-pu, middle part of the Hua-tung Coast.

Fig. 5-26. (a) A view of a cluster of boring-shell (*Jouannetia sp*.) burrows drilled into mudstone (Takangkou Formation) at Chi-chi, north part of the Hua-tung Coast. These shells, now located around 3 m above the sea level, have been dated ~0.9 ka cal BP by radiocarbon methods. (b) Close view of the shells and their burrows.

4-1: Contact between arc volcaniclastics and overlying forearc flysch sediments of the Fanshuiliao Formation: Beichi, Fuli Road no. 23, Bridge no. 5.

At stop 4-1 (see Fig. 5-27 for location) it exposes the uppermost part of the Tuluanshan Formation with epiclastics and the lowest section of the fine-grained turbidites of the Fanshuliao Formation (Fig. 5-28, Chen and Wang, 1988; Chen , 1997b). According to Chen (1997b), the epiclastic sandstone and conglomerate of the Tuluanshan Formation are up to 200 m thick at the locale. Conglomerates are matrix-supported with rounded andesite and limestone clasts up to 10 cm long. The epiclastic sandstones are thinly-bedded, non-welded and composed of detrital fossils and fragmented phenocrysts, displaying Bouma sequence typical of the products of turbidity currents. These deposits, which comprise high proportions of resedimented clasts that were originally accumulated in shallow waters, are interpreted as accumulated in a submarine and distal volcano-apron environment (Chen, 1997b).

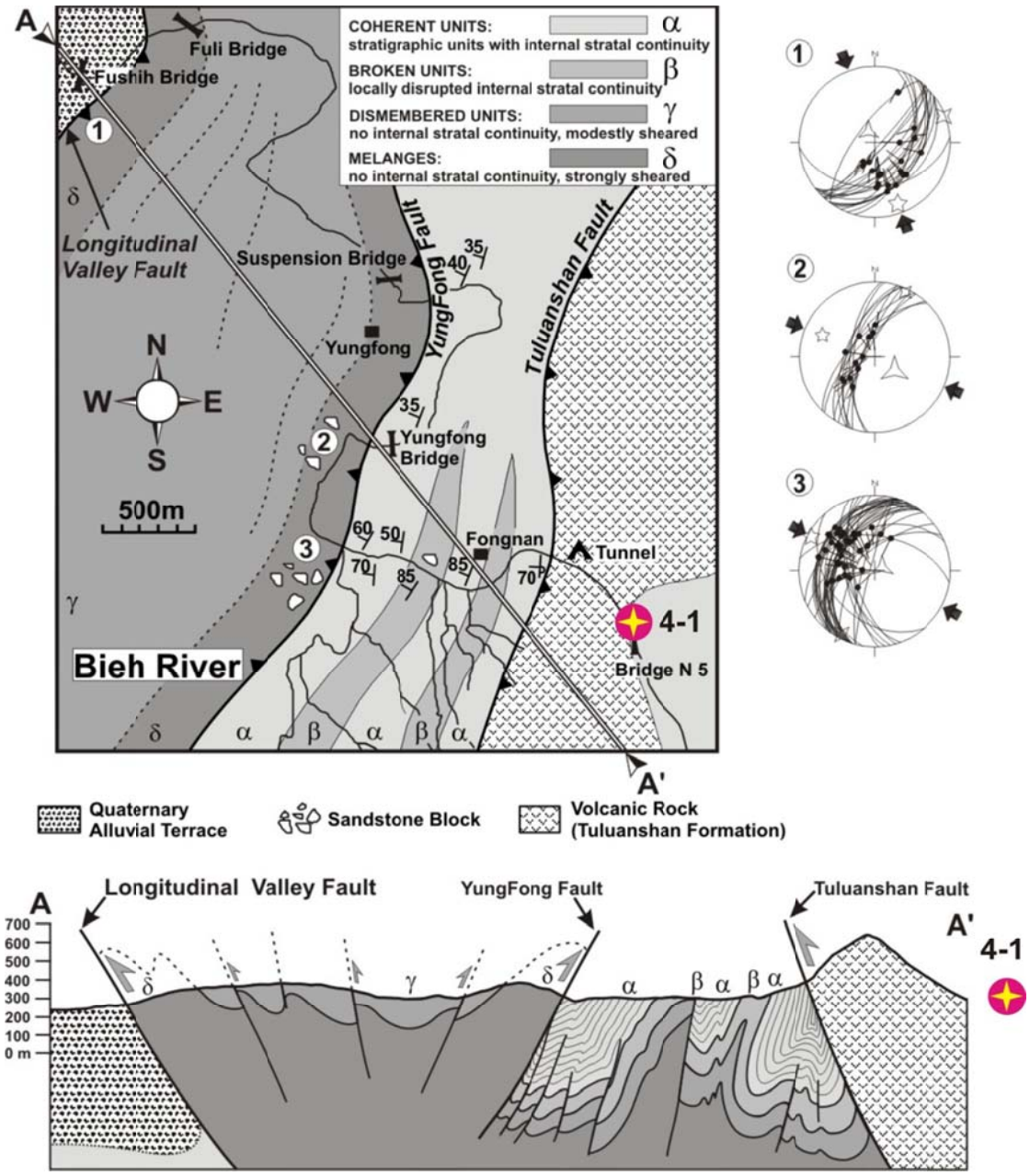

Fig. 5-27. Geological map and cross-section of the area of the Beichi River (Chang et al., 2000). Three stereographic plots of striated scaly foliations measured in area. Lower hemisphere equal-area projection, striated faults as thin curves with dots; inward directed segments for reverse slip, outward directed ones for normal slip, double half segments for strike-slip; paleostress axes as 5-, 4- and 3- branch stars for maximum compressive stress, intermediate stress and minimum stress respectively. Large convergent arrows indicate directions of compression. Circles with numbers refer to stop locations.

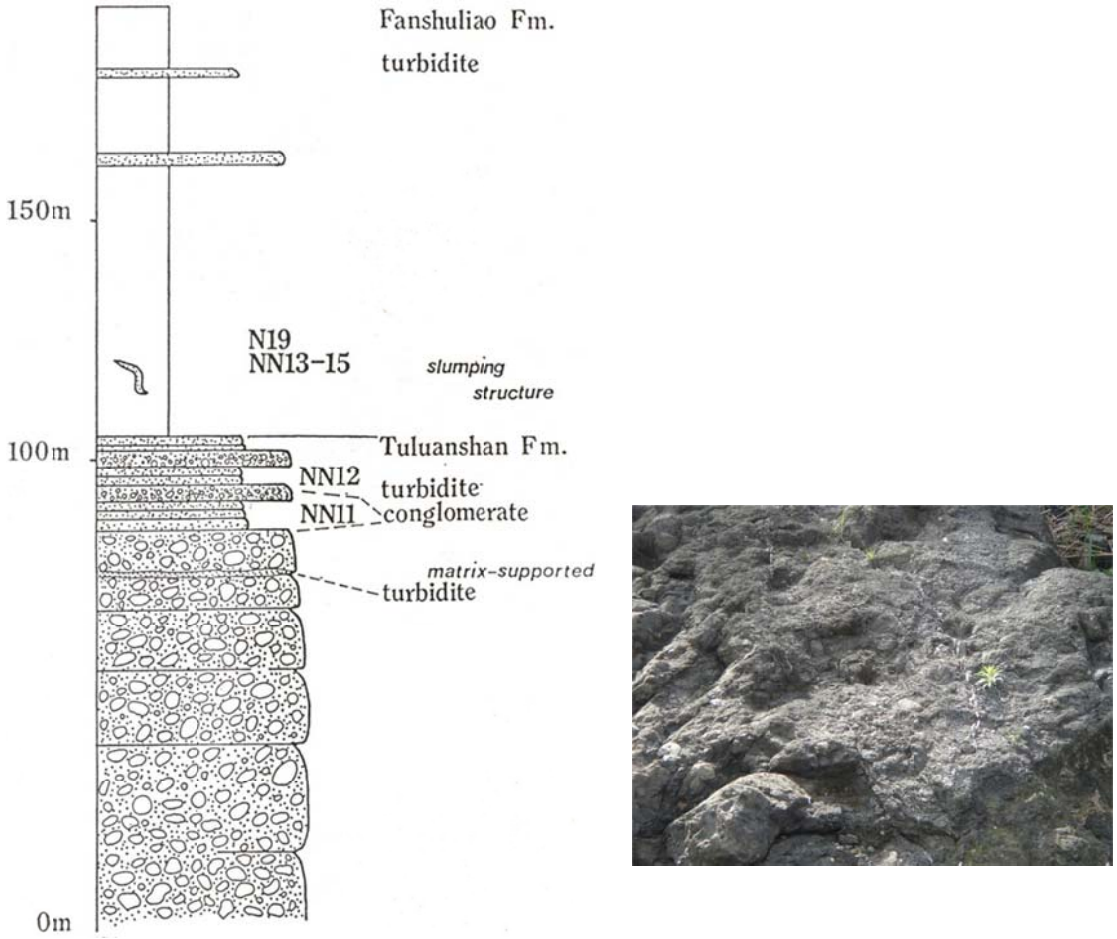

Fig. 5-28. Stop 4-1. Stratigraphic column (from Chen and Wang, 1988) and photo (conglomerate of the Tuluanshan Formation) at stop 4-1, Beichi (see Fig. 5-23 for stop location).

Stop 4-2: The creeping Chihshang Fault: Chishang village

The village of Chinyuan is located on the surface trace of the Chihshang fault (Fig. 5-29). The Chinyuan channel, which is situated on a small alluvial fan in Chinyuan, is also one of the observatory sites to monitor the rapid creeping Chihshang fault.

Three fractures zones in the concrete retaining walls along a NW-SE to E-W trending water channel within a distance of about 100 m have been observed since 1991. These fractures have been considered as surface breaks of the Chihshang fault (Chu et al., 1994; Angelier et al., 1997). Progressive shortening across each fractures zone were monitored once or twice per year by direct measurement on the walls since 1991 (e.g., Angelier et al., 2001). In 1998, three creepmeters have installed to straddle each fractures zone to record daily creep data (Fig. 5-30). Furthermore, dozens benchmarks of a dense geodetic network of about 200 m wide were setup along the retaining walls of the channel since 1998. These data together show that a rapid horizontal shortening across three fractures of a collective rate of 22-27 mm/yr

from 1992-1998 and a decreasing rate of 13-15 mm/yr from 1999-2003 before the Chengkung earthquake. Furthermore, the daily recorded creep data from creepmeter show clearly a seasonal variation of surface deformation: quiescence during dry season and rapid creep during wet season. We interpret that the fault motion has been strongly influenced by rain or ground water at the shallow surface level.

Field investigations and measurements after the 2003 Chengkung earthquake revealed relatively little co-seismic surface near fault deformation: about 1 cm of collective horizontal shortening recorded by three creepmeters across the three abovementioned fractures. Field observation showed no clear surface breaks other than these three pre-existing fractures at the Chinyuan site. Geodetic measurements of the Chinyuan network, one before and three after the earthquake, reveal a significant post-seismic creep (Fig. 5-32). The near fault deformation was characterized by a major anticline fold and a minor back-fold in the hanging wall of the fault (Fig. 5-33). Whereas the vertical elevation change was mimicking the fold structure, the horizontal deformation was mostly released by brittle fractures (i.e., the three fractures) in the concrete retaining walls and the water channel. The maximum vertical elevation change, which is located at the easternmost benchmark, showed a progressive post-seismic creep: 5 cm, 8 cm, and 10 cm at 25 days, 105 days, and 340 days, respectively, following the earthquake. The total horizontal shortening across the surface fault zone was 5 cm, 8 cm, and 10 cm at 25 days, 105 days, and 340 days, respectively.

A recent trenching showed that the fault does not break through the uppermost alluvial deposits, which appear to attend to more than 10 m in thickness. This is consistent with the fact that the near fault deformation was predominated by an anticline fold, implying that the fault is strongly coupled, if not totally locked, in the shallow surface level. Thus, we interpret the fractures in the retaining walls as a result of brittle response of bending of the concrete construction. Two fractures are located near the surface tip of the primary fault and one fracture is located near the surface tip of the probable backthrust. Lee et al. (2005) interpreted the locked segment at the shallow surface as an effect of velocity strengthening due to surface unconsolidated deposits by applying the frictional instability along the fault.

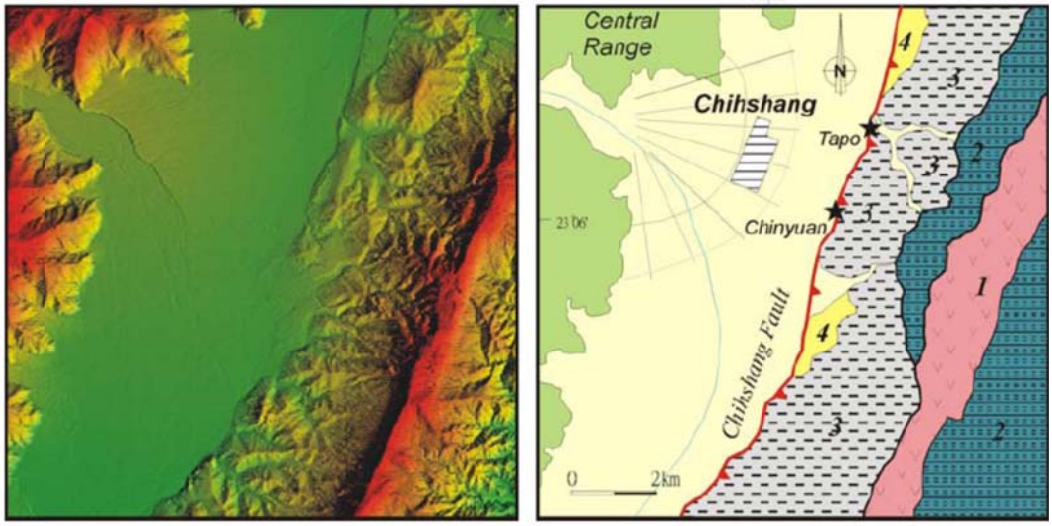

Fig. 5-29. General morphologic features and geology of the active Chihshang Fault (after Lee et al., 2001). Left side: the digital elevation model's (DEM) shading image. Right side: geological interpretation of the DEM. Geological units of the Coastal Range: 1: Touluanshan Formation, 2: Takangkou Formation, 3: Lichi Mélange, 4: Quaternary terrace. The Chihshang Fault is situated on the western margin of the Coastal Range. The two stars indicate the sites of creepmeters.

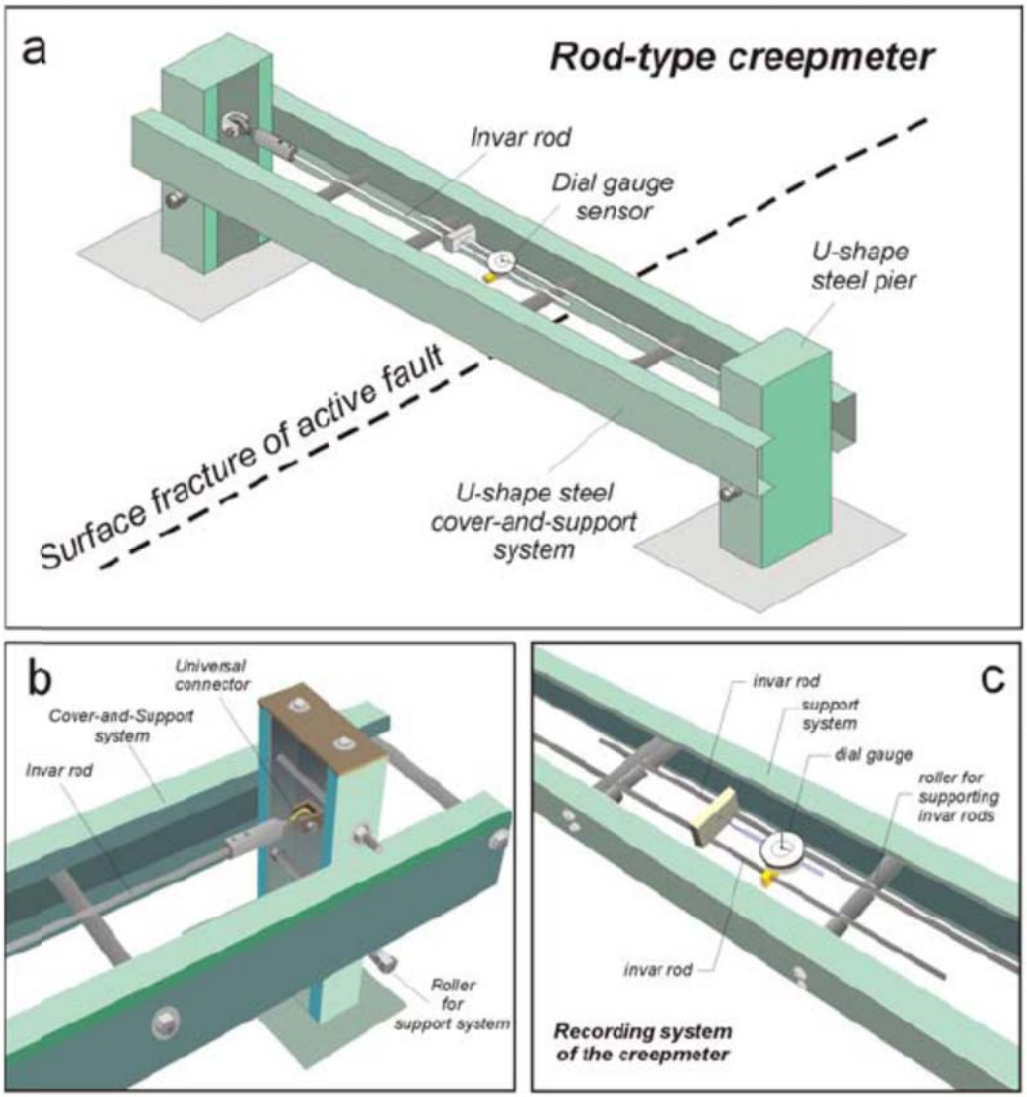

Fig. 5-30. (a) Schematic representation of the rod-type creepmeter across an active fault. The instrument measures the horizontal displacement between the anchored piers on the opposite sides of the active fault. (b) Details of the pier end of the creepmeter. The invar rods are attached on each pier by a universal connector and are supported by the rollers fixed on a U-shaped steel cover-and-support system. (c) Details of the middle part of the creepmeter. The relative horizontal movement of two invar rods can be measured by a mechanical dial gauge sensor. The resolution of the dial gauge is up to 0.01 mm and ranging to 50 mm. (from Lee et al., 2001)

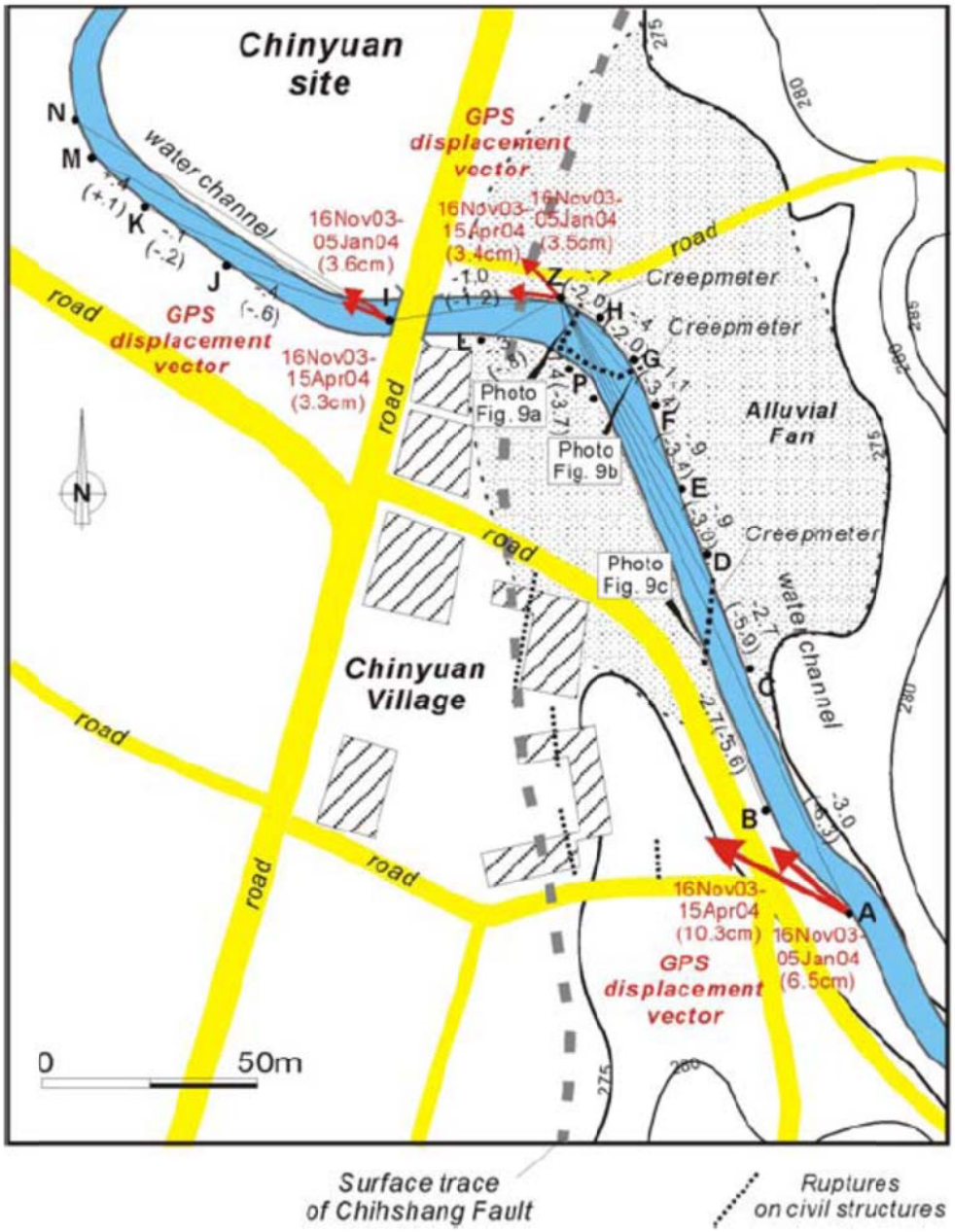

Fig. 5-31. Geodetic network and results of horizontal distance changes and GPS horizontal displacements related to the 2003 Chengkung earthquake at the Chinyuan site. The contours lines show that the site is located on a small alluvial fan (marked in grey dots). The values between the benchmarks indicate locations of measurement of horizontal distance changes. The GPS displacement vectors are with respect to a continuous GPS station SHAN in the Longitudinal Valley.

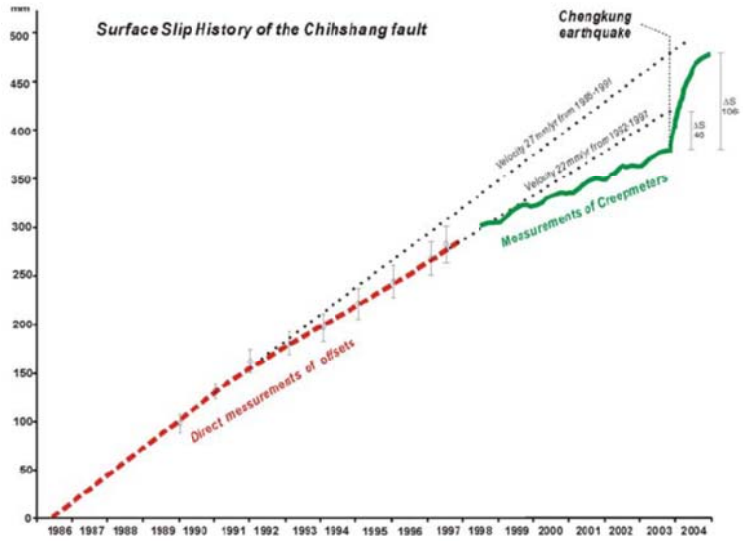

Fig. 5-32. Shortening across the Chihshang Fault, from mid-1986 to December 2004, with tentative estimate of strain deficit before the Chengkung earthquake (Dec. 10, 2003) (From Lee et al., 2005). Shortening (mm) versus time (years). Dashed line: results 1986-1997. Solid line: results 1998-2003, Chinyuan creepmeters. Uncertainties as error bars (for creepmeter data, within curve thickness). Dotted lines: extrapolation of aseismic creep shortening until the Chengkung earthquake: upper bound from 1986-1991, lower bound from 1992-1997, respectively giving minimum strain deficits of 106 mm and 46 mm in Dec. 2003.

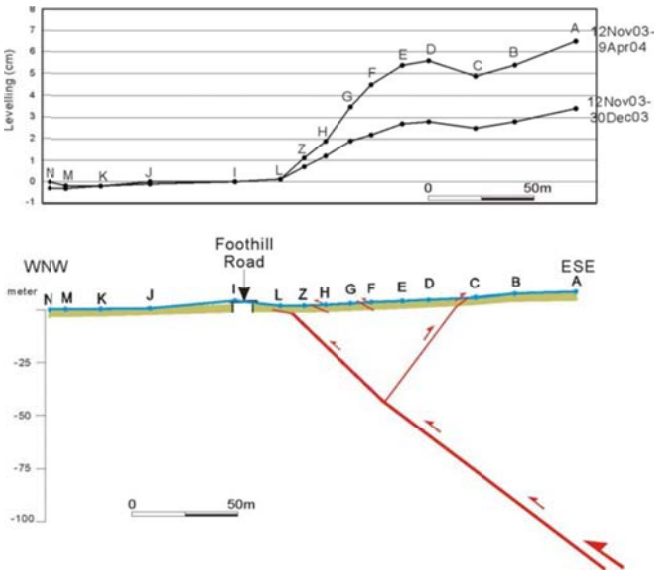

Fig. 5-33. Results of distance-angle and levelling measurements across the surface fault zone of the Chihshang fault and geological interpretation at Chinyuan site (From Lee et al., 2005).

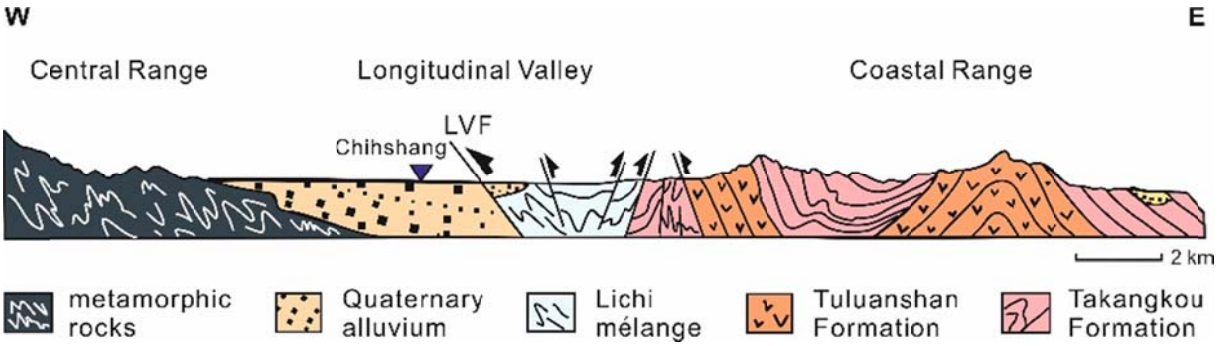

Fig. 5-34. A simplified geologic cross section of eastern Taiwan near Chihshang (after Mu et al., 2011). LVF = Longitudinal Valley Fault.

Stop 4-3: Luyeh Terrace: Active fault scarp and growing fold in the Longitudinal Valley, terraces of Lungtien and Gautai

Lungtien and Gautai are located at high large terraces within the Longitudinal Valley in the Luyeh area (Fig. 5-35). Large terrestrial fluvial deposits, which extend from north of Luyeh to the entire Peinanshan area, appear to be products of the Peinan River and the Luyeh River from Pleistocene to present-day. Along the Luyeh river banks, at least 3-5 terraces can be observed at the different heights, indicating a rapid uplift and river incision in the area. The village of Lungtien is situated on the highest and largest, and presumably the oldest terrace of the Luyeh River. An N-S trending geomorphic scarp occurs at the Lungtien terrace.

In the trip, we will observe this scarp of Luyeh fault. The scarp of about 8-12 m high shows the east side going up. GPS data during the last 2-3 years indicate horizontal shortening occurred across the scarp (Chen et al., 2005). Together with the leveling data, it indicates that this scarp represents an active reverse fault scarp. In addition, we can also observe fractures with compressive features in the retaining walls at the foot of the scarp. This reverse fault scarp likely represents the surface trace of the Luyeh fault, which has been previously mentioned, although description is very limited. A few topographic profiles with detailed measurements across the scarp showed a growing anticlinal fold, which is presumably related to the reverse fault, in the hanging wall. We interpret this as that the Luyeh fault is probably locked at the shallow surface level. The Luyeh fault extends farther south and it likely affects significantly the deformation of the Peinanshan massif. The Peinanshan massif is composed of Plio-Pleistocene shallow marine to fluvial deposits (Chi et al., 1983). This massif is deformed by two faults on its both sides, the Luyeh fault to the west and the Lichi fault to the east (Fig. 5-38). At the top of Gautai, we can observe folded strata of the Peinanshan syncline. In addition, several levels of the terraces of the Luyeh River show clearly this growing syncline: older the terrace is (i.e., higher), more titled.

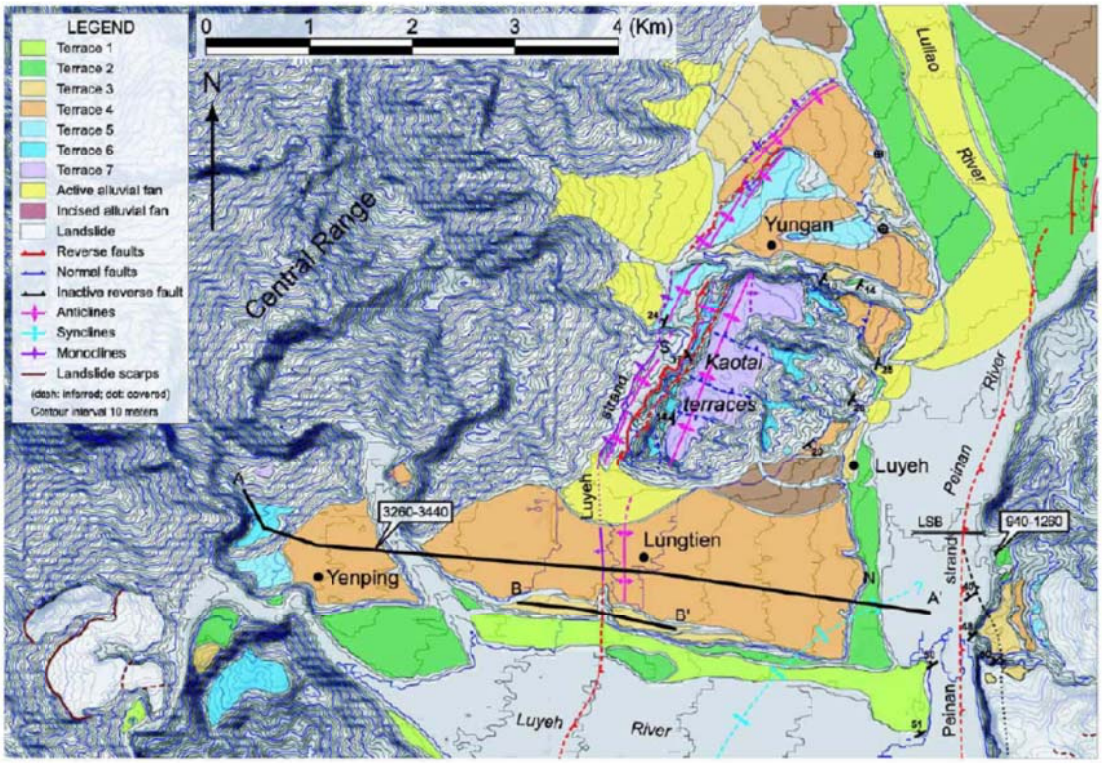

Fig. 5-35. Detailed map of geomorphic features and active structures of the Gautai terraces area. Note that the names of terraces indicate only the relative ages of the terraces and do not imply correlation of the terraces; that is, terrace 4 north of the Luyeh River may not be the same age as terrace 4 elsewhere. The Luyeh strand, a major strand of the Longitudinal Valley fault, runs along the western edge of the Gautai terraces and has produced a monoclinal scarp on the Lungtien terrace to the south. To the north, the Luyeh strand dies out just south of the Luliao River. The other strand of the Longitudinal Valley fault, the Peinan strand, runs within the Peinan River valley and through the Luanshan Bridge (LSB) about 200 m from the eastern end of the bridge. Ages of terraces are calibrated ages (2s), in cal BP.

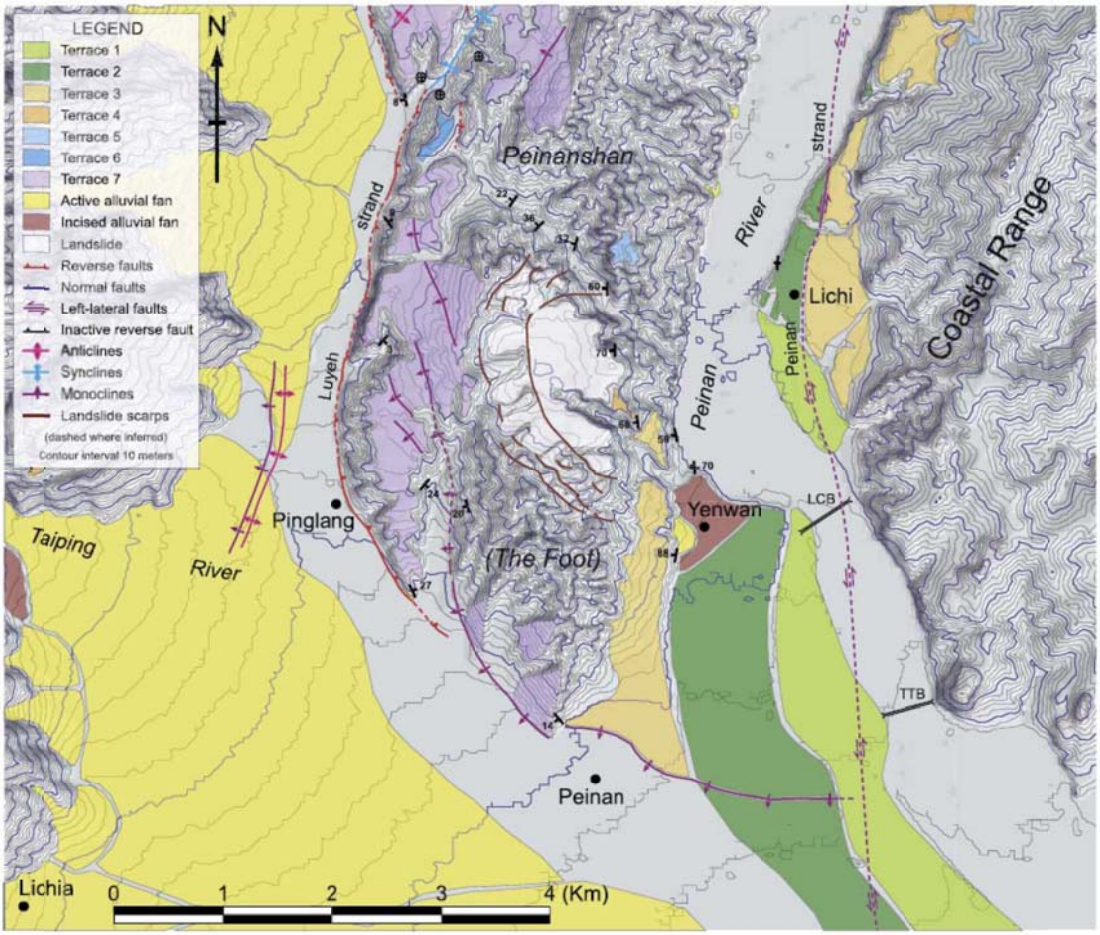

Fig. 5-36. Detailed map of geomorphic features and active structures of the southern Peinanshan area. The Luyeh strand runs along the western front of the Peinanshan, but becomes an E-W striking monocline that wraps around the southernmost part of the Peinanshan. The Peinan strand traverses the Peinan River valley, but produces a small N-S scarp on the terraces near Lichi.

Stop 4-4: Lichi Melange: Lichi Village

The Lichi Melange is widely distributed in the southern part of the Coastal Range. It also extends northward along the western margin of the Coastal Range to Lehe, forming a narrow band of 1-3 km wide and 70 km long. The type locality crops out at Lichi Village near Taitung. The mélange is composed of thick mudstone, mixed with a variety of exotic blocks. Badland topography is the most characteristic of the Lichi Melange. According to the drilling data of the Chinese Petroleum Company, the thickness of the mélange is greater than 1 km (Meng and Chiang, 1965). The exotic blocks are mostly ophiolitic fragments and sandstone. Other lithological varieties include greywacke, shale, limestone, conglomerate and andesitic agglomerate. The most distinguished exotic block is the so-called East Taiwan Ophiolite (ETO; Liou et al., 1977b). The ETO comprises all the components for a typical ophiolite sequence –

peridotite, gabbro, serpentinite, diabiasic dike, plagiogranite, basalt and red clay. Paleontological studies indicate that the mélange contains microfossils of ages ranging from Oligocene to Middle Pliocene (time span of ca. 30 Ma). Based on the youngest fossils, the deposition of the Melange is commonly assumed to begin in the Middle or Upper Pliocene (ca. 3 Ma).

		Lichi Mélange	Kenting Mélange
similarities	Matrix	Intensely sheared mudstones without distinctive stratification. Some layers with coherent stratification have been locally reported	
	Texture	Scaly foliation, dense pattern of small faults with slickenside lineations (mainly thrust and strike-slip in type, also normal)	
	Exotic blocks	Ophiolitic blocks (including basic to ultrabasic rocks) and sedimentary blocks (including sandstone, sandstone/shale interbeds, shales and limestones), metric to kilometric in size	
	Boundary structure	Bounded by west-verging thrusts at both eastern and western boundaries of mélange zone	
	Footwall	Quaternary fluvial deposit (both Lichi and Kenting) and coral reef (Kenting only) in the west	
	Tectonic regime	Mainly NW-SE compression indicated by fault slip data and other structures inside the mélange	
differences	Clay mineral	illite (48.8%), chlorite (8.4%), kaolinite (13.9%), smectite (1.9%) and mixed-layer clay minerals (27.0%)	Illite (57.8%), chlorite (10.3%), duckite (11.5%), montmorillonite (2.0%) and mixed-layer clay minerals (18.6%)
	Age of matrix	Rather well constrained, 3.5~3.7 Ma	Large dispersion of ages, approximate range 1 to10 Ma
	Exotic blocks	Include both Miocene and Pliocene sedimentary rocks and Miocene volcanic rocks (with volcanic breccias, tuffs, and volcaniclastic turbidites) issued from the Luzon Arc	Include Miocene turbiditic blocks, but does not include Pliocene sedimentary rocks and Miocene volcanic rocks
	Pebbly layer	Locally reported (especially in the rivers of the central segment)	Not found (but many conglomerate blocks exposed)
	Limestone included	Pliocene Kangkou Limestone (around the summit of the volcanic arc east to the mélange)	Pleistocene Hengchun Limestone (apron coral reef and lagoon phase limestone exposed in west of the mélange)
	Hanging wall strata	Miocene volcanic basement overlaid by Pliocene turbidites to the east	Miocene turbidite formation to the east
	Geographic location	Along the southwestern flank of the Coastal Range, east of the Central Range and Longitudinal Valley	In a narrow area of low hills that bound the main range of Hengchun Peninsula (souther extension of Central Range) to the west
	Geological location	Between the Taiwan accretionary prism/Central Range and the Luzon volcanic arc	Between the foreland of the Taiwan belt and the western flank of the southern Taiwan accretionary prism
	Origin of ophiolite	Basement of forearc basin (probably the Philippine Sea oceanic crust)	South China Sea oceanic crust
	Tectonic origin	Forearc mélange: originates from the thrusted strata at the front of a forearc basin west of, and attached to, the Luzon Arc	Formed at the front of an accretionary prism above the subduction zone, representing the relic of a submarine trench.

Fig. 5-37. Stop 4-6. (A) Lichi Melange at the type-locality of Lichi Village (Geologic park). (B) Table listing the similarities and differences for the Lichi Melange and the

Kengting Melange.

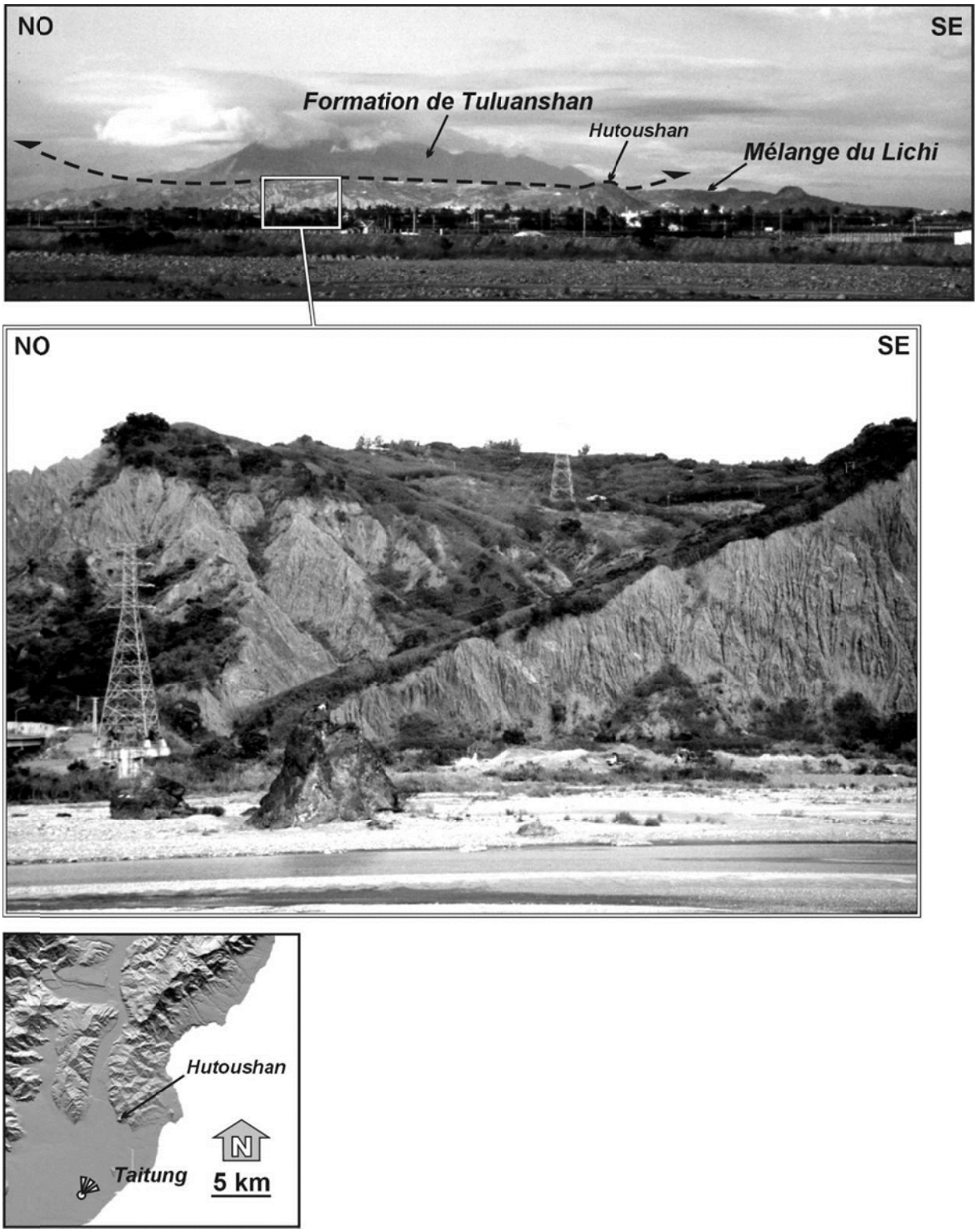

Fig. 5-38. Typical outcrop of the Lichi Melange near the Lichi Bridge.

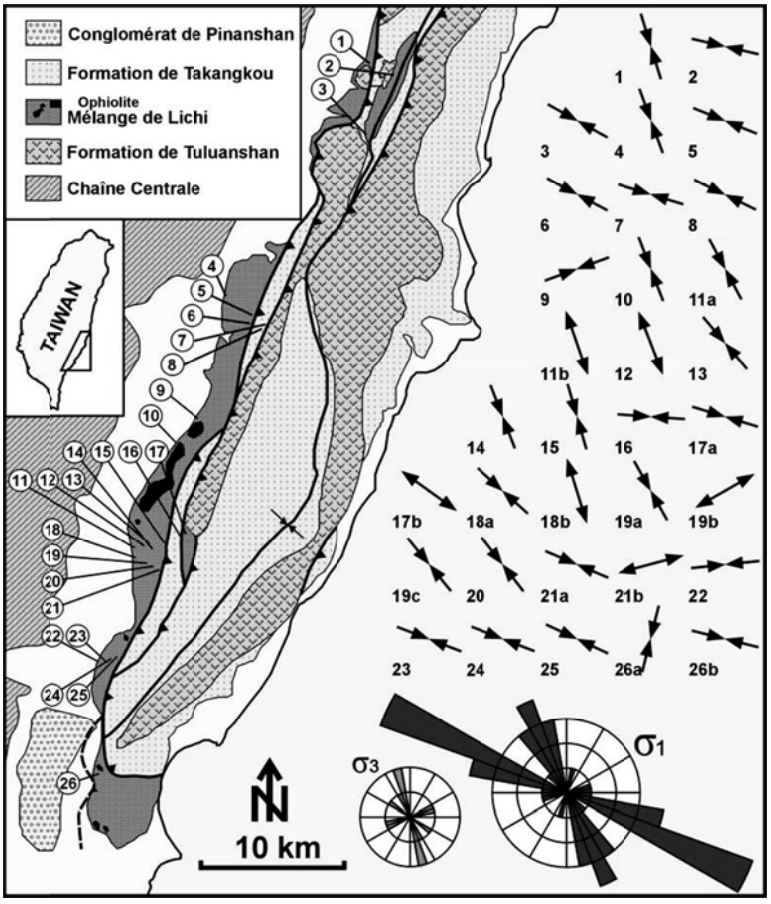

Fig. 5-39. Distribution of paleostress axes reconstructed in the Lichi Melange, and statistical distribution of the trends of compression (convergent arrows) and extension (divergent arrows). Numbers near arrows refer to site location in map. The rose diagram of σ 1 trends shows a main regional trend N100°–120°E and a secondary trend of N140°–170°E.

Stop 4-5: Fukang: Exotic sandstone block (Fukang Sandstone) in the Lichi Melange

A huge classical sandy turbidite block (over one km in dimension) is exposed along the coast north of the Fukang fishing port (Figs. 5-40, 41). The sandstone block is overturned. Its composition is similar to that of Loshui Formation exposed on the east coast of Hengchun Peninsula. Late Miocene (NN11) nannofossils have been reported from this sandstone block (Chi, 1981). This age is similar to Hengchun Peninsula turbidites, but older than the Plio-Pleistocene forearc turbidites and the muddy matrix of the Lichi Melange (3.5-3.7 Ma) in the Coastal Range. Again, fission track analysis on zircon grains separated from the sandstone block here shows an age pattern similar to those of the Hengchun Peninsula, but differs from the forearc turbidites in the Coastal Range.

At the Fukang (Hsiaoyeliu scenic area) where the sandstone is polished by

long-term wave actions, this sandstone block is dominated by very thick sandy turbidites deposited by high-concentration turbidity currents with abundant climbing ripples and loading/dewatering structures, such as flames, dishes and pillars, indicative of rapid deposition. Also, notice that the sandstone is capped unconformably by uplifted coral-reef complexes, which have been dated ranging from a few hundred years to 7.5 ka cal BP (Peng et al., 1977; Yamaguchi and Ota, 2004).

Fig. 5-40. Topographic map showing the distribution of the Fukang Sandstone block outlined by a red line (from Central Geological Survey).

Fig. 5-41. The Fukang Sandstone, a Miocene exotic block in the Lichi Melange.

Stop 5-1: Miocene slate/sandstone: Taimali, Taitung

Deformation of the southernmost Central Range of Taiwan: Polyphasage folding and faulting

In the Taiwan Island, the late Cenozoic collision of Eurasian Plate with the Luzon arc provides an opportunity to observe the arc-continent collision. However, many phenomena and structures recorded in the field demonstrate that the model of arc-continent collision is not sufficient for explaining the Taiwan Mountain building processes; for example, the rapid uplift and exhumation of the metamorphic rocks, the east-west trending fold-and-thrust systems in the southeastern Taiwan, the tectonic rotation of the Hengchun peninsula, the escape phenomenon in the Ilan and Pingtung Plains, etc. All these are very difficult to be interpreted by using a “simple collision mechanism”.

At this stop, we focus on the structural record of southern Taiwan mountain range, in order to clarify the process of deformation in the growing accretionary prism. In view of geological stratigraphy, the southern Taiwan is underlain by thick series of Miocene deposits, including dark gray argillites, flysch deposits with occasional interbeds of gray compact sandstone, and disseminated marly nodules. Lots of field works have been developed in this study to extract the tectonic stress of this region. The transpressional stress and structures are largely distributed in this

area and afford us to measure particle deformation, which is an important key to reconstruct geotectonic history *in situ* of region. Following are some of our preliminary result.

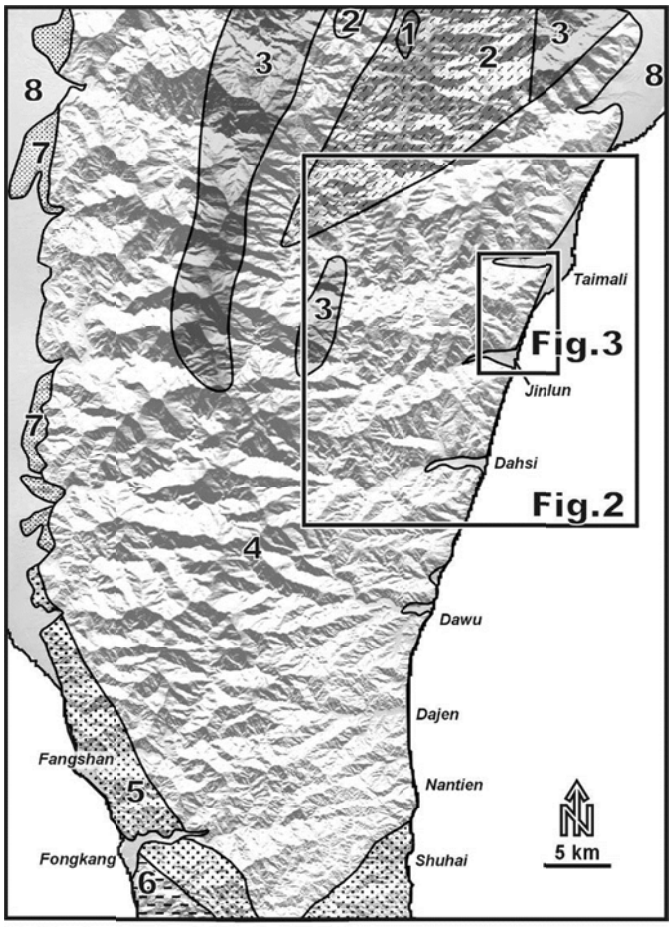

Fig. 5-42. Topographic and geological map of the southernmost Central Range (geological data after the Central Geological Survey). Topography clearly shows the well-aligned enechelon structure pattern in the eastern flank of the Central Range. The location of Fig. 5-43 (i.e. Fig. 2) is indicated.

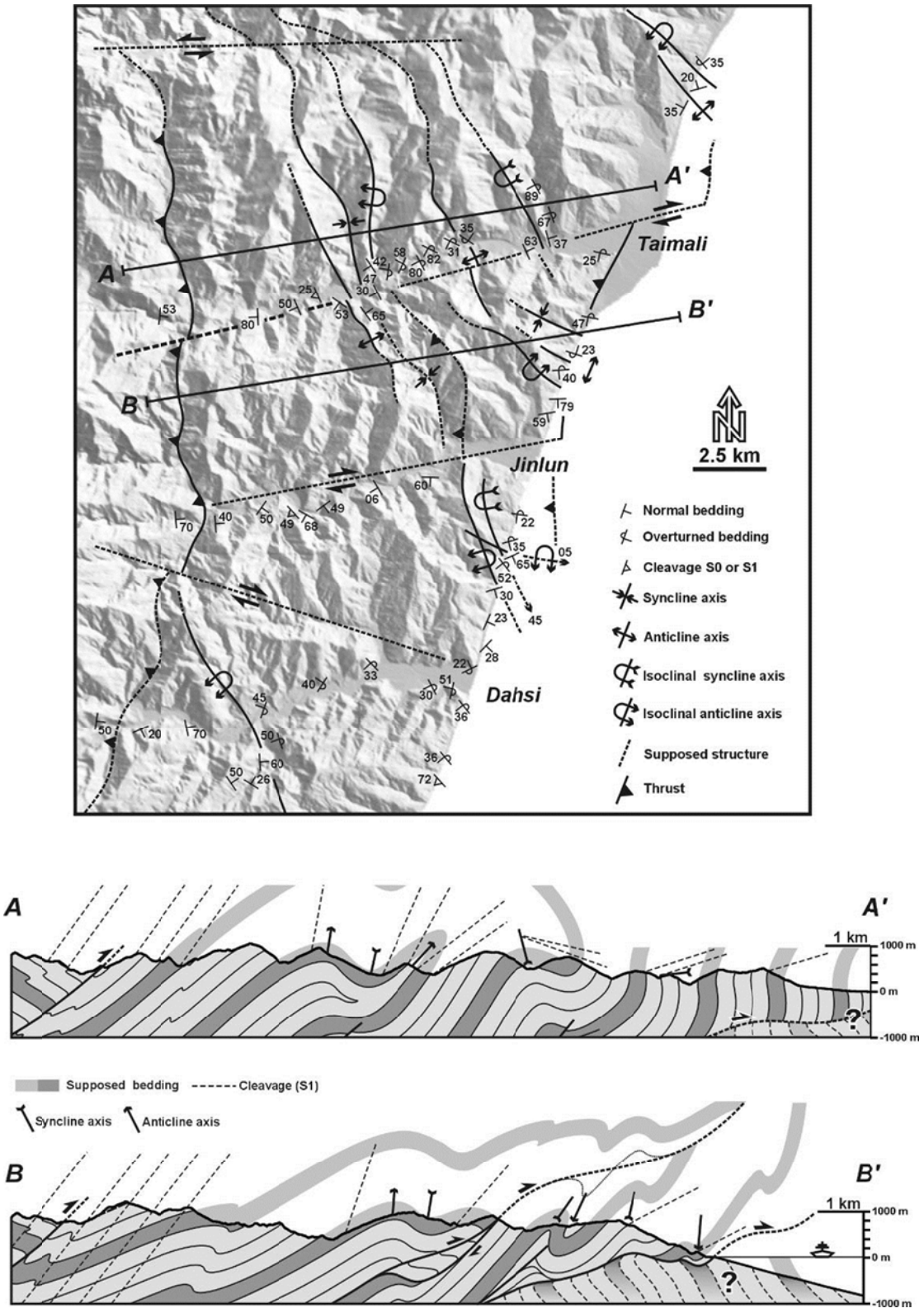

Fig. 5-43. General geological map and profiles of the eastern flank of the southernmost Central Range. Location in Fig. 5-42. Fault slip data analysis in Fig. 5-46.

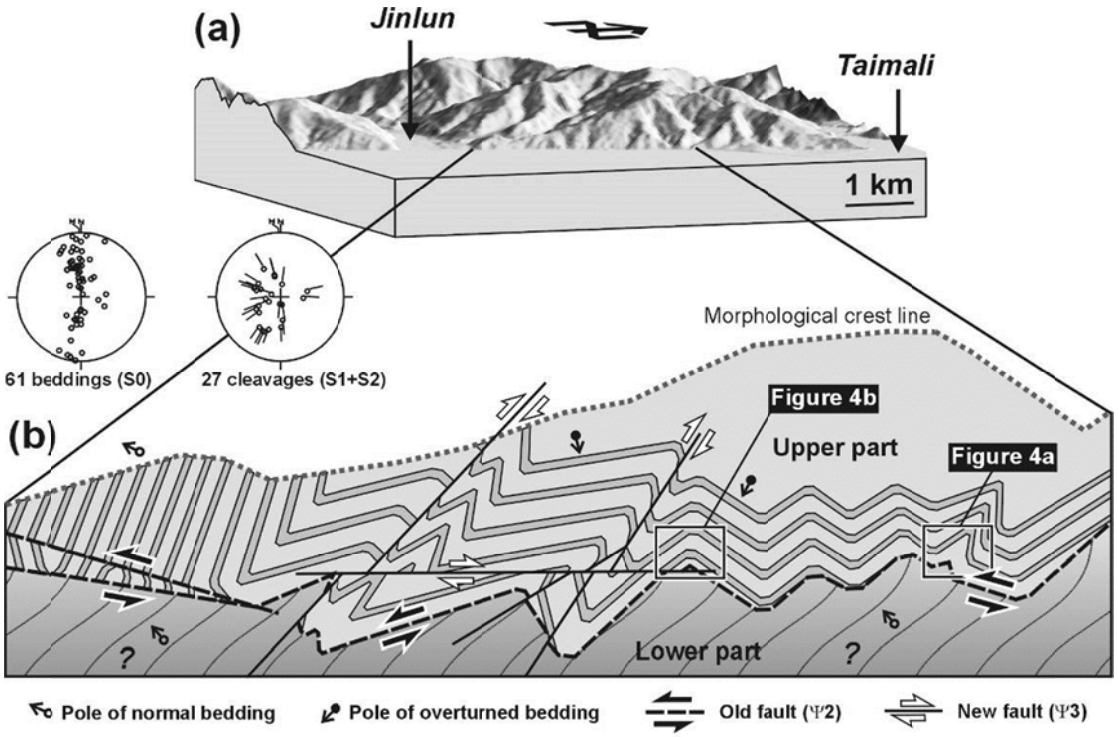

Fig. 5-44. Interpreted structural section in the Lushan Formation of the Taimali beach. Diagrams show lower hemisphere Schmidt projection of measured bedding and cleavages, respectively. Locations of Figures 4a and 4b are indicated.

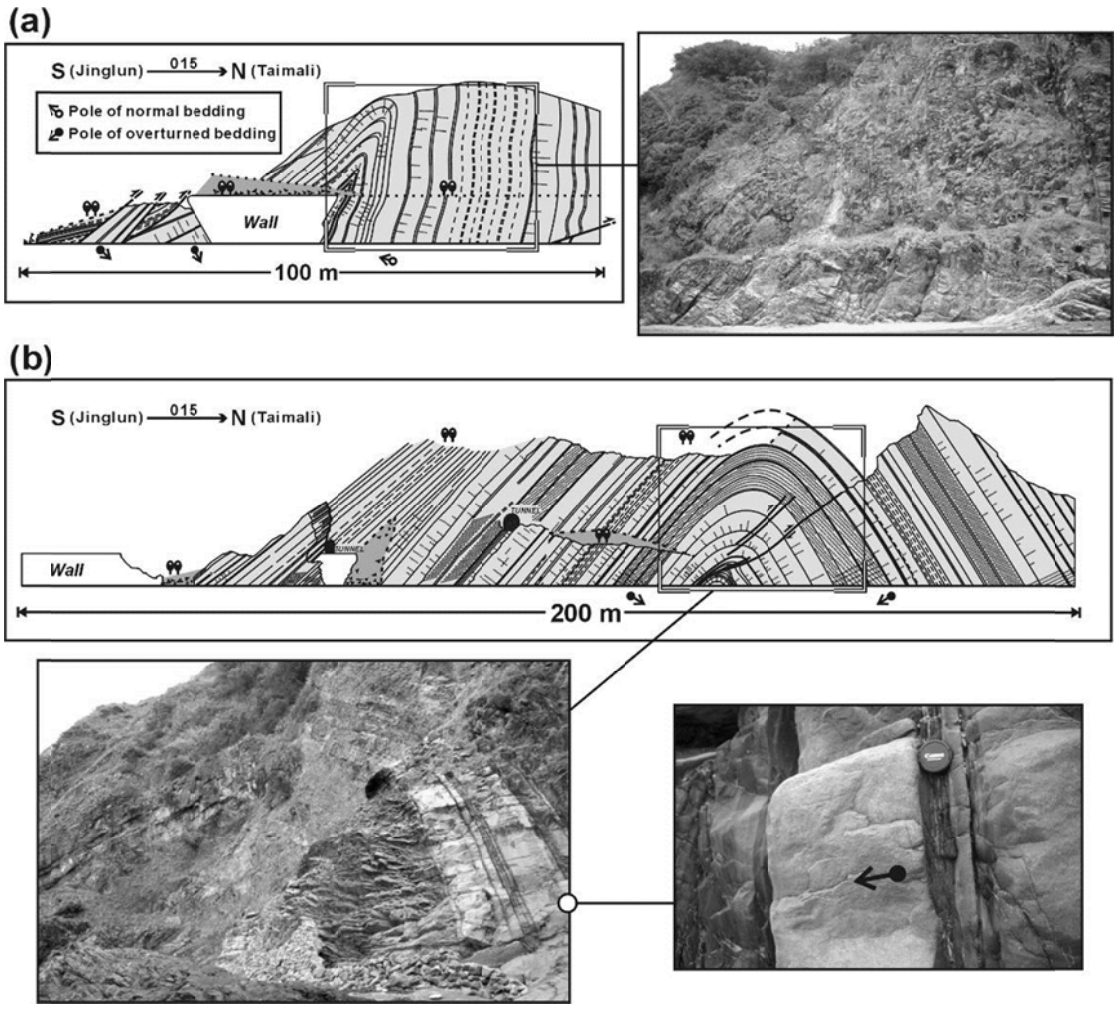

Fig. 5-45. East-west striking antiforms in the Lushan Formation of the Taimali beach. Many sedimentary structures (including graded bedding, flute cast, cross bedding, loading structure, etc.) indicate that the strata were overturned before this folding.

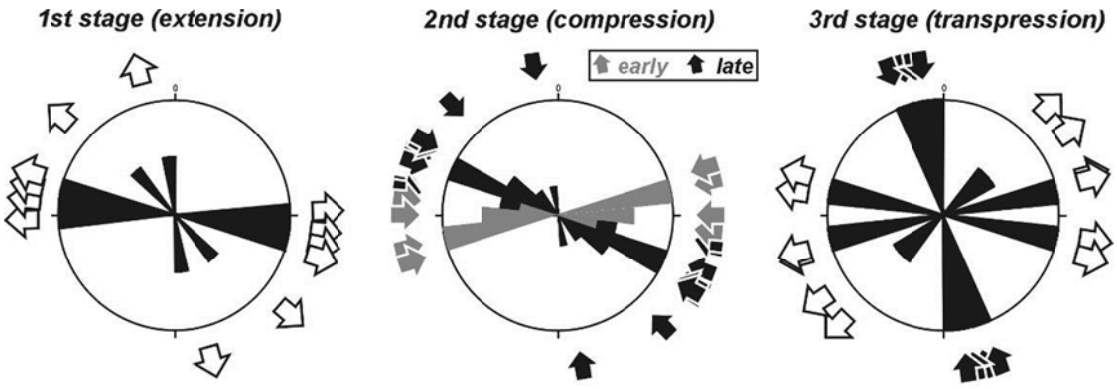

Fig. 5-46. Summary of paleostress direction recorded in the eastern flank of the southernmost Central Range. Three stages of paleostress could be recognized in this area. White divergent arrows: trends of extension. Black and gray convergent arrows: trends of compression.

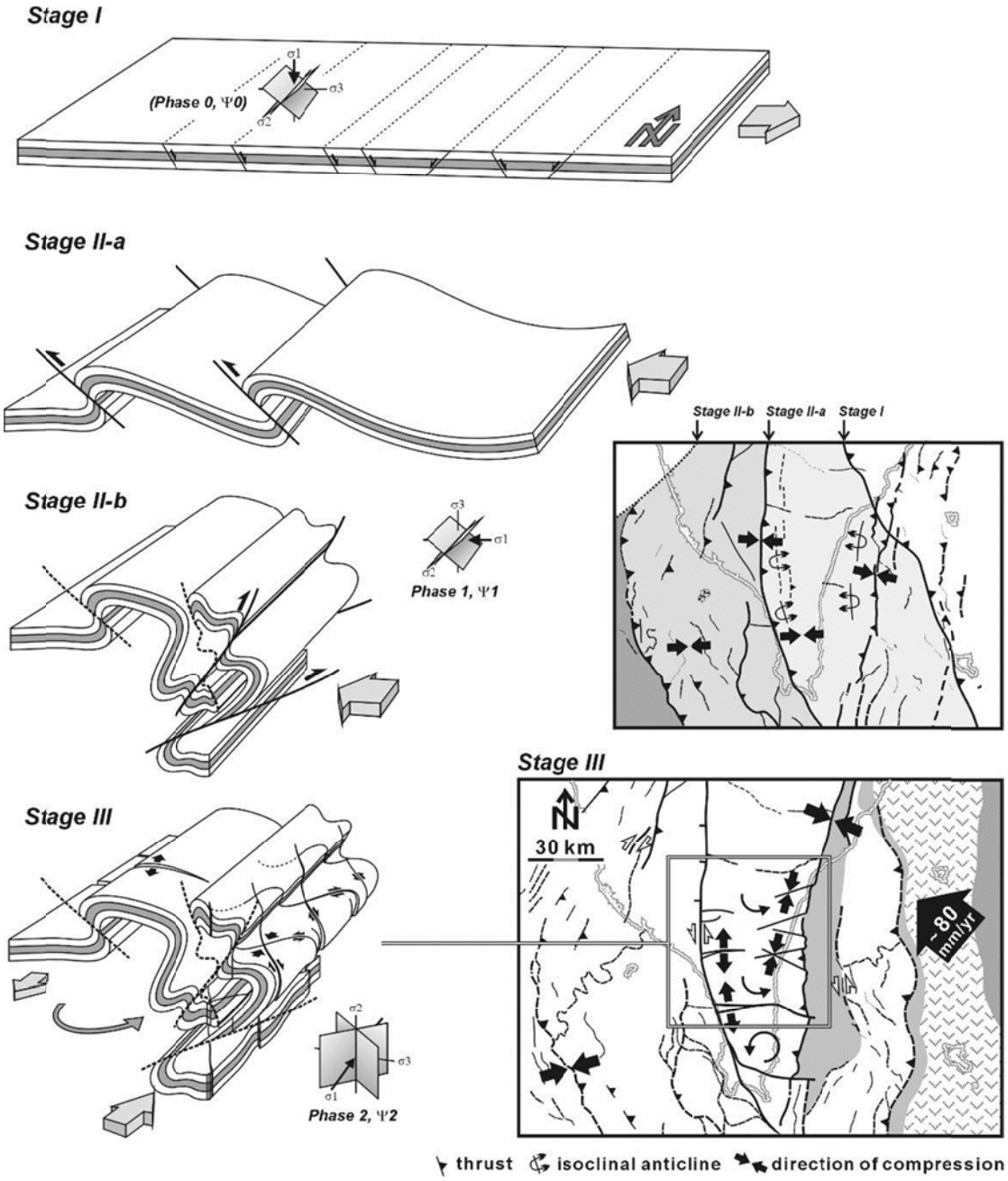

Fig. 5-47. Summary of the tectonic evolution of the southernmost Central Range. Note the apparent change in paleostress orientations during Stage III, as a consequence of the rotation of the mountain blocks and the intense arc collision.

Stop 5-2: A distant view of the Hengchun Western Terrace: Chienshih, Bridge 394.

At this stop, the shape and geometry of the Western Hengchun Hill can be observed. Three distinct geological units are distributed in the Hengchun Peninsula: the Middle-Late Miocene Mutan Formation turbidite in the east, the Plio-Pleistocene shallow marine sequences in the west, and the Kengting Melange along the Hengchun Velley. The high uplift rate in this area suggests fast rising of the block west of the Hengchun fault. Also, two reddish-green igneous blocks are exposed at Chienshan. The Chienshan blocks are strongly sheared and altered and consist mainly unsorted, unstratified angular fragments of basalt, diabase, gabbro, and anothosite (Page and Lan, 1983).

Fig. 5-48. A distant view toward the south at stop 5-2. The view shows the eastward-dipping West Hengchun Terrace (恆春西台地) on the right which is caused by a westward thrusting fault at depth according to Chen et al. (2005); Hengchun Longitudinal Valley in the middle; Hengchun Fault (恆春斷層), a sinistral-oblique thrust fault, which brings the older Miocene and Pliocene rocks on top of the Pleistocene sequence that underlies the West Hengchun Terrace. Chienshan (尖山), on the left, is one of the exotic block consisting of basaltic agglomerates and encased in the Kenting Formation. (Photo from Chen, W.-S. et al., 2000)

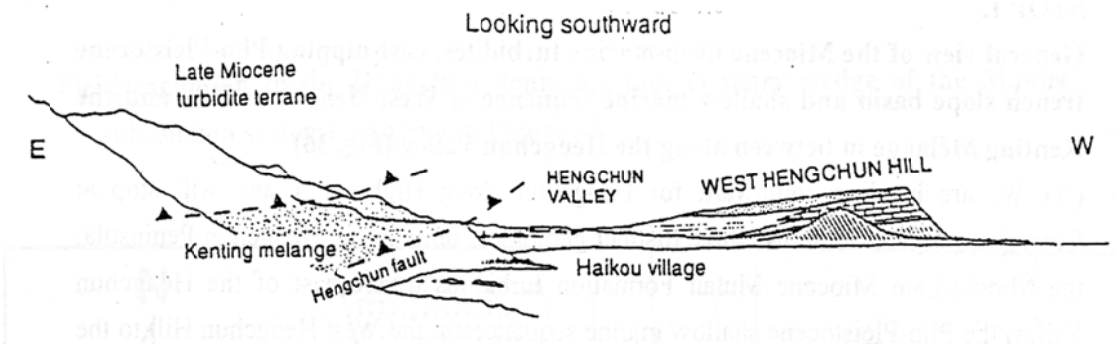

Fig. 5-49. Sketch of general geology of the Hengchun Peninsula viewed from Chienshan and relationship of formations and faults in the Hengchun Peninsula (drew by CP Chang in 1994).

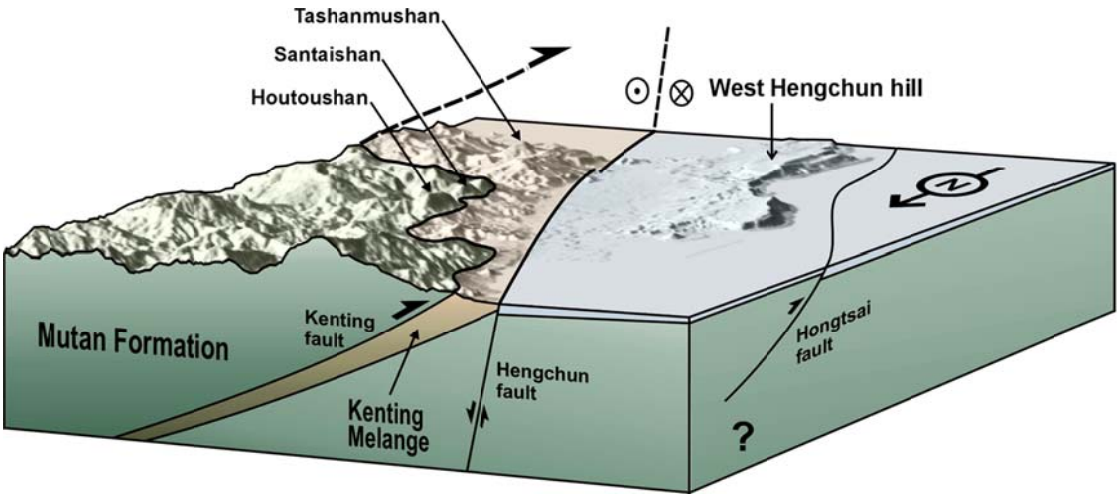

Fig. 5-50. The geometrical distribution of the shear features in the Kenting Mélange suggests that this zone dips to the east with an angle of about 30° or less. In order to avoid confusion, Chang et al. (2003) proposed to name the shear zone as the "Kenting Fault". To the east, in the hanging wall of the Kenting Fault, the Mutan Formation has been thrust westward along the Kenting Mélange and formed the principal mountain range of the Hengchun peninsula. To the west, in contrast with the sinuous upper boundary of the mélange zone, the western boundary of the Kenting Mélange is a linear structure, which is cut by the steeply east-dipping Hengchun Fault.

Stop 5-3: Shimen Conglomerate

The Miocene Shihmen Conglomerate is a late Miocene feeder channel along the Sschungchi river. The graves include qaurtzose sandstone, granite, schist, marl, gabbro, diabase, basalt, dacite and rhyolite. Most gravels are subrounded. Mafic igneous and meta-igneous lithic clasts form a natural gorge with both fining and

coarsening upward cycles. The presence of mafic rocks during the collision must be explained in any models of geological evolution of the Hengchun Peninsula.

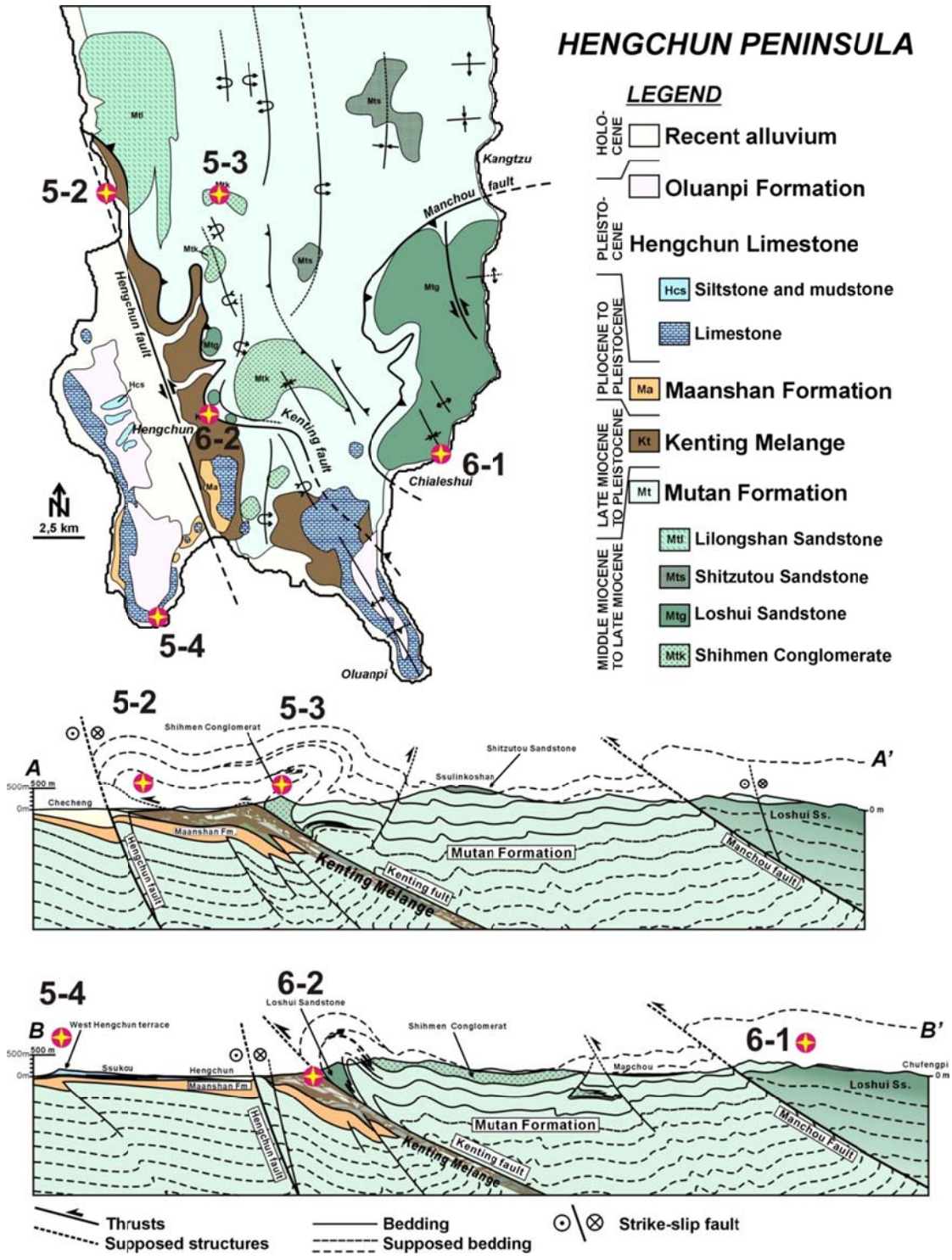

Fig. 5-51. General geological map and profiles of the Hengchun peninsula (Chang et al., 2003). The strike-slip component of strike-slip motion is indicated in the cross-sections by small circles with cross and dot.

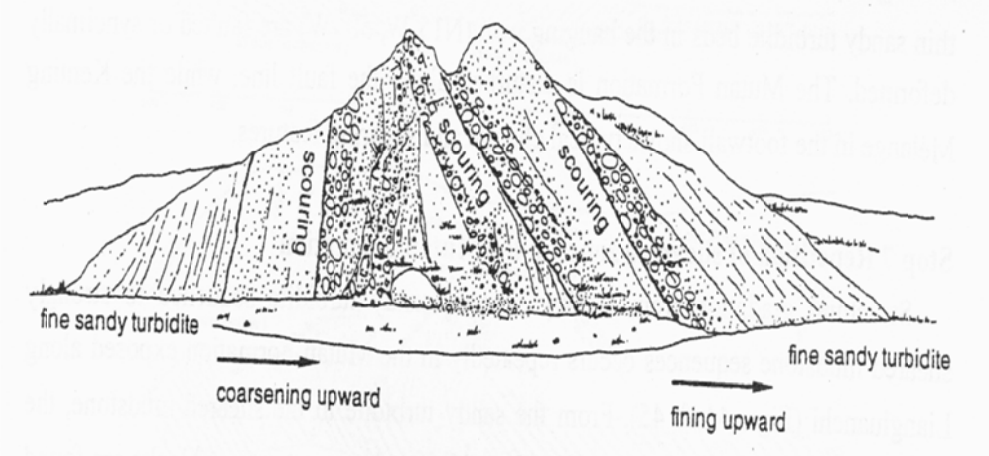

Fig. 5-52. Stop 5-3. Channel features preserved in the Shihmen Conglomerate (drew by CP Chang in 1994).

Stop 5-4: Hengchun Limestone: Maobitou

Situated on the southernmost tip of the southwest cape, Maobitou looks out to Oluanpi across the Bashi Channel, and got its name from a cat-like rock that broke off from the cliffs. Here you will find a typical coral reef coast, with interesting landforms such as fringing reef shores, slumping cliffs, eroded fissures, columns, and potholes.

Fig. 5-53. An aerial photograph of the Maobitou (Stop 5-4, from Chen, W.-S et al., 2000).

Fig. 5-54. Lower Pleistocene Limestone (Hengchun Limestone) showing tabular cross bedding exposed at Maobitou.

Stop 6-1. Miocene deep sea sandy turbidites: Chiaoloshui

At this stop we will observe a Miocene sandstone sequence, the Loshui Sandstone, deposited in a deep-sea fan (Fig. 5-55). Deep-sea sandstones and slumped turbidites are two main lithological characteristics in this coastal section. Typical turbidite features such as normal graded bedding with parallel lamination at base followed by climbing current ripples and mud drapes at top (Fig. 5-56A). Flute casts (Fig. 5-56B), slumped beds (Fig. 5-56C), dish structures (Fig. 5-56D), and erosional surfaces with rip-up-clasts are common features for thick and massive sandstone beds. Deep-sea traces of various ichnogenera, such as *Paleodictyon, Chondrites, Scolicia, Sublorenzina, Spirodesmos, Helminthopsis, Helminthoida, Planolites*, and *Belorhaphe* are frequently observed.

The strata here strike about N20°E with a dip of 20° to NE. The direction of flute casts is from south to north with a mean direction at 330°. No south-directed flute casts have ever been found. The north-directed paleocurrents in the Loshui Sandstone is a great contrast to the north-to-south paleocurrent direction measured also by flute casts in the Lilungshan Sandstone, western Hengchun Peninsula.

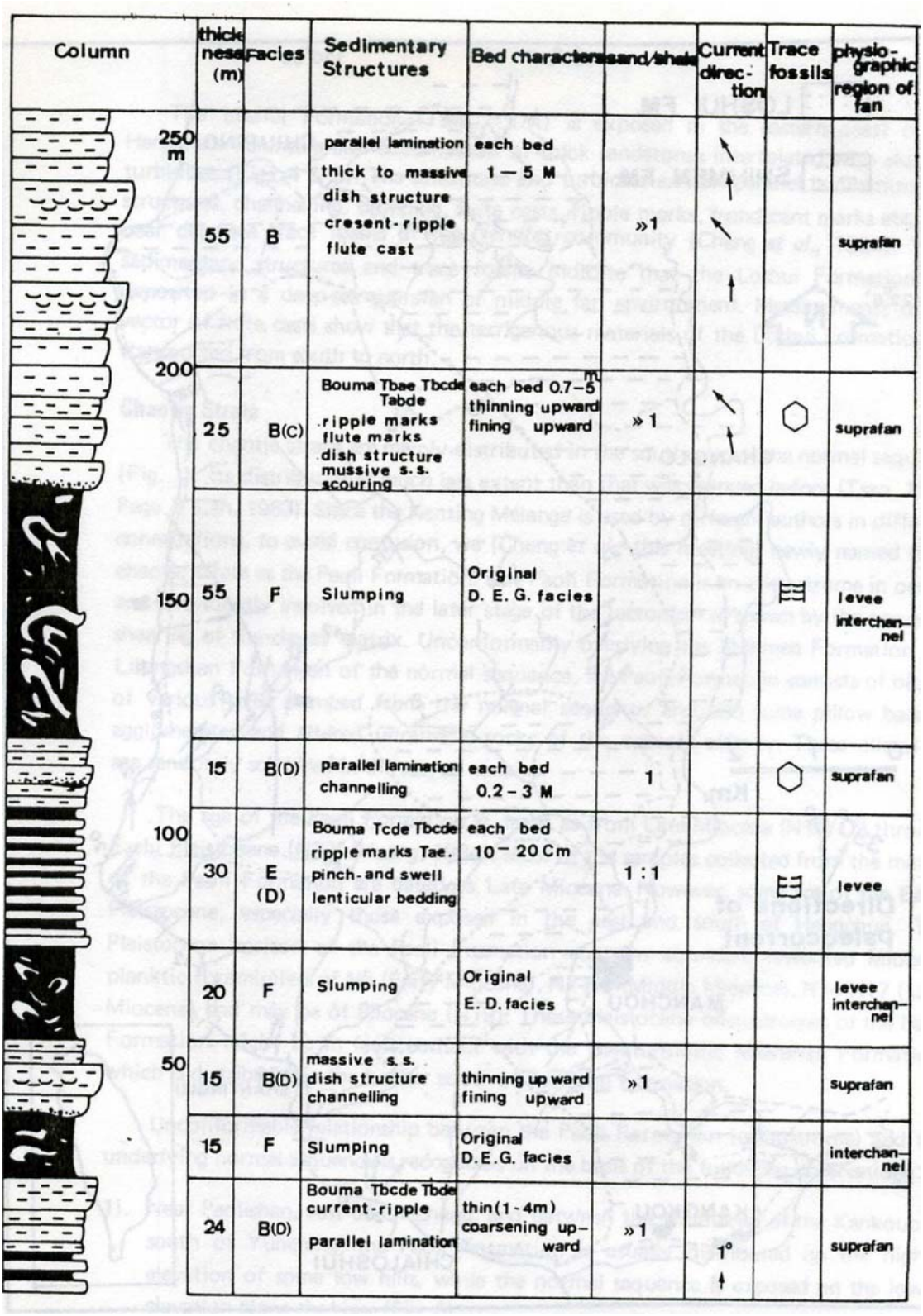

Fig. 5-55. Sedimentological log of the lower part of the Loshui Sandstone (Cheng et al., 1984) at Stop 6-1.

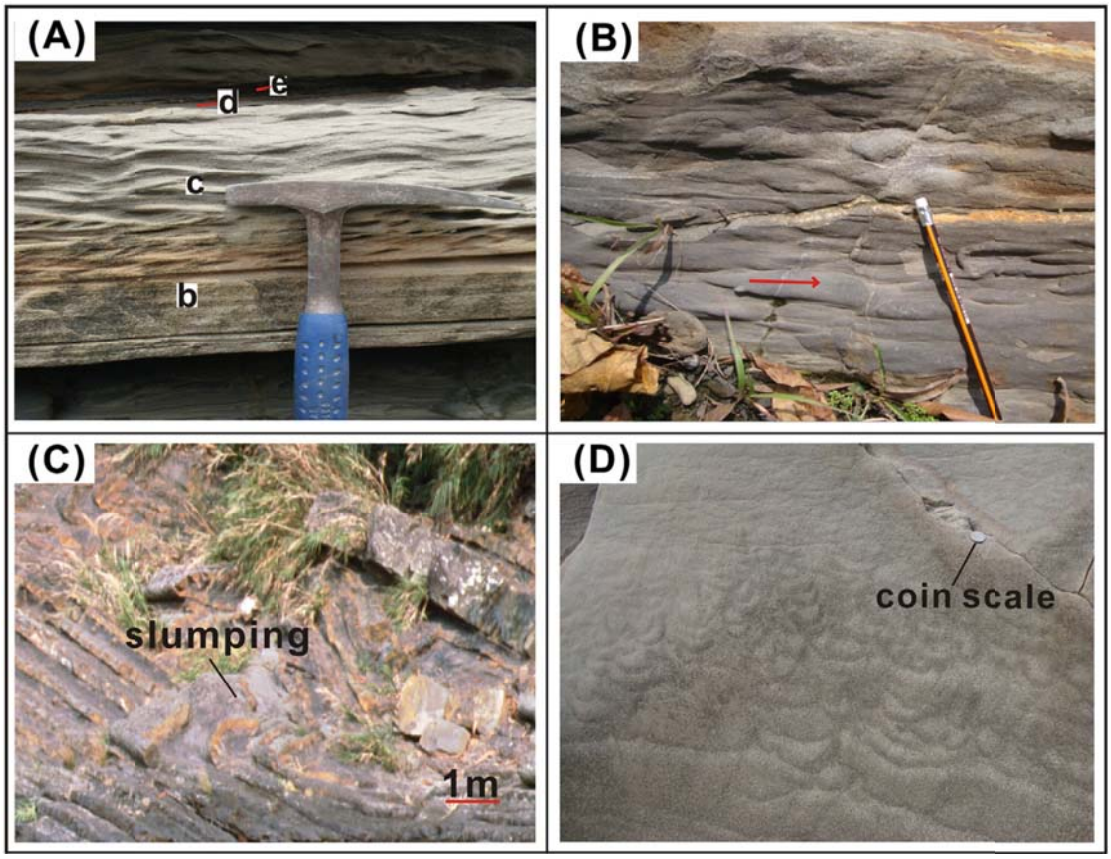

Fig. 5-56. Field photos at Hengchun Peninsula. (A) Turbidite strata with typical Bouma sequence, Tb-e, found in Loshui Formation, (B) flute cast can be seen easily in Mutan Formation and Loshui Sandstone (arrow pointing downstream), (C) slumping phenomenon in the Loshui Sandstone, (D) dish and plume structure are common in Sandstone showing a rapid deposition. (from Zhang et al., 2014)

Stop 6-2: Kenting Melange and gas seepages: Chuhou, Hengchun

Following Highway 200 from Hengchun to Manchou, the bus will pass the ancient East Gate of the Hengchun Town before reaching the famous Chuhou (Gasfires) (Fig. 5-57). The gas seepage at Chuhou is located in the Kenting Formation, and contains many fissures through which natural gas leaks to the surface and ignites.

An excellent exposure north to the “gas seepage” shows the typical features of the Kenting Mélange (Fig. 5-58). The exposure exhibits badland topography. Millimeter to meter sized blocks are mostly sheared and distributed randomly in the pervasively sheared argillaceous matrix. No stratification is visible in the mélange. White clay mineral dickite marks the shearing surface in the argillaceous matrix. In addition to some basalt blocks, major blocks found in the mélange are quartz-rich sandstone characterized by extension structures.

To the north of the Kenting Melange, the Mutan Formation is in contact with the mélange by a high-angle fault (strike N3°W/67° dipping to W; Figs. 5-59 and 5-60). Thin sandy turbidite beds in the hanging wall (N15°W, 50°W) are faulted or synclinally deformed. The Mutan Formation is disturbed along the fault line, while the Kenting Mélange in the footwall shows typical chaotic and shearing features.

Fig. 5-57. Flare of gas at dusk at Chuhou (From Chen, W.-S et al., 2000).

Fig. 5-58. An outcrop of the Kenting Formation north of Stop 6-3 at Chuhou

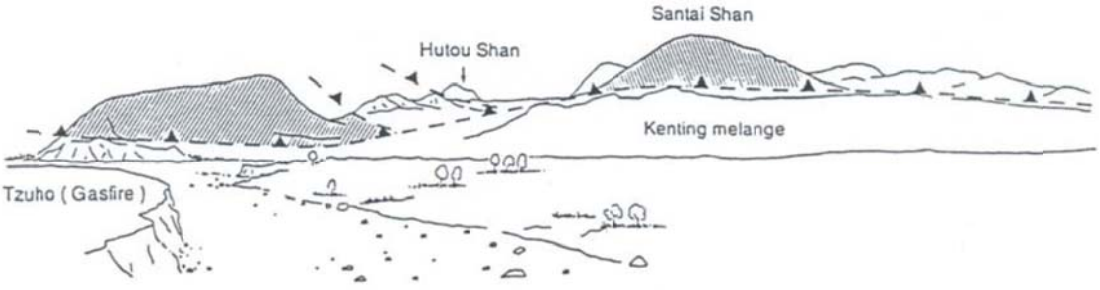

Fig. 5-59. A sketch of structures between the Kenting Mélange and the Mutan Formation (shaded) at Chuhou.

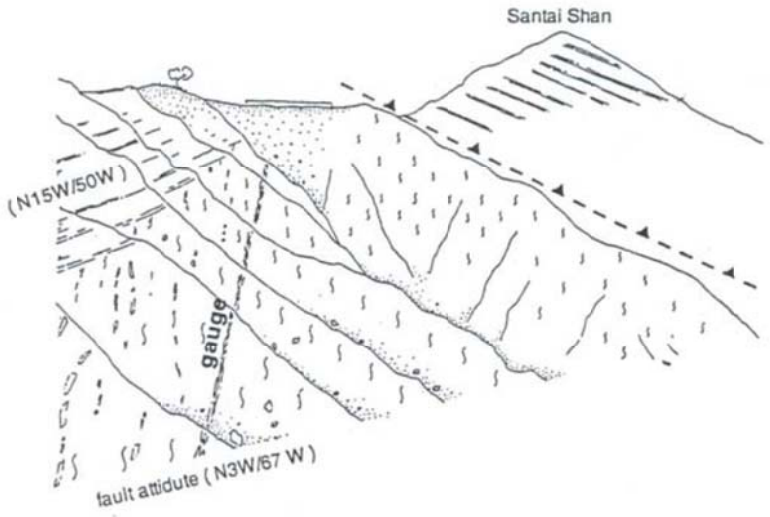

Fig. 5-60. Fault contact between the Kenting Mélange and the Mutan Formation at a good exposure north of Chuhou.

Stop 6-3: Chelungpu Fault Preservation Park (Chushan): Surface rupture by 1999 Chi-Chi earthquake (Mw 7.6)(Huang et al., 2016)

The 1999 Chi–Chi earthquake in Taiwan introduced earthquake geologists to two phenomena of ground rupture associated with thrust faulting that had been uncommonly observed previously. Taiwanese geologists noted early in their field investigations that one rarely observed a fault in the escarpment at the leading edge of a thrust. Rather, one commonly observed a monocline–like escarpment. The heights of monocline–like escarpments ranged from 10 m in the north to 1 m in the south over the 100 km length of the N–S part of the Chi–Chi rupture. The second feature they recognized in a few places is that there can be a *ground deformation–zone* associated with the escarpment. Although the most intense deformation typically occurred at the escarpment, there was typically noticeable deformation nearby, especially in the hanging wall of the thrust. The deformation caused much of the damage to dwellings, large structures and infrastructure of communities through which the rupture passed.

Taliwun village at Chushan, Nantou, where Chelungpu Fault Preservation Park is located is a rare place where one can still see the damage to dwellings within the Chi-Chi deformation-zone and the mononcline-like escapement. One of the best possible illustrations of relations between shapes of escarpments and subsurface structures is exposed in a trench of the Chelungpu Fault Preservation Park, a division of the Taiwan National Museum of Natural Science, near the south end of 1999 Chi–Chi deformation–zone (Fig. 5-51). The site of the trench was excavated twice. The purpose of the first excavation in 2002 is for the study of paleoearthquake on Chelungpu fault. Afterwards, the trench was filled up to avoid weathering and erosion. The second excavation in 2012 is for education and display purposes. Thus, the 2012 excavated trench is preserved at the Park. In addition, some damaged dwellings within the Chi-Chi deformation-zone remain tens of meters northeast of the Park.

Prior to the 1999 earthquake, the ground at the site of the Chushan trench was an essentially flat building site, sloping gently SW. There was a one-storey brick building with a yard and a vegetable garden at the site prior to the 1999 earthquake. After the earthquake, but before the trench was excavated, the ground surface in the escarpment appeared as a low warp. The trace of a monocline-like escarpment passed through the site of the house and formation of the escarpment destroyed the house. The Chushan trench was excavated with its long axis (Fig. 5-51A) passing through the escarpment. The exposures of sedimentary units and the structures in the two walls of the trench are spectacular. The trench provided an ideal combination of wonderful exposure, distinctive stratigraphic units, material

properties conducive to faulting, and variety of structures (Figs. 5-52, 5-53, 5-54, 5-55 and 5-56).

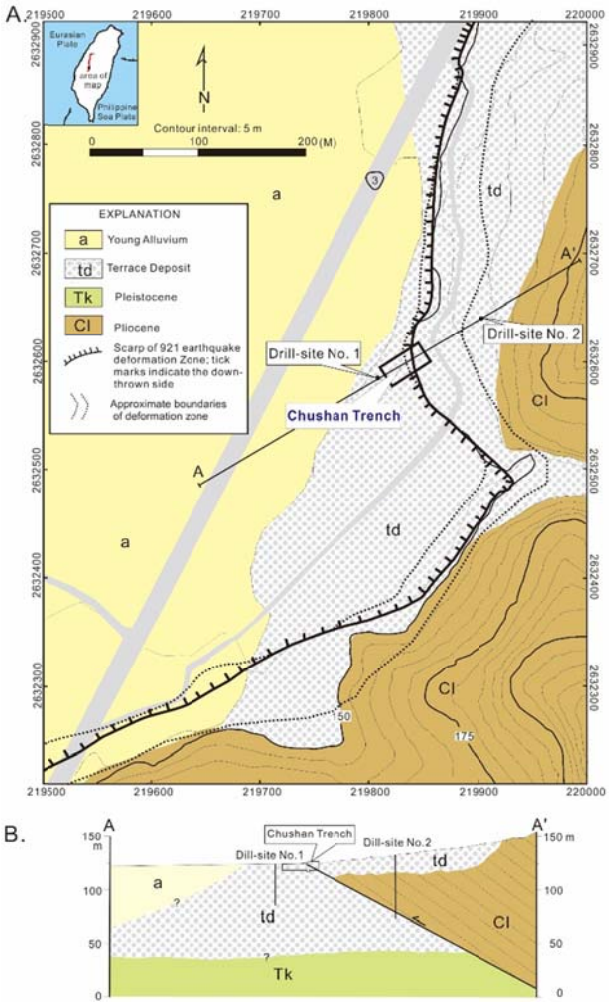

Fig. 5-51. Local geologic setting of Chushan trench in the village of Tanliwun, Taiwan. The trench is named after the city of Chushan, 5 km SW of Tanliwun. A. Chushan trench is on a low terrace. Young alluvium spreads out west of Chushan trench. The hills adjacent to the trench are composed mainly of Pliocene rocks. B. Cross section of area of Chushan trench. The boreholes were drilled as part of the trenching project. The trench and borehole no. 2 suggest a reverse fault dipping eastward that slipped a few m during the 1999 earthquake. Over a long time, the Pliocene rocks in the hanging wall have been lifted up several hundred meters (Huang et al., 2016).

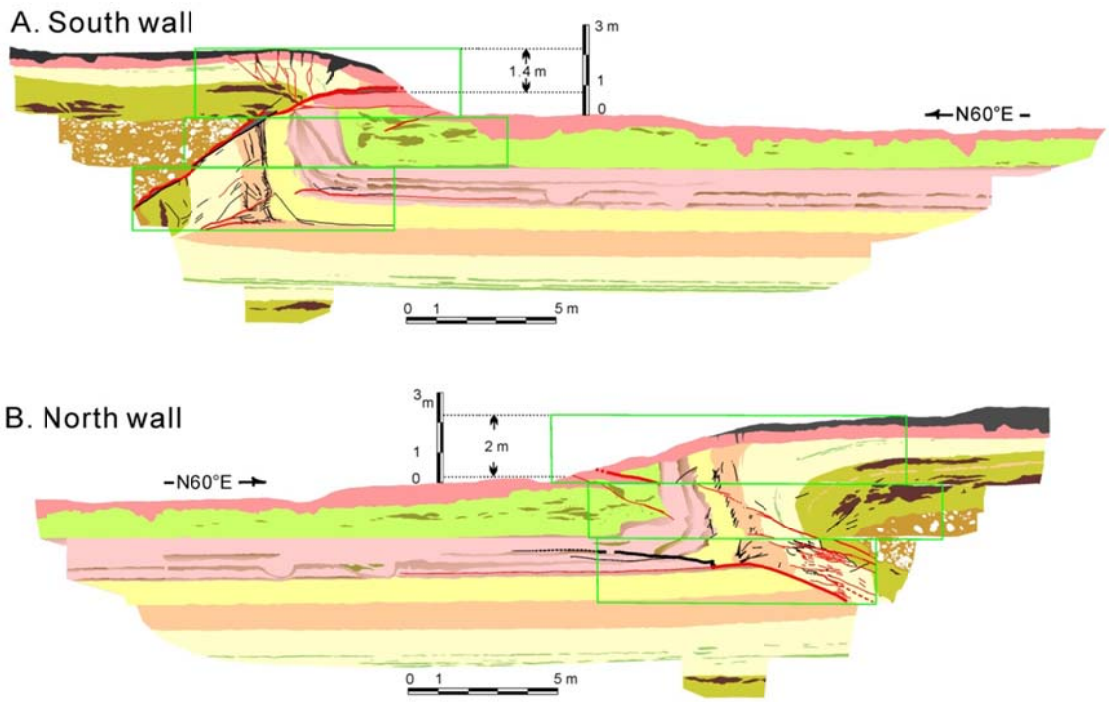

Fig. 5-52. Profiles of the ground surface and cross sections of south wall (A) and north wall (B) of Chushan trench excavated in 2002 (slightly modified from Chen et al., 2007). Thicknesses of red and black lines indicate different offsets on faults: The thicker the line, the larger the offset. Faults in red were judged to have been active during Chi-Chi earthquake. Faults in black were dormant. Faults in areas bounded with are shown in detailed maps in Figs. 5-53B and 5-54B.

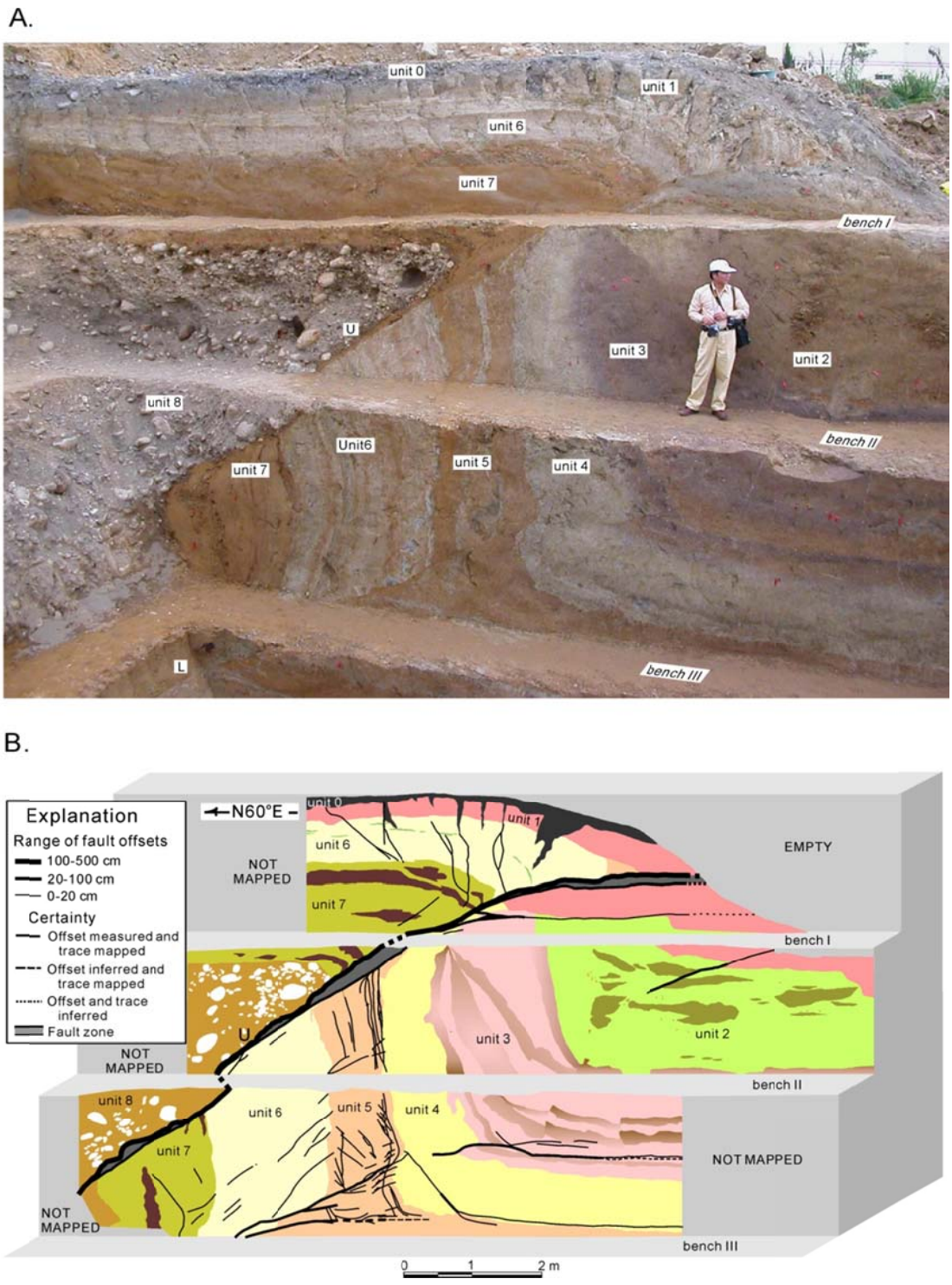

Fig. 5-53. Structures exposed in the south wall of Chushan trench excavated in 2002. Unit 0: man-made fill. Unit 1: top soil. Unit 2: yellowish brown clayey, sandy silt with lenses of gravel. Unit 3: packages of brown clayey, sandy silt overlain by dark violet clayey sandy silt at top of each package. Unit 4: bluish sandy, clayey silt. Unit 5: brown clayey sandy silt with two thin beds of gray silt or silty clay. Unit 6: light gray sandy clayey silt. Unit 7: brown clayey sandy silt with lenses of gravel. Unit 8: bouldery, cobbly gravels. A. NE end of south wall of Chushan trench. B. Map of same area of south wall, showing stratigraphic units, faults and a highly asymmetric syncline. The upper main fault (U) is indicated by heavy solid lines. It strikes parallel

to the short, NE wall of the trench and dip toward the NE. Two branches of the lower main fault (L) indicated by medium-thick solid lines are exposed in Unit 6 and Unit 5. The structure exposed in the south wall is in essence a fault zone and a highly asymmetric syncline, the steep limb of which is truncated by the upper main fault.

A.

B.

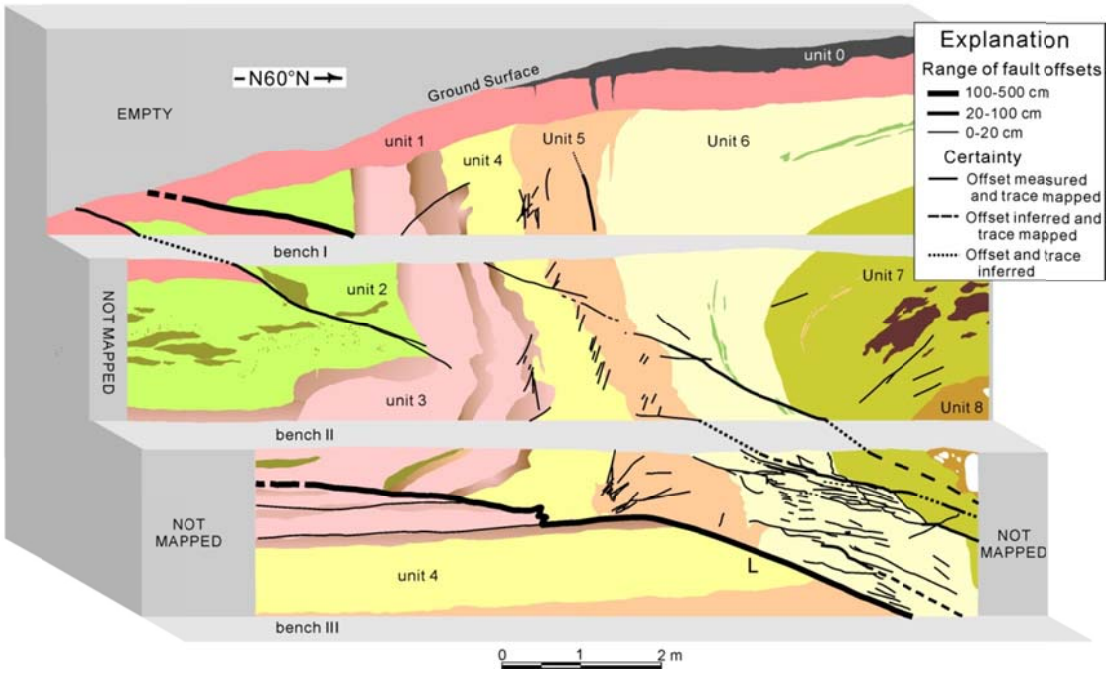

Fig. 5-54. Structures exposed in the north wall of Chushan trench excavated in 2002. Stratigraphic units defined in caption to Fig. 5-53A. A. NE end of north wall. B. Map of same area, showing stratigraphic units and faults. The fault zone in the north wall of the Chushan trench contains the main lower (L) fault within the face of the third bench in the trench. The maximum apparent dip is 27° and the maximum apparent slip is about 3 m for this fault. The lower main fault becomes three horizontal faults within the face of the third bench. The pebbly bouldery cobbly gravel, Unit 8, overlying the main fault was deformed into a nearly recumbent anticline. Unit 7 is conformable with the gravel and with Unit 6. Unit 6 forms a more open anticlinal hinge. It reappears in the footwall of the lower main fault as a horizontal layer in the wall of the fourth bench.

Fig. 5-55. Structures exposed in the south wall of Chushan trench excavated in 2012. The difference of structures on the south walls in between 2012 and 2002 (Fig. 5-53A) is difficult to tell. [Photograph by Liu Yung-Chu]

Fig. 5-56. Structures exposed in the north wall of Chushan trench excavated in 2012. The difference of structures on the north walls in between 2012 and 2002 (Fig. 5-54A) is observable, in particular, via Unit 4. Unit 4: bluish sandy, clayey silt. [Photograph by Liu Yung-Chu]

References

Angelier, J., Lee, J.-C., Hu, J.-C. and Chu , H.-T. (2003) Three-dimensional deformation along the rupture trace of the September 21st, 1999 , Taiwan earthquake: a case study in the Kuangfu school. J. Struct. Geol., 25, 3, 351-370.

Barrier, E. and Chu, H.-T. (1984) Field trip guide to the Longitudinal Valley and the Coastal Range in Eastern Taiwan. Sino-French Colloquium, pp.27-49.

Barrier, E. and Muller, C. (1984) New observations and discussion on the origin and age of the Lichi Melange. Mem. Geol. Soc. China, 6, 303–326.

Biq, C. (1971) Comparison of melange tectonics in Taiwan and in some other mountain belts. Petrol. Geol. Taiwan, 9, 79-106.

Biq, C. (1973) Kinematic pattern of Taiwan as an example of actual continent–arc collision. Report of the Seminar on Seismology. US–ROC Cooperative Science Program 25, 149–166.

Biq, C. (1977) The Kenting Mélange and the Manila Trench. Proc. Geol. Soc. China 20, 119-122.

Byrne, T. (1998) Pre-collision kinematics and a possible modern analog for the Lichi and Kenting melanges, Taiwan. J. Geol. Soc. China 41, 535-550.

Byrne, T. (1995) Deformation partitioning and tectonic exhumation in the pre-collision zone of the Taiwan orogenic belt. EOS, AGU Transactions, 76(46), F635.

Chai, B.H.T. (1972) Structure and tectonic evolution of Taiwan. Am. J. Sci., 272, 389–422.

Chang, C.-P., Angelier, J. and Huang, C.-Y. (2000) Origin and evolution of a melange: the active plate boundary and suture zone of the Longitudinal Valley, Taiwan. Tectonophysics, 325, 43-62.

Chang, L.-S. (1963) A biostratigraphic study of the so-called Hori Slate in central Taiwan based on smaller foraminifera. Proc. Geol. Soc. China, 6, 3-17.

Chang, L.-S. (1967) A biostratigraphic study of the Tertiary in the Coastal Range, eastern Taiwan, based on smaller foraminifera. (I. Southern Part). Proc. Geol. Soc. China, 10, 64-76.

Chang, L.-S. (1968) A biostratigraphic study of the Tertiary in the Coastal Range, eastern Taiwan, based on smaller foraminifera. (II. Northern Part). Proc. Geol. Soc. China, 11, 19-33.

Chang, L.-S. (1969) A biostratigraphic study of the Tertiary in the Coastal Range, eastern Taiwan, based on smaller foraminifera. (III. Middle Part). Proc. Geol. Soc. China, 12, 89-101.

Chang, L.-S. (1970) A biostratigraphic study of the so-called slate formation on the

east flank of the Central Range between Tawu and Taimali, southeastern Taiwan, based on smaller foraminifera. Proc. Geol. Soc. China, 13, 129-142.

Chang, L.-S., and Chen, T.-H. (1970) A biostratigraphic study of the Tertiary along the Hsiukuluanchi in the Coastal Range, eastern Taiwan, based on smaller foraminifera. Proc. Geol. Soc. China, 13, 115-128.

Chang, L.-S. (1972). Eocene/Miocene hiatus and N Conglomerate in the Central Range of Taiwan. Proc. Geol. Soc. China, 15:93–98.

Chang, S.S.-L. (1971) Subsurface geologic study of the Taichung basin. Petrol. Geol. Taiwan, 8, 21-45.

Chang, S.S.-L. and Chi, W.-R. (1983) Neogene nannoplankton biostratigraphy in Taiwan and the tectonic implications. Petrol. Geol. Taiwan, 19, 93-147.

Chen, C.-H. (1977) Some stratigraphic problems of the Hsuehshan Range of Taiwan. Proc. Geol. Soc. China, 20, 61-70.

Chen, C.-H. (1979) Geology of the east-west cross-island highway in central Taiwan. Mem. Geol. Soc. China, 3, 219-236.

Chen, P.-H., Huang, T.-C., Huang, C.-Y. and Chiang, M.-C., Lo, S.-R. and Kuo, C.-L. (1977) Paleomagnetic and coccolith stratigraphy of Plio-Pleistocene shallow marine sediments, Chuhuangkeng, Miaoli. Petrol. Geol. Taiwan, 14, 219-239.

Chen, S.C. and Wu, C.-H. (2006) Slope stabilization and landslide size on Mt. 99 Peaks after Chichi Earthquake in Taiwan. Environmental Geology, 50(5), 623-636.

Chen, W.-C., Chu, H.-T. and Lai, T.-C. (2000) Surface ruptures of the Chi-Chi Earthquake in the Shihgang Dam area. Spec. Publ. Centr. Geol. Surv., 12, 41-62.

Chen, W.-S. (1991) Origin of the Lichi Mélange in the Coastal Range, eastern Taiwan. Spec. Publ. Central Geol. Surv., 5, 257–266.

Chen, W.-S. (1997a) Mesoscopic structures developed in the Lichi Mélange during the arc–continent collision in the Taiwan region. J. Geol. Soc. China, 40, 415–434.

Chen, W.-S. (1997b) Lithofacies analyses of the arc-related sequence in Coastal Range, eastern Taiwan. J. Geol. Soc. China, 40(2), 313-338.

Chen, W.-S., Chow, M.-H. and Lee, K. (2000) An In-depth Travel Guide for the Hengchun Peninsula. Yuan-Liou Publishing, Taipei, Taiwan, 271pp. (in Chinese)

Chen, W.-S., Ridgeway, K. D., Horng, C.-S., Chen, Y.-G., Shea, K.-S. and Yeh, M.-G. (2001) Stratigraphic architecture, magnetostratigraphy, and incised-valley systems of the Pliocene-Pleistocene collisional marine foreland basin of Taiwan. Bull. Geol. Soc. Am., 113, 1249-1271.

Chen, W.-S. and Wang, Y. (1988) Volcaniclastic and biogenic sequence of the Tuluanshan Formation, Coastal Range, Taiwan. Symposium on the Arc-continent Collision and Orogenic Sedimentation in eastern Taiwan and Ancient Analogs, Field Guidebook, 6-1~6-27.

Chen, W.-S., Lee, W.-C., Huang, N.-W., Yen, I-C., Yang, C.-C., Yang, H.-C., Chen, Y.-C. and Sung, S.-H. (2005) Characteristics of accretionary prism of Hengchun Peninsula, southern Taiwan: Holocene activity of the Hengchun Fault. Western Pacific Earth Sciences, 5, 129-154. (in Chinese)

Chen, Y.-G. and Liu, T.-K. (1993) Holocene radiocarbon dates in Hengchun Peninsula and their neotectonic implications. J. Geol. Soc. China, 36(4), 457-479.

Cheng, Y.-M. and Wei, K.-Y. (1983) The calcareous nannofossils and larger foraminifera Lepidocyclina in the Kangkou Limestone, Coastal Range, eastern Taiwan. Tih-Chih, 4(2), 51-66.

Chi, W.-R., Namson, J. and Suppe, J. (1981) Record of plate interactions in the Coastal Range, eastern Taiwan. Mem. Geol. Soc. China, 4, 155-194.

Chi, W.-R. (1982) The calcareous nannofossils of the Lichi Melange and the Kenting Melange and their significance in the interpretation of plate-tectonics of the Taiwan region. Ti-Chih, 4(1), 99-114.

Chi, W.-R., and Chu, H.-T. (1982) Calcareous nannofossils from the fillings of the columnar joints of the Wushihpi andesites, Coastal Range, eastern Taiwan. Acta Geologica Taiwanica, 21, 195-200.

Chi, W.-R., Huang, H.-M. and Wu, J.-C. (1983) Ages of the Milun and Pinanshan Conglomerated and their bearings on the Quaternary movement of eastern Taiwan. Proc. Geol. Soc. China, 26, 67-75.

Chou, J.-T. (1973) Sedimentology and palaeogeography of the Upper Cenozoic System of western Taiwan. Proc. Geol. Soc. China, 16, 111-143.

Chou, J.-T. (1980) Stratigraphy and sedimentology of the Miocene in western Taiwan. Petrol. Geol. Taiwan, 17, 33-52.

Chu, H. T., Shen, P. and Jeng, R. C. (1988) The origin of chromitite from the Kenting melange, southern Taiwan. Proc. Geol. Soc. China, 31:33-52.

Chung, J.-K. and Shin, T.-C. (1999) Implication of the rupture process from the displacement distribution of strong ground motions recorded during the 21 September 1999 Chi-Chi, Taiwan earthquake. Terrestrial, Atmospheric and Oceanic Sciences, 10(4), 777-786.

Chung, S.-L. and Sun, S.-S. (1992) A new genetic model for the East Taiwan Ophiolite and its implications for Dupal domains in the Northern Hemisphere. Earth Plant. Sci. lett., 109, 133-145.

Chung, S.-L., Sun, S.-S., Tu, K., Chen, C.-H. and Lee, C.-Y. (1994) Late Cenozoic basaltic volcanism around the Taiwan Strait, SE China: product of lithosphere-asthenosphere interaction during continental extension. Chem. Geol., 112, 1–20.

Clark, M.B., Fisher, D.M., Lu, C.-Y. and Chen, C.-H. (1993) Kinematic analyses of the

Hsuehshan Range, Taiwan: a large-scale pop-up structure. Tectonics, 12, 205-218.
Clark, M.B. and Fisher, D.M. (1995) Strain partitioning and crack-seal growth of chlorite-muscovite aggregates during progressive noncoaxial strain: an example from the slate belt of Taiwan. J. Struct. Geol., 17(4), 461-474.
Covey, M. (1986) The evolution of foreland basins to steady state: evidence from the western Taiwan foreland basin. In Allen, P.A. and Homewood, P., editors, Foreland Basins, Int. Assoc. Sedimentol., Spec. Publ., 8, 77-90.
Crespi, J.M., Chan, Y.-C. and Swaim, M.S. (1996) Synorogenic extension and exhumation of the Taiwan hinterland. Geology, 24(3), 247-250.
Davis, D., Suppe, J. and Dahlen, F.A. (1983) Mechanics of fold-and-thrust belts and accretionary wedges. J. Geophys. Res., 88, 1153-1172.
Ernst, W.G. (1977) Olistostromes and included ophiolite debris from the Coastal Range of eastern Taiwan. Mem. Geol. Soc. China, 2, 97–114.
Ernst, W.G., Liou,J.-G. and Moore, D.E. (1981) Multiple metamorphic events recorded in Tailuko amphibolites and associated rocks of the Suao-Nanao area, Taiwan. Mem. Geol. Soc. China, 4, 391-441.
Ernst, W.G., Ho, C.-S. and Liou, J.-G. (1985) Rifting, drifting, and crustal accretion in the Taiwan sector of the Asiatic continental margin. In Howell, D.G., editor, Tectonostratigraphic terranes of the Circum-Pacific region. Circum-Pacific Council for En. Min. Res. Earth Sciences Series, 1, 375-389.
Ernst, W.G. and Jahn, B.-M. (1987) Crustal accretion and metamorphism in Taiwan, a post-Palaeozoic mobile belt. Phil. Trans. Roy. Sco. Lond., 321, 129-161.
Fuller, C.W., Willett, S.D., Fisher, D., Lu, C.-Y. (2006) A thermomechanical wedge model of Taiwan constrained by fission-track thermochronometry. Tectonophysics, 425, 1-24.
Ho, C.S. (1977) Mélanges in the Neogene sequence of Taiwan. Mem. Geol. Soc. China, 2, 85–96.
Ho, C.S., (1988) An introduction to the geology of Taiwan: explanatory text of the geology map of Taiwan, 2nd Ed., Ministry of Economic Affaires, R.O.C., 192p.
Ho, H.-C. and Chen, M.-M. (2000) Geologic map and explanatory text of Taiwan: Taichung Sheet, scale 1:50,000. Centr. Geol. Surv., Taiwan.
Hsu, T.-L (1956) Geology of the Coastal Range, eastern Taiwan. Bull. Geol. Surv. Taiwan, 8, 39-63.
Hsu, T.-L. (1976) The Lichi Mélange in the Coastal Range framework. Bull. Geol. Surv. Taiwan, 25, 87-95.
Hsu, K.J. (1988) Mélange and the mélange tectonics of Taiwan. Proc. Geol. Soc. China, 31, 87–92.
Huang, C.-Y. and Cheng, Y.-M. (1983) Oligocene and Miocene planktonic foraminiferal

biostratigraphy of northern Taiwan. Proc. Geol. Soc. China, 26, 21-56.
Huang, C.Y., Wu, W.Y., Chang, C.P., Tsao, S., Yuan, P.B., Lin, C.W., Xia, K.Y. (1997) Tectonic evolution of accretionary prism in the arc-continent collision terrane of Taiwan. Tectonophysics 281, 31-51.
Huang, C.Y., Yuan, P.B., Lin, C.W., Wang, T.K., Chang, C.P. (2000) Geodynamic processes of Taiwan arc-continent collision and comparison with analogs in Timor, Papua New Guinea, Urals and Corsica. Tectonophysics, 325, 1-21.
Huang, C.Y., Yuan, P.B., Tsao, S.J. (2006) Temporal and spatial records of active arc-continent collision in Taiwan: A synthesis. GSA Bulletin 118(3/4), 274-288.
Huang, T.-C. (1980a) Calcareous nannofossils from the slate terrane west of Yakou, Southern Cross-Island Highway. Petrol. Geol. Taiwan, 17:59–74.
Huang, T.-C. (1980b) Oligocene to Pleistocene calcareous nannofossil biostratigraphy of the Hsuehshan Range and Western Foothills in Taiwan. Geology and Palaeontology of Southeast Asia, 21:191–210.
Huang, T.-C. and Ting, J.-S. (1981) Calcareous nannofossil biostratigraphy of the upper Neogene in the shallow-sea deposits of Taiwan. Ti-Chih, 3, 105-119. (in Chinese)
Huang, T.-C. (1982) Tertiary calcareous nannofossil stratigraphy and sedimentation cycles in Taiwan. In Proceedings of the Second ASCOPE Conference and Exhibition, pages 837–886, Manila, Philippines.
Huang, T.-C. and Chi, W.-R. (1979) Calcareous nannofossils of the subsurface pre-Miocene rocks from the Peikang Basement High and adjacent areas in western central Taiwan (part II, Palaeocene). Petrol. Geol. Taiwan, 16, 95–129.
Huang, T.-Y. (1969) Some planktonic foraminifera from a borehole at Shihshan, near Taitung, Taiwan. Proc. Geol. Soc. China, 12, 103-119.
Huang, T.-C. (1976) Neogene calcareous nannoplankton biostratigraphy viewed from the Chuhuangkeng section, northwestern Taiwan. Proc. Geol. Soc. China, 19, 7-24.
Huang, W.-J., Chen, W.-S., Lee, Y.-H., Yang, C.C., Lin, M.-L., Chiang, C.-S., Lee, J.-C., and Lu, S.-T. (2016) Insights from heterogeneous structures of the 1999 Mw 7.6 Chi-Chi earthquake thrust termination in and near Chushan excavation site, central Taiwan Journal of Geophysical Research, doi: 10.1002/2015JB012174.
Jahn, B.-M. and Liou, J.-G. (1977) Age and geochemical constraints of glaucophane schists of Taiwan. Mem. Geol. Soc. China, 2, 129-140.
Jahn, B.-M., Liou, J.-G. and Nagasawa, H. (1981) High pressure metamorphic rocks of Taiwan: REE geochemistry, Rb-Sr ages and tectonic implications. Mem. Geol. Soc. China, 4, 497-520.
Jahn, B.-M., Martineau, F., Peucat, J. J. and Cornichet, J. (1986) Geochronology of the Tananao Schist Complex, Taiwan, and its regional tectonic significance.

Tectonophysics, 125, 103–124.
Jahn, B.-M. (1988) Pb-Pb dating of young marbles from Taiwan and its tectonic implications. Nature, 332, 429-432.
Jahn, B.-M. and Cuvellier, H. (1994) Pb-Pb and U-Pb geochronology of carbonate rocks and direct dating of sedimentary sequences: an assessment. Chem. Geol., 115, 125-151.
Juang,W.-S. (1996) Geochronology and geochemistry of basalts in theWestern Foothills, Taiwan. Bulletin of the National Museum of Natural Sciences, 7, 45–98.
Juang, W.-S. and Bellon, H. (1984) The potassium-argon dating of andesites from Taiwan. Proc. Geol. Soc. China, 27, 86-100.
Juang, W.-S. and Bellon, H. (1986) Potassium-argon ages of the Tananao Schist in Taiwan. Mem.Geol. Soc. China, 7:405–416.
Kao, H., and Chen, W.P. (2000) The Chi-Chi Earthquake sequence: Active, Out-of-Sequence Thrust Faulting in Taiwan. Science. 288, 2346-2349.
Karig, D.E. (1973) Plate convergence between the Philippines and the Ryukyu Islands. Mar. Geol., 14, 153–168.
Lan, C.-Y., Lee, T., and Wang-Lee, C. M. (1990) The Rb-Sr isotopic record in Taiwan gneisses and its tectonic implication. Tectonophysics, 183, 129–143.
Lan, C.-Y., Jahn, B.-M., Mertzman, S.A. and Wu, T.-W. (1996) Subduction-related granitic rocks of Taiwan. J. Asian Earth Sciences, 14, 11-28.
Lee, C.-J. (1991) Depositional aspects of Eocene in Taiwan and some tectonic implications. Spec. Publ. Centr. Geol. Surv., 6, 189–206.
Lee, J.-C., Angelier, J. and Chu, H.-T. (1997) Polyphase history and kinematics of a complex major fault zone in the northern mountain belt: the Lishan Fault. Tectonophysics, 274, 97-115.
Lee, J.-C., Angelier, J., Chu, H.-T., Yu, S.-B. and Hu, J.-C. (1998) Plate-boundary strain partitioning along the sinistral collision suture of the Philippine and Eurasian plates: Analysis of geodetic data and geological observation in southeastern Taiwan: Tectonics, 17, 6, 859-871.
Lee, J.-C., Chu, H.-T., Angelier, J., Chan, Y.C., Hu, J.C., Lu, C.Y. and Rau, R.J. (2002) Geometry and structure of northern surface ruptures of the 1999 Mw=7.6 Chi-Chi, Taiwan earthquake: influence from inherited fold belt structures. J. Struct. Geol., 24(1), 173-192.
Lee, Y.-H. and Yang, C.-N. (1994) Structural evolution in the Tayulin area of the Central Range. Bull. Centr. Geol. Surv., 9, 77-105.
Lin, A. T. and Watts, A. B. (2002) Origin of the West Taiwan basin by orogenic loading and flexure of a rifted continental margin. J. Geophys. Res., 107, ETG2-1 – 2-19.
Lin, A.T., Watts, A.B. and Hesselbo, S.P. (2003) Cenozoic stratigraphy and subsidence

history of the South China Sea margin in the Taiwan region. Basin Research, 15(4), 453-478.

Lin, C.-H., Yeh, Y.-H., Yen, H.-Y., Chen, K.-C., Huang, B.-S., Roecker, S.W. and Chiu, J.-M. (1998) Three-dimensional elastic wave velocity structure of the Hualien region of Taiwan: Evidence of active crustal exhumation. Tectonics, 17, 89-103.

Liou, J.G., Suppe, J. and Ernst, W.G. (1977a) Conglomerates and pebbly mudstones in the Lichi Mélange, eastern Taiwan. Mem. Geol. Soc. China, 2, 115–128.

Liou, J.-G., Lan, C-Y. and Ernst, W.G. (1977b) The East Taiwan Ophiolite. Mining Research Service Organization (Taipei) Special Publication, 1, 212 pp.

Liou, J.-G. (1981) Petrology of metamorphosed oceanic rocks in the Central Range of Taiwan. Mem. Geol. Soc. China, 4, 291-341.

Liu, C.-S., Huang, I.-L. and Teng, L. S. (1997) Structural features off southwestern Taiwan. Mar. Geol., 137, 305-319.

Lo, C.-H. and Onstott, T.C. (1995) Rejuvenation of K-Ar systems for minerals in the Taiwan mountain belt. Earth Planet Sci. Lett., 131, 71-98.

Lo, C.-H. and Yui, T.-F. (1996) $^{40}Ar/^{39}Ar$ dating of high-pressure rocks in the Tananao basement complex, Taiwan. J. Geol. Soc. China, 39, 13–30.

Ma, K.F., Song, T.R., Lee, S.J. and Wu, H.I. (2000) Spatial slip distribution of the September 20, 1999, Chi-Chi, Taiwan, earthquake (Mw7.6) – Inverted from teleseismic data. Geophys. Res. Lett., 27(20), 3417-3420.

Ma, K.-F., Mori, J., Lee, S.-J. and Yu, S.-B. (2001) Spatial and temporal distribution of slip for 1999 Chi-Chi, Taiwan, earthquake. Bull. Seismol. Soc. Am., 91, 1069-1087.

Ma, K.-F., Tanaka, H., Song, S.-R., Wang, C.-Y., Hung, J.-H., Tsai, Y.-B., Mori, J., Song, Y.-F., Yeh, E.-C., Soh, W., Sone, H., Kuo, L.-W. and Wu, H.-Y. (2006) Slip zone and energetics of a large earthquake from the Taiwan Chelungpu-fault Drilling Project. Nature, 444, doi:10.1038/nature05253.

Meng, C.-Y. and Chiang, S.-C. (1965) Subsurface data from the wildcat SS-1, Shihshan, Taitung. Petrol. Geol. Taiwan, 4, 283-286.

Ota, Y., Lin, Y.-N.N., Chen, Y.G., Chang, H.-C. and Hung, J.-H. (2006) Newly found Tunglo active fault system in the fold and thrust belt in northwestern Taiwan deduced from deformed terraces and its tectonic significance. Tectonophysics, 417, 305-323.

Page, B.M. and Lan, C.Y. (1983) The Kenting melange and its record of tectonic events. Mem. Geol. Soc. China, 5:227-248.

Page, B.M. and Suppe, J. (1981) The Pliocene Lichi Mélange of Taiwan: its plate tectonic and olistostromal origin. Am. J. Sci. 281, 193–227.

Pelletier, B. and Stephan, J. F. (1986) Middle Miocene obduction and late Miocene beginning of collision registered in the Hengchun Peninsula: geodynamic

implications for the evolution of Taiwan. Tectonophysics, 125:133-160.
Reed, D.L., Lundberg, N., Liu, C.S., Luo, B.Y., 1992. Structural relations along
Richard, M., Bellon, H., Maury, R. C., Barrier, E. and Juang, W.-S. (1986) Miocene to Recent calc-alkaline volcanism in eastern Taiwan: K-Ar ages and petrography. Tectonophysics, 125, 87-102.
Rin, C.-C. (1935) Stratigraphic studies of the younger Tertiary and Pleistocene formations of Toyohara district, Taityu Prefecture, Taiwan (Formosa). Mem. Faculty of Sci. and Agriculture Taihoku, Imperial University, 13, 13-30.
Shyu, J.B.H., Sieh, K.,Chen, Y. and Liu, C.-S. (2005) Neotectonic architecture of Taiwan and its implications for future large earthquakes, J. Geophys. Res., 110, B08402, doi:10.1029/2004JB003251.
Song, S.-R. and Lo, H.-J. (1988) Volcanic geology of Fengpin-Takangkou area, Coastal Range of Taiwan. Acta Geologica Taiwanica, 26, 223-235.
Sun, S.-C. (1982) The Tertiary basins of offshore Taiwan. In: Proceedings of the Second ASCOPE Conference and Exhibition (Ed. by A. Salivar-Sali), pp.125-135.Manila, Philippines.
Sung Q. (1991) Explanatory text of the geologic map of Taiwan, scale 1:50,000 sheets 69, 70, 72 Hengchun Peninsula. Central Geological Survey, Taipei.
Suppe, J. (1980) A retrodeformable cross section of northern Taiwan. Proc. Geol. Soc. China, 23, 46–55.
Suppe, J. (1981) Mechanics of mountain-building and metamorphism in Taiwan. Mem. Geol. Soc. China 4, 67– 90.
Teng, L.S. (1979) Petrographical study of the Neogene sandstones of the Coastal Range, eastern Taiwan. (I. Northern Part). Acta Geologica Taiwanica, 20, 129-155.
Teng, L.S. (1981) On the origin and tectonic significance of the Lichi Formation, Coastal Range, eastern Taiwan. Ti-Chih, 2, 51–62. (in Chinese)
Teng, L.S. (1982) Stratigraphy and sedimentation of the Suilien Conglomerate, Northern Coastal Range, eastern Taiwan. Acta Geologica Taiwanica, 21, 201-220.
Teng, L.S. and Lo, H.-J. (1985) Sedimentary sequences in the island arc settings of the Coastal Range, eastern Taiwan. Acta Geologica Taiwanica, 23, 77-98.
Teng L.S. (1987) Tectonostratigraphic facies and geologic evolution of the Coastal Range, eastern Taiwan. Mem. Geol. Soc. China, 8, 229-250.
Teng, L.S. and Chen, W.-S. (1988) Stratigraphy and geologic history of the Coastal Range, eastern Taiwan. Symposium on the Arc-continent Collision and Orogenic Sedimentation in eastern Taiwan and Ancient Analogs, Field Guidebook, 4-1~4-25.
Teng, L. S. (1990) Geotectonic evolution of late Cenozoic arc-continent collision in Taiwan. Tectonophysics, 183, 57–76.

Teng, L. S., Wang, Y., Tang, C.-H., Huang, C.-Y., Huang, T.-C., Yu, M.-S. and Ke, A. (1991) Tectonic aspects of the Paleogene depositional basin of northern Taiwan. Proc. Geol. Soc. China, 34, 313–336.

Teng, L.S. (1992) Geotectonic evolution of Tertiary continental margin basins of Taiwan. Petrol. Geol. Taiwan, 27, 1-19.

Teng, L.S., Lee, J.-C. and Hsu, C.-B. (2002) Soft-sediment deformation in the Fanshuiliao Formation of the Coastal Range, eastern Taiwan. Bull. Centr. Geol. Surv., 15, 103-137.

Teng, L. S. and Lin, A.T. (2004) Cenozoic tectonics of the China continental margin: insights from Taiwan. in Malpas, J., Fletcher, C. J., Aitchinson, J. C. & Ali, J. (eds) Aspects of the Tectonic Evolution of China. Geological Society, London, Special Publications, 226, 313-332.

Tsai, H. and Sung, Q.C. (2003) Geomorphic evidence for an active pop-up zone associated with the Chelungpu fault in central Taiwan. Geomorphology, 56, 31-47.

Tsai, Y.-B. (1986) Seismotectonics of Taiwan. Tectonophysics 125, 17– 37.

Tsan, S. F. (1974a) The Kenting Formation: a note on Hengchun Peninsula stratigraphy. Proc. Geol. Soc. China 17, 131-133.

Tsan, S. F. (1974b) Stratigraphy and structure of the Hengchun Peninsula, with special reference to a Miocene olistostrome. Bull. Geol. Surv. Taiwan 24, 99-108.

Usami, M. (1939) Explanatory text of the geologic map of Taiwan, Karenko Sheet. Government-General of Taiwan Pub. 862, 21pp.

Wang, C.-S. (1976) The Lichi Formation of the Coastal Range and arc–continent collision in eastern Taiwan. Bull. Geol. Surv. Taiwan, 25, 73–86.

Wang, Y. and Chen, W.-S. (1993) Geologic Map of Eastern Coastal Range (Northern Sheet), Scale 1:100000. Centr. Geol. Surv. Taipei.

Wang-Lee, C. and Wang, Y. (1987) Tananao terrane of Taiwan: its relation to the late Mesozoic collision and accretion of the southeast China margin. Acta Geol. Taiwanica, 25, 225-239.

Wei, K-Y. and Cheng, Y.-M. (1982) Calcareous nannofossils from the Fanshuliao-chi section, Coastal Range, eastern Taiwan. Acta Geologica Taiwanica, 21, 177-194.

Wu, F.T., Rau, R.-J. and Salzberg, D. (1997) Taiwan orogeny: thin-skinned or lithospheric collision? Tectonophysics, 274, 191-220.

Yang, K.-M., Huang, S.-T., Wu, J.-C., Ting, H.-H., Mei, W.-W., Lee, M., Hsu, H.-H. and Lee, C.-J. (2007) 3D geometry of the Chelungpu thrust system in central Taiwan: its implications for active tectonics. Terr. Atmos. Ocean. Sci., 18(2), 143-181.

Yang, T.Y., Liu T.-K and Chen, C.-H. (1988) Thermal event records of the Chimei Igneous Complex: constraint on the ages of magma activities and the structural

implication based on fission-track dating. Acta Geol. Taiwanica, 26, 237-246.
Yang, T. F., Tien, J.-L., Chen, C.-H., Lee, T. and Punongbayan, R. S. (1995) Fission-track dating of volcanics in the northern part of the Tiwan-Luzon arc, eruption ages and evidence for crustal contamination. SE Asian Earth Sci, 11(2), 81-93.
Yang, T.F., Yeh, G.H., Fu, C.C., Jiang, J.H., Wang, C.C., Lan, D. F., Chen, C-H., Walia, V. and Sung, Q.C. (2004) Composition and exhalation flux of gases from mud volcanoes in Taiwan. Environmental Geology, 46, 1003-1011.
Yang, C.-C. (1997) Depositional environments of the Chishui Shale, Cholan and Toukoshan Formations, Central Taiwan. MSc thesis, Institute of Geology, National Taiwan University, 120pp. (in Chinese)
Yen, T.-P. (1954) The gneisses of Taiwan. Bull. Geol. Surv. Taiwan, 5, 1-100.
Yen, T.-P. (1960) A stratigraphic study of the Tananao Schist in northern Taiwan. Bull. Geol. Surv. Taiwan, 12, 53-66.
Yen, T.-P. (1963) The metamorphic belts within the Tananao Schist terrain of Taiwan. Proc. Geol. Soc. China, 6, 72-74.
Yen, T.-P. and Rosenblum, S. (1964) Potassium-argon ages of micas from the Tananao Schist terrane of Taiwan - A preliminary report. Proc. Geol. Soc. China, 7, 80-81.
Yen, T.-P. (1967) Structural analysis of the Tananao Schist of Taiwan. Bull. Geol. Surv. Taiwan, 18, 1-110.
Yu, H.-S. and Chou, Y.-W. (2001) Characteristics and development of the flexural forebulge and basal unconformity of Western Taiwan Foreland Basin. Tectonophysics, 333, 277–291.
Yui, T.-F., Lu, C.-Y. and Lo, C.-H. (1988) A speculative tectonic history of the Tananao Schist of Taiwan. Proc. Geol. Soc. China, 31(2), 7-18.
Yui, T.-F. and Lo, C.-H. (1989) High-pressure metamorphosed ophiolitic rocks from the Wanjung area, Taiwan. Proc. Geol. Soc. China, 32, 47-62.
Yui, T.-F. and Lan, C.-Y. (1991) Isotopic compositions of Tananao marble in the Tungao area, northeastern Taiwan: a chronological consideration. Spec. Publ. Centr. Geol. Surv., 5, 161-172.
Yui, T.-F., Wu, T.-W. and Lu, C.-Y. (1994) Geochemical characteristics of metabasites from the slate formations of Taiwan. J. Geol. Soc. China, 37, 53-67.

Appendix 1: 國立中央大學地球科學系台灣地質野外考察行程規劃

日期(2018)	野外露頭點
14 Jan. **(第 1 天)** 林殿順 黃文正 郭力維	中央山脈變質岩 **早上 6:30 AM 中大開車** 1-1：朝陽漁港：中央山脈變質岩 1-2：天祥層：天祥 1-2：白沙橋 1-3：長春祠　住:花蓮康橋飯店
15 Jan. **(第 2 天)** 林殿順 黃文正 郭力維	海岸山脈秀姑巒溪（由西往東） 2-1：德武河階 2-2：八里灣層 2-3：奇美村秀姑巒溪河床：奇美斷層及八里灣層（2 處露頭） 2-4：都巒山層(長虹橋) 住:花蓮康橋飯店
16 Jan. **(第 3 天)** 林殿順 郭力維	海岸山脈北段沿海岸 3-1：海岸山脈最北端、花蓮溪口：嶺頂，中新世火山碎屑岩 3-2：水璉礫岩(鹽寮十號橋) 3-3：石門礫岩 3-4：石梯坪 3-5：烏石鼻 住:池上
17 Jan. **(第 4 天)** 林殿順 郭力維	海岸山脈西南側 4-1：鷺溪五號橋 4-2：池上斷層 4-3：鹿野高台 4-4：利吉村 4-5：富岡砂岩 住 :東台大飯店
18 Jan. **(第 5 天)** 林殿順 郭力維	5-1：太麻里海邊 5-2：尖山外來岩塊 5-3：恆春四重溪石門礫岩及四重溪層 5-4：恆春石灰岩：恆春西台地 住:恆春小丑魚度假村

19 Jan. **(第 6 天)** 林殿順 郭力維	6-1：佳樂水砂岩 6-2：墾丁層(出火) 6-3：烏山頭水庫六甲斷層槽溝開挖 回程中大

Field leaders

Andrew T. Lin (林殿順)	National Central University, Taiwan	andrewl@ncu.edu.tw
Wen-Jen Huang (黃文正)	National Central University, Taiwan	huang22@ncu.edu.tw
Li-Wei Kuo (郭力維)	National Central University, Taiwan	liweikuo@ncu.edu.tw

Field assistants:

蔡仲霖	National Central University, Taiwan	tcl10721@gmail.com
謝宜廷	National Central University, Taiwan	s950718g@gmail.com

In case of emergency, one may contact the personnel with the following cell phone numbers:

Bus driver's (游莊章先生) contact: 0932-365532;

* The regional code of Taiwan is +886

Student Participants

1.	楊楚伶	18.	張簡婉晴
2.	孟婷茹	19.	林鈺真
3.	江宜佳	20.	顏佳平
4.	孫綺謙	21.	林鼎竣
5.	李政熹	22.	陳　翔
6.	莊子寬	23.	李俊德
7.	陳伯源	24.	陳文瑜
8.	葉正陽	25.	陳昱先
9.	李健瑀	26.	鄭雲澤
10.	郭顯定	27.	王家佑
11.	柯源峰	28.	彭睿平
12.	胡祖寧	29.	莊博滄
13.	吳宜儒	30.	宋冠毅
14.	陳昭邑	31.	蔡昇均
15.	呂宜庭	32.	蕭立揚
16.	郭玫穎	33.	林皓鍇
17.	徐郁捷	34.	張　立

Appendix 2: Geological Map of Taiwan